Targeting the RB pathway in tumor cells

María Caballero de la Torre

PhD Thesis UPF

Barcelona, 2021

Treball dirigit pel Dr. Francesc Posas Garriga i la Dra. Eulàlia de Nadal Clanchet

Departament de Ciències Experimentals i de la Salut (DCEXS-UPF) i Institut de Recerca Biomèdica (IRB Barcelona)

Programa de Doctorat en Biomedicina de la Universitat Pompeu Fabra

No se equivoca el que prueba diferentes caminos para conseguir sus metas, se equivoca aquel que por temor a equivocarse no experimenta.

ACKNOWLEDGMENTS

Han sido 5 años en los que he aprendido y trabajado mucho, he pasado por situaciones duras y he cometido errores, pero he aprendido de ellos y he vivido momentos memorables rodeada de gente maravillosa. Me quedo con los mejores recuerdos y quiero dar sinceros, profundos y cuantiosos agradecimientos a todos los que me habéis acompañado en este camino.

En primer lugar, quiero agradecer a mis directores de tesis, Francesc Posas y Laia de Nadal, por darme la oportunidad de formar parte de un grupo admirable, por su trabajo y dedicación permanente, por sus consejos, enseñanzas, orientación y por la gran confianza que han depositado en mí para desarrollar este proyecto, ¡muchas gracias!

Quiero agradecer especialmente a las cuatro personas con las que he trabajado en este proyecto de RB. A Manel por guiarme en los primeros pasos, por tu paciencia y por enseñarme a desenvolverme de manera autónoma en el laboratorio. A Santi por compartir conmigo la fuente de conocimiento enciclopédico de tu cabeza, porque es difícil encontrar una persona con la que sea tan fácil compenetrarse y que valga tantísimo como tú. Thanks to Rado for helping me with the last experiments of the thesis, it's a pity that we've only shared the last year because I still have a lot to learn from you. A Israel por aportarme tantos conocimientos de screening y descubrirme el mundo de desarrollo de fármacos, por tu gran interés, ganas de mejorar, esfuerzo, proactividad y cooperatividad infinita.

Al equipo de "mammals" por esos eternos "meetings" donde compartimos nuestros logros y fracasos. To Predrag, I still remember the first day we arrived together at the laboratory as it is said in Spanish: we are "el punto y la I". Thank you for having been by my side these years! A Adri y a Iván por estar ahí a las buenas y a las malas, por el buen funcionamiento de la sala de cultivos, por ayudarme con multitud de experimentos y análisis de datos, por aguantar mis locuras y por

divertirnos juntos. A Cesc porque fomentas un muy buen ambiente en el laboratorio.

Al resto del laboratorio de Cell Signaling, por hacerme crecer científica y personalmente y porque no me imagino un grupo de trabajo mejor. A Anna mi grandísima compañera de batallas, por haberte convertido en mi informante (papeleos, fechas de entrega y solicitudes que para mí son imposibles de recordar), asesora, confidente, y sobre todo cómplice y amiga. A Aida no te agradecemos todo lo que haces constantemente, siempre velando porque el laboratorio funcione y no nos falte de nada, por tus "disagree", porque las comidas contigo son mucho más a menas. A Mariona, Carme, Alba, Seisi y David por ser conocedores como nadie del mundo de la ciencia, vuestros consejos han sido prácticos y tremendamente útiles, os admiro profundamente. A Pablo y Gerard por vuestro compañerismo y apoyo moral. A Nico porque, aunque vayas de "malote", hay que quererte. A Hansol, María Quintana y Guillem por recordarme la ilusión del comienzo, disfrutad del camino que os queda por descubrir. A antiguos miembros del laboratorio Silvia y Berta por enseñarme tanto en mis comienzos y ser tan geniales. A Ramón, Jana, Cate, Pedro, Arnau, René y Arturo que siempre que os veo me produce inmensa alegría. A Montse por tu apoyo inigualable, por estar siempre dispuesta a organizar planes y ayudarme a desconectar de la rutina. Laieta, Eva y Sira (del lab de Javier) las reuniones con vosotras curan el alma.

A los compañeros que dejamos en el PRBB Marc, Leire, y a todos los miembros del lab de "pombe", os hemos echado de menos. También a las nuevas amistades que hemos conocido en el IRB, Alicia, Anna Ferrer, Marta, Lorena, Marina, Joel y al resto gente del lab de Riera, Méndez, Gomis, Azorin, Nebreda, Serrano etc. A Henar y las chicas de Oncohéroes. A Marta Taulés, Toni, Jaume Comas, Tanya Yates y a los demás miembros de servicios y personal del IRB/PCB que son un gran apoyo en nuestros

experimentos, gracias por hacer que nuestra llegada al IRB haya sido tan acogedora.

A Pepa Toro y Antonio Chiloeches por brindarme la primera oportunidad de pisar un laboratorio y darme alas para continuar. A mis chicas de la universidad de Alcalá Eva, Bea, Alicia, Nadia, Ana, Chus, Ceci, y a mis "cachorr@s" (Andrés, Rocío, Laura, Cris, Eva, Yeli, Javi, Lucía y Lore) que los reencuentros con vosotros son superlativos.

A la música, ese mundo mágico donde eres libre para expresar y sentir y a aquellos que lo hacen posible en especial a Diego Miguel-Urzanqui por tu dedicación, infinita paciencia y compromiso, a la orquesta de la UPF, a la del PRBB y a la agrupación musical Ntra. Sra. de Riánsares.

Dicen que los amigos son la familia que escoges, y yo tengo a los más grandes y son piezas esenciales de mi tesoro personal. A Luis mi fiel, empático, comprensivo, paciente y divertido compañero de aventuras. A mi Rodri, persona que acuño el término "lagartear", por tu cariño incondicional y estar siempre pendiente de mí. A Guillem por su arte culinario que me ha salvado la vida en tiempos de estrés, por compartir locuras y amenizar la casa con tu música. A Elena Fagín por ser la alegría de la huerta "murciana" y mejor planificadora de eventos que conozco. A Sofia por los pensamientos intensos, por las escuchas pacientes y buenos consejos. A Marcos por tus análisis racionales que suelen hacerme ver la realidad con más claridad y a Clara porque simplemente contigo todo mejora un 10000x. A Elena Moreno por las charlas profundas y por esos "bailesitos" que nos animan la vida. Almudena y Ernest mis "filetos" favoritos siempre aportando cariño y alegría al grupo. A Marc por ser el máximo experto en cuestiones marítimas. Al gran Javi porque eres bueno y grande a partes iguales. A Adri y Paloma por aportar diversión y risas. A Barri, Enrique y Jacobo vuestras visitas a Barcelona nunca decepcionan.

A Estefa por quererme tanto, por estar siempre a mi lado, por impulsarme a crecer y por tener un impacto tan grande en mi vida que siempre me voy a quedar corta para expresar mi gratitud. A mis amigos de Tarancón los Frankachelos y la Tremolina "mis musiquillos" porque el aburrimiento no existe con vosotros. A Lore y Aitor porque tenéis la magia de sacarme un sinfín de carcajadas, por los carnavales, viajes, lloros y alegrías compartidas. A Tere Cardeñosa y Yelina por ser imprescindibles a lo largo de mi vida, aunque no siempre podemos vernos.

A Rubén por creer en mí, por ser partícipe de mis éxitos, amenizarme la vida y hacerme feliz.

A mi familia que siempre me recibe con los brazos abiertos y grandes sonrisas llenas de fuerza. Quiero resaltar a mis tres tías Pili, Sole y Mari sois el sabio pilar que nos sustenta a todos, siempre al pie del cañón. Al resto de mis primos, tíos y aquellos que nos cuidan desde arriba, sois mi refugio, mi hogar y mi raíz.

A mi hermano porque eres el mayor regalo que me dieron de niña, por las aventuras y recuerdos de la infancia y las tonterías y momentos de adultos. A mi padre por estar a mi lado apoyándome siempre, por tu esfuerzo y por los sacrificios que has hecho para que yo tuviera lo mejor en todos los sentidos. A mi madre por protegerme, por comprenderme, por conocerme más que yo misma, por ser tan valiente, por guiarme y enseñarme a luchar por mis sueños. Gracias a los tres por enseñarme a ser feliz, por apoyarme incondicionalmente, por ser mis referentes y porque todo lo que soy os lo debo a vosotros. Os quiero.

¡MILLONES DE GRACIAS!

SUMMARY

The Retinoblastoma protein (RB) is an essential negative regulator of the G1/S transition of the cell cycle. RB is cyclically inactivated by cyclin-dependent kinases (CDKs) during cell cycle progression. Mutations in components of the RB signaling pathway lead to oncogenesis. Our group described a new regulatory mechanism of RB by p38 stress-activated MAPK. In response to environmental stresses, p38 phosphorylates RB in the N-terminal region, at S249/T252 residues, revealing a new interaction surface between RB and the E2F transcription factor. RB phosphorylation by p38 leads to an increase in the affinity of RB for E2F that represses E2F-dependent gene expression and halts cell cycle progression. Of note, expression of a p38-phosphomimetic RB version decreases proliferation of cancer cell lines and tumors in mice even in the presence of high CDK activity (Gubern et al., 2016; Joaquin et al., 2016). Furthermore, RB phosphorylated at S249/T252 promotes tumor immunity by inhibiting NFKB transcriptional activity and PD-L1 expression. Indeed, the expression of an RB-derived phosphomimetic peptide decreases the upregulation of PD-L1 induced by radiation therapy and increases the therapeutic effectiveness of radiation *in vivo* (Jin et al., 2018).

The discovery of this novel mechanism of RB regulation represents an opportunity for developing new drugs to treat cancer diseases. In this thesis, we designed and developed an assay that monitors the RB activity in cultured cell to identify compounds that emulate or yield the effect of S249/T252 phosphorylation of RB, turning RB into a super-repressor insensitive to CDK inactivation. This assay has been optimized for High-Throughput Screenings

(HTSs) for drug discovery. More than 9.000 compounds from three different chemical libraries were assayed as a proof of concept. This screening led to the detection of several active compounds (hits). 32 hits were validated by IC50 and cytotoxicity analyzes and 22 out of them were prioritized for further analyzes. These 22 candidates were classified according to their mechanism of action on the RB signaling pathway by several secondary assays. Our data indicated that 11 drugs inhibited tumor cell growth, 7 out of them arrested the cell cycle in G1 and 2 increased the affinity of E2F1-RB. Moreover, 1 compound inhibited CDK activity and another compound activated p38 MAPK. Additionally, we characterized a smaller RB-E2F1 interaction region, which are helping us to characterize the impact of the hits more accurately, limiting the interaction surface of selected small molecules with these proteins.

Our screening assay has confirmed the success and feasibility of a new RB targeting strategy. We are now assaying a HTS with larger chemical libraries (a total of 150,000 compounds). The compounds that directly increased the RB-E2F1 binding will offer a new and promising cancer therapeutic strategy, applicable to most types of cancers, with clear advantages over the traditional approach. These activators of RB not only will offer anti-proliferative therapy to cancer patients but also will be able to boost immune response by decreasing PDL1 expression.

La proteína de Retinoblastoma (RB) es un regulador negativo esencial en la transición G1/S del ciclo celular. RB se inactivada cíclicamente por quinasas dependientes de ciclina (CDKs) durante la progresión del ciclo celular. Mutaciones en los componentes de la vía de señalización de RB conducen a oncogénesis. Nuestro grupo describió un nuevo mecanismo regulador de RB por la proteína p38 MAPK activada por estrés. En respuesta al estrés ambiental, p38 fosforila a RB en la región N-terminal, en los residuos S249/T252, revelando una nueva superficie de interacción entre RB y el factor de transcripción E2F. Esta fosforilación provoca un aumento de la afinidad de RB por E2F que reprime la expresión génica dependiente de E2F y detiene la progresión del ciclo celular. Cabe destacar que la expresión de un mutante RB p38-fosfomimético disminuye la proliferación de líneas celulares cancerosas y tumores en ratones, incluso en presencia de una alta actividad de CDK (Gubern et al., 2016; Joaquin et al., 2016). Además, RB fosforilado en S249/T252 promueve la inmunidad tumoral al inhibir la actividad transcripcional de NFKB y la expresión de PD-L1. De hecho, la expresión de un péptido fosfomimético derivado de RB disminuye la expresión de PD-L1 inducida por la radioterapia y aumenta la eficacia terapéutica de la radiación *in vivo* (Jin et al., 2018).

El descubrimiento de este mecanismo de regulación de RB representa una oportunidad para desarrollar nuevos fármacos para tratar el cáncer. En esta tesis, hemos diseñado y desarrollado un ensayo que monitoriza la actividad de RB en células en cultivo para identificar compuestos que emulan o mimetizan el efecto de la fosforilación S249/T252 de RB, convirtiendo a RB en un súper

represor insensible a la inactivación de CDK. Este ensayo se ha optimizado para pruebas de detección de alto rendimiento (HTS) para el descubrimiento de fármacos. Mediante este ensayo, hemos analizado más de 9.000 compuestos de tres bibliotecas químicas diferentes. Este cribado condujo a la detección de varios compuestos activos (hits), de los cuales 32 fueron validados por análisis de IC50 y citotoxicidad y 22 de ellos fueron priorizados para análisis adicionales. Estos 22 candidatos se clasificaron según su mecanismo de acción en la vía de señalización de RB mediante varios ensayos secundarios. Nuestros datos indicaron que 11 fármacos inhiben el crecimiento de células tumorales, 7 de ellos detienen el ciclo celular en G1 y 2 aumentan la afinidad de E2F-RB. Además, 1 compuesto inhibe la actividad de CDK y otro compuesto activa p38 MAPK. Además, también hemos identificado una región de interacción RB-E2F1 más pequeña, lo que nos está ayudando a caracterizar el impacto de los hits con mayor precisión, limitando la superficie de interacción de las moléculas pequeñas seleccionadas con estas proteínas.

Nuestro ensayo de cribaje ha confirmado el éxito y la viabilidad de esta nueva estrategia dirigida a RB como diana. Actualmente, estamos ensayando un HTS con bibliotecas químicas más novedosas y grandes (un total de 150.000 compuestos). Los compuestos que directamente incrementan la unión de RB-E2F ofrecen una nueva y prometedora estrategia terapéutica contra el cáncer con claras ventajas sobre el enfoque tradicional y aplicable a la mayoría de los tipos de cánceres. Estos compuestos activadores de RB no solo ofrecerán una terapia anti proliferativa a los pacientes con cáncer,

sino que también podrán inducir la respuesta inmune al disminuir la expresión de PDL1.

PREFACE

Cancer is the name given to a group of systemic diseases characterized by the uncontrolled growth of abnormal cells with the potential to invade or spread to other parts of the body. Cancer is one of the main causes of death globally. During 2020, more than 19 million people were diagnosed with cancer and 10 million cancer deaths were registered according to World Health Organization.

The latest research reveals that cancer is a multidimensional process with specific characteristics at the cellular, tissue and organism levels (Smith et al., 2020).The pathogenesis of cancer is the result of multiple genetic and epigenetic alterations. In the course of this multistep oncogenic process, cells obtain certain capacities, including self-sufficiency in growth cues, unlimited proliferation and resistance to antiproliferative and apoptotic (Fouad and Aanei, 2017; Hanahan and Weinberg, 2011). Moreover, during oncogenesis, tumor and surrounding stromal cells are strongly modified, attracting new blood vessels, avoiding immune detection, and ultimately, invading and metastasizing to other tissues (Ganesh and Massagué, 2021). Macroscopic cancer hallmarks have also been described as a result of the interaction between cancer and the whole organism. These systemic characteristics are as follows: global inflammation, novel connections between the primary tumor, bone marrow, and distal metastasis, inhibition of immunity, metabolic changes leading to cachexia, propensity for thrombosis, and neuroendocrine changes (Paul, 2020).

The main cause of these cancer-related phenotypic characteristics can be divided into two broad classes, namely the activation of oncogenes and the inactivation of tumor suppressor

genes. An oncogene is a gene that undergoes aberrant genetic or epigenetic alterations that increase its expression or lead to uncontrolled activity of the protein it encodes. In the context of tumorigenesis, activation of oncogenes triggers cell proliferation and evasion of apoptosis, thereby leading to uncontrolled cell growth (Cisowski and Bergo, 2017). Tumor suppressor genes stand at the opposite side in cell growth regulation, normally serving to inhibit cell proliferation and tumor development. In many types of cancer, these genes are lost or inactivated, thereby removing negative regulators of cell proliferation and also contributing to the uncontrolled growth of tumor cells (Guo et al., 2014; Kontomanolis et al., 2020). Even though during tumorigenesis, tumor suppressors are as important as oncogenes, most of the current molecular targeted therapies are oncogene inhibitors (Baudino, 2015; Peuget et al., 2020). This is due to regaining the activity of inactivated tumor suppressor genes has been shown to be more difficult to achieve.

The Retinoblastoma protein (RB) is an essential tumor suppressor and mutations in components of the RB signaling pathway lead to oncogenesis. Understanding how RB controls the process of the cell cycle and prevents tumor development has been key to design an innovative drug detection strategy targeting RB. Here, we developed a cell-based assay to monitor RB activity and identify small molecules that increase the tumor suppressive capacity of RB. We set up the assay for use in high-throughput screening (HTS) and established secondary validation methods. The results obtained in this thesis represent a remarkable improvement in drug discovery and will allow to introduce novel compounds in the clinic.

TABLE OF CONTENTS

INTRODUCTION

RETINOBLASTOMA TUMOR SUPPRESSOR

Retinoblastoma (RB), the first tumor suppressor gene to be identified in a rare childhood retina tumor and was cloned more than 35 years ago (Friend et al., 1986; Knudson, 1971). Since then, RB homologous proteins or closely related family members have been found in a huge number of plant and animal species, thereby indicating their biological relevance (Van Den Heuvel and Dyson, 2008).

The importance of RB proteins lies in their fundamental role in the regulation of the cell cycle. Although RB pocket proteins control all the phases of the cell cycle, their main function is to modulate the G1-S transition. RB interacts with the E2F family of transcription factors and represses the expression of essential cell cycle genes by its direct interaction with E2F or acting as adaptor protein that recruit chromatin remodelers. RB proteins undergo hyperphosphorylation in order to allow the cell to enter the S phase. This phosphorylation state of RB leads to its separation from the E2F proteins family, thereby allowing the transcription of the genes necessary for S phase progression and cell proliferation (Fiorentino et al., 2013).

The loss or aberrant inactivation of RB proteins is one of the most predominant events in cancer and contributes to pathological cell proliferation leading to oncogenesis. Although some tumors harbor mutations in RB, it is usually the altered expression of RB regulators such as Cyclin D, CDK4 and CDK6 or the inactivation of CDK regulators that lead to RB inactivation (Malumbres and Barbacid, 2001). Indeed, the hyperactivation of CDKs is one of the

most common mechanisms leading to the loss of RB function and causing uncontrolled cell proliferation (Peyressatre et al., 2015).

Beyond its function as cell cycle regulator, RB plays an important role in other cell processes, such as maintenance of chromosome stability (Manning et al., 2010), induction and maintenance of senescence (Chicas et al., 2010), apoptosis (Hilgendorf et al. 2013; Ianari et al. 2009), differentiation (Thomas et al., 2003), and angiogenesis (Gabellini et al., 2006). Given the key roles of these processes in preventing tumor progression, they could all contribute to the tumor suppressor function of RB.

1.1. The pocket protein family

Based on sequence similarity, the RB protein family is composed of RB (p105 or RB1 gene), p107 (RBL1 gene), and p130 (RBL2 gene) (Friend et al., 1986; Lee et al., 1987). All three RB family members are collectively known as the “RB pocket proteins” or “RB proteins” family.

Within this family, RB is the most widely characterized protein, while structural data from p130 and p107 proteins are still limited. Despite this, sequence analysis reveals that p130 and p107 contain structural domains analogous to those of RB. The RB, p107 and p130 proteins have amino-terminal domains (107N and 130N), pocket domains and carboxy-terminal domains (107C and 130C) with similar structural elements (Figure 1). RB shows approximately 25% sequence homology with p107 and p130, whereas p107 and p130 share 54% identity with each other (Dick and Rubin, 2013a).

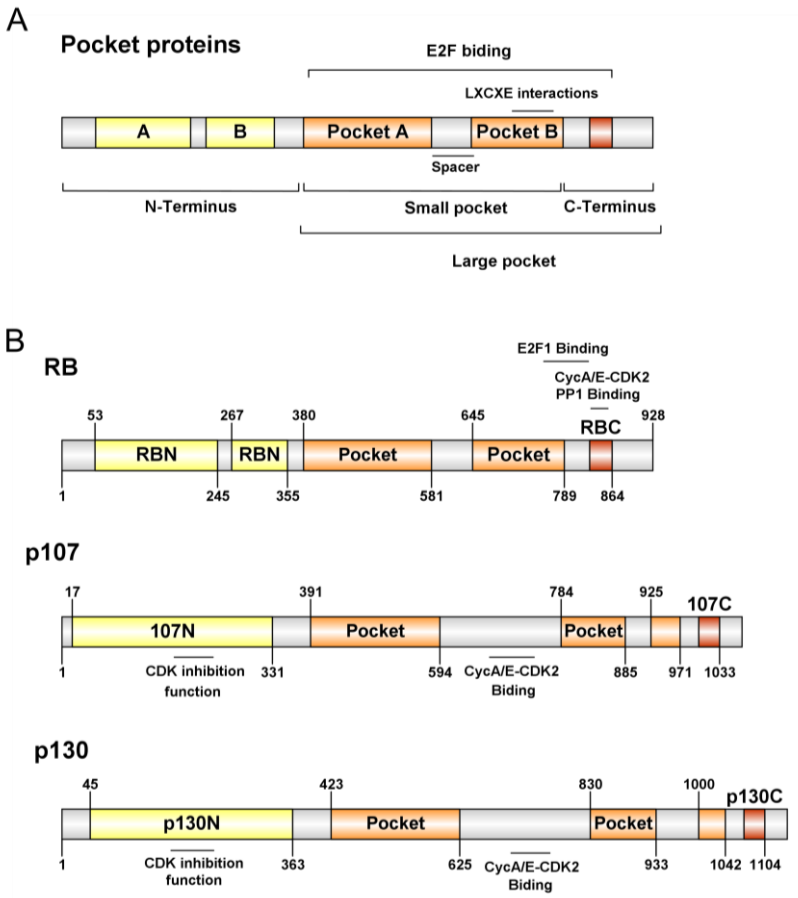

Figure 1. Schematic representation of the pocket protein family. A. Both the "large pocket" and "N-terminus" act as minimal E2F interaction domains independently. The "large pocket" is the minimal domain of growth-suppressing and the small pocket (included in the large pocket region) is the region required to bind to oncoviral proteins through their LXCXE motif. **B.** Comparison of pocket proteins structures. The key structural differences between RB, p107 and p130 are highlighted. Adapted from Henley-Dick, 2012 and Dick-Rubin, 2013.

The most preserved amino acid fragment among RB proteins is the small pocket region, which contains the A and B domain separated by a flexible spacer. Shortly after the discovery of RB, several viruses were found to target RB for its inactivation during

cellular transformation (Dyson et al., 1989) and the small pocket was defined as the minimal fragment of RB capable of interacting with viral oncoproteins (Hu et al., 1990). Each of these viral proteins contains a LXCXE peptide motif that is crucial for stable interaction with RB family proteins (Münger et al., 1989; Whyte et al., 1989). Apart from the viral proteins, a wide range of cellular proteins, such as chromatin modulators, have been reported to contain an LXCXE motif that allows them to interact with RB, p107 and p130 (Balog et al., 2011; Dick, 2007) (Figure 1A). The most widely characterized pocket protein interactions occur with the E2F family of transcription factors. However, the small pocket is not enough to interact with E2Fs, and the C-terminal domain is also needed. Both the small pocket and C-terminal domain comprise the so-called large pocket region, which interacts with E2Fs and suppresses the transcription of the cell cycle control genes (Hiebert et al., 1992a) .

Finally, the N-terminal region has a single globular entity formed by two Cyclin-like folds, very similar to the A and B boxes located in the RB pocket and these domains are preserved in all members of the pocket proteins family (Hassler et al., 2007). In fact, it has been described that the N-terminal region also act as a minimal E2F interaction domain independently to the large pocket domain (Gubern et al., 2016) (Figure 1 A).

Remarkably, there are few obvious structural differences between RB, p107 and p130 (Wirt and Sage, 2010). RB contains two exclusive features, namely a docking site for E2Fs and a C-terminal short amino acid region that is competitively occupied by CDKs or protein phosphatase 1 (PP1) (Henley and Dick, 2012). Several structures in

both p107 and p130 are absent in RB, such as the characteristic insertions in the B domain at their small pockets. In the case of p130, this region is subjected to regulatory phosphorylation to maintain protein stability (Litovchick et al., 2004). Additionally, p107 and p130 show longer spacer regions than RB, allowing them to bind stably with CDK complexes and a region in the N-terminus related to CDK inhibition (Woo et al., 1997) (Figure 1 B). Although these RB pocket proteins show a high degree of structural similarity, they perform redundant or very different functions depending on the binding partners and cellular context (Classon and Harlow, 2002).

1.2 RB phosphorylation effects and its structural function

RB pocket proteins are phosphorylated on multiple sites, mainly by CDK. Among these proteins, the phosphorylation code of RB protein is the most characterized. Early studies of RB phosphorylation levels showed that these phosphorylation events modulate RB activity (Mittnacht, 1998a). As mentioned above, the main function of RB is the control of the cell cycle by regulating the transcription of E2F dependent genes. Non phosphorylated RB is active, and it results in transcriptional repression and the arrest of cell cycle progression. RB works as a protein interaction scaffold, associating with a huge number of transcriptional co-repressor proteins. Analysis of RB structure facilitated the understanding of its interaction with different proteins and how the phosphorylation events regulate these interactions (Rubin et al., 2005).

The two most important structural domains of RB are the N-terminal domain (RBN) and the domain of the pocket protein, apart from various disordered sequences which include loops such as

RBNL within RBN, RBPL inside of the pocket, RBIDL that connects the pocket to the N-terminal domain and the C-terminal domain (RBC) (Rubin et al., 2005). The RB protein has 16 CDK phosphorylation sites, serine (Ser) or threonine (Thr) residues followed by Proline (Pro), in the disordered spacer regions (RBNL, RBPL, RBIDL, RBC). However, mass spectrometry studies have shown that only 13 of these sites are phosphorylated in cells (Dephoure et al., 2008; Olsen et al., 2010) (Figure 2 A).

The different phosphorylation events induce conformational changes that cause RB inactivation by hindering E2F binding. RB phosphorylation by CDKs break the interaction with specific proteins, favoring the folding on itself and rendering this folding structure incompatible with RB binding partners (Burke et al., 2010, 2012; Hassler et al., 2007).

E2F interacts with several domains of non-phosphorylated RB. A key interaction surface is between a cleft flanked by the two helical subdomains in the pocket region of RB and the E2F transactivation domain ($E2F^{TD}$) (Lee et al., 2002; Xiao et al., 2003). In addition, the RBC binds to E2F and its heterodimer partner DP ($E2F^{MB}$–DP^{MB}) (Figure 2 B, C).

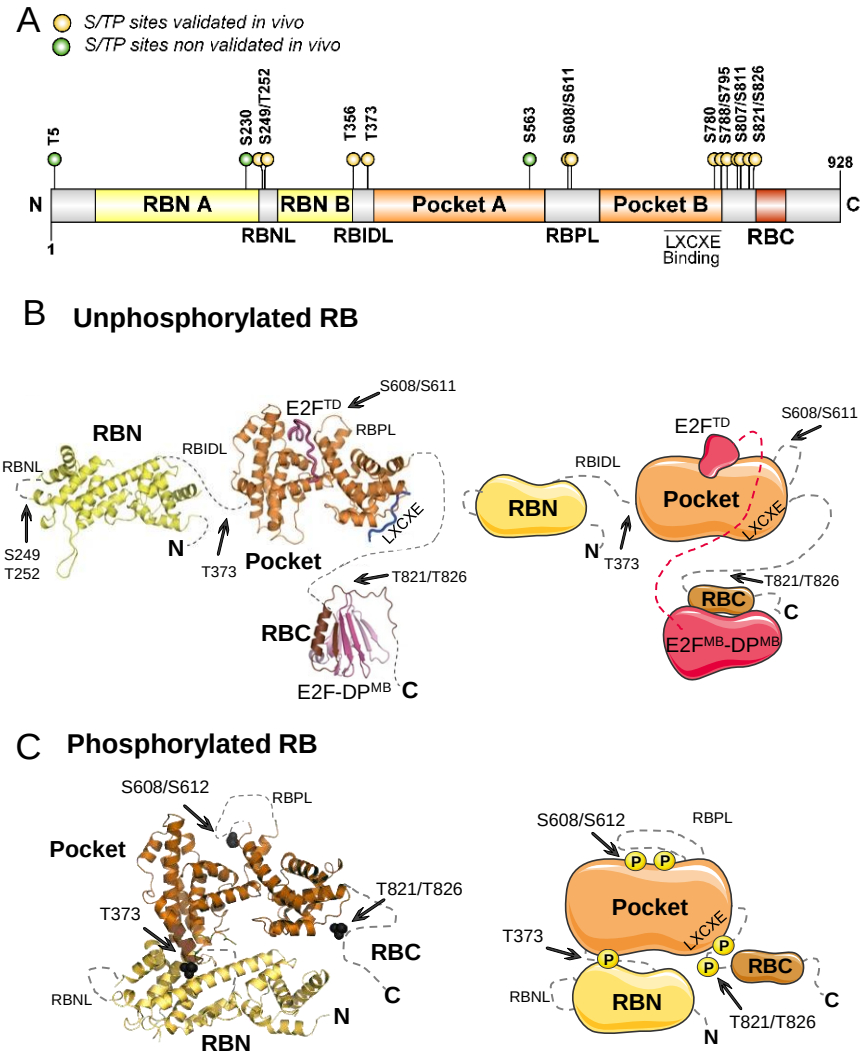

Figure 2. Model of phosphorylation sites of RB and its protein interactions.

A. Representation of the consensus S/TP phosphorylation sites of RB located along its sequence. **B.** Crystal model and schematic diagram of unphosphorylated RB. RB presents two binding E2F surfaces. The pocket domain interacts with the E2F transactivation domain ($E2F^{TD}$) and the RB C-terminus (RBC) binds to E2F and its heterodimer partner DP ($E2F^{MB}$–DP^{MB}). The pocket domain has a cleft in its second helical subdomain, which binds linear LXCXE sequences of different proteins. **C**. Crystal model and schematic diagram of phosphorylated RB. T373 phosphorylation drives the association of the RB C-terminus (RBC) and the pocket

domains, whereas phosphorylation of S608, S612, T821 and T826 induces conformational changes resulting in the inhibition of the RB–E2F and RB-LXCXE protein complexes. Adapted from Rubin, 2013.

The regulatory role of RB in the cell cycle is largely determined by its phosphorylation state. In early G1, Cyclin D-CDK4,6 complexes phosphorylate the S249, T252, T356, S608, S788, S807, S811 and S826 sites of RB. Afterwards, Cyclin D-CDK4,6 or Cyclin E-CDK2 mediate the phosphorylation of T5, T373, and S795, and at the end of G1, Cyclin E-CDK2 complexes phosphorylate S612 and T821, as shown by *in vitro* experiments (MacDonald and Dick, 2012; Zarkowska and Mittnacht, 1997). Individual mutations in the diverse phosphorylation residues are not enough to override the RB function in the cell cycle, thereby demonstrating that no single site prevents the interaction of RB with E2F. On the contrary, modifications on most RB phosphorylation sites block E2F-RB binding (Brown et al., 1999; Knudsen and Wang, 1997). The first phosphorylation events of the C-terminal domain lead to structural modifications of RB, which change the intramolecular interactions and give rise to the exposure of previously hidden CDK phosphorylation sites. As cells progress through the cell cycle, new available phosphorylation sites are enabled, thus altering the molecular structure of the E2F binding cleft and resulting in the separation of RB from E2F (MacDonald and Dick, 2012). Therefore, knowledge of the molecular effects of these phosphorylation events is fundamental to understand RB-E2F dissociation mechanisms (Burke et al., 2010).

RB phosphorylation at T821/T826 induces a conformational change in the protein. In this regard, the RBC joins to the pocket

domain, thereby preventing interaction with the LXCXE motif of protein partners, such as viral protein and histone deacetylase (Harbour et al., 1999; Knudsen and Wang, 1996; Rubin et al., 2005). In the same way, residues T821/T826 immediately precede the RB C-terminal domain sequence required for RB-E2F1^{MB}-DP^{MB} binding and the phosphorylation in these sites prevents RB-E2F association. RB contains other sites susceptible to phosphorylation that alter the binding with E2F. The phosphorylation of S608/S612 mediates RB pocket loop interaction with the pocket domain in a manner that mimics and competes with E2F. In addition, T373 phosphorylation generates a hydrophobic surface that binds a cleft in the N terminus, thus allosterically disrupting E2F binding (Burke et al., 2010, 2012). The allosteric inhibition mechanism regulated by phosphorylated T373 and competitive control by the phosphorylation at S608/S612 are clearly different. The allosteric regulation consist of a conformational change to release bound E2Fs and other protein interactions at the LXCXE cleft, while the competitive binding of RB prevents the association of free E2F (Burke et al., 2012).

Regions of RB phosphorylation outside the pocket domain able to mediate associations with other proteins remain poorly understood. Due to its highly disordered nature, the N-terminal fragment of RB has only been partially crystallized and none of the published crystal structures of the protein contain the loop region comprising the phosphorylation residues (S249/T252) (Burke et al., 2010, 2012; Hassler et al., 2007). Consequently, it is difficult to determine the effects of phosphorylation sites in the RBN.

Several studies showed that E1A-like inhibitor of differentiation (EID1) binds to RB when cells commit to differentiation and that this binding drives EID1 degradation. The S249/T252 phosphorylation located in the RBN disrupts the association between EID1 and RB (Ahlander et al., 2008; Hassler et al., 2007; Khidr and Chen, 2006). Nevertheless, molecular modeling predictions proposed that the RBN displays a similar structure to that of the RBC, which interacts with E2F (Gubern et al., 2016), thus suggesting a potential additional surface in RB for E2F interaction. The high degree of similarity of the RBN with the two structured domains of the pocket domain suggests that RB evolved through duplication event (Hassler et al., 2007).

1.3 The role of RB proteins in the cell cycle

The cell cycle is an ordered set of events that leads to cell division. During the cycle, cells proceed through a series of precisely timed and closely regulated stages of growth, DNA replication, and division that produces two identical daughter cells. The cell spends most of its time in what is called G1, where it grows and prepares itself for the S phase, in which the cell replicates its chromosomes. Once an extra set of all the genetic material has been completed, the cell moves into the G2 stage, where the chromatin starts to condense. Finally, the cell undergoes Mitosis (M) and completes its division into two daughter cells. Cell cycle progression harbors a high degree of complexity and occurs only under favorable conditions in order to avoid the accumulation of replication errors within the genome of the daughter cells. Cell cycle control involves the participation of key regulatory proteins, including the RB pocket protein family, E2Fs, Cyclin-CDK

complexes, CDK inhibitor (CKI) proteins, and chromatin-remodeling and modifying complexes.

1.3.1 E2F transcription factors

The most documented activity of RB proteins is the regulation of cell cycle progression through its interaction with E2Fs (Dick and Rubin, 2013b). The complex mechanism of E2F-dependent gene regulation controls cell entry into S phase and the initiation of DNA replication. RB-E2F binding blocks the recruitment of transcriptional activators and acts as an interaction platform for repressors, thereby inhibiting the expression of E2F-dependent genes and, hence, blocking the transition from G1 to S phase (Chinnam and Goodrich, 2011; Van Den Heuvel and Dyson, 2008).

The E2F family of transcription factors is composed of 8 members (E2F1-8), often subdivided into activators and repressors (DeGregori and Johnson, 2012; Trimarchi and Lees, 2002). Although cell cycle transcriptional activators and repressors have opposing functions, E2F activators and repressors have similar structural domains. Most of them present a heterodimerization domain that allows them to bind to transcription factor DP (Dimerization Partner). The interaction with DP offers a second DNA binding site, which enhances the stability of E2F binding. Most E2Fs have an RB pocket protein binding site, allowing binding between E2F and RB when RB proteins are hypophosphorylated.

E2Fs 1–3a, the transcriptional activators, interact with RB and are periodically expressed during the cell cycle, peaking at the G1–S phase transition. E2F3b (another distinct transcript encoded in the

same locus as E2F3a), E2F4 and E2F5 are canonical transcriptional repressors that remain constitutively expressed throughout all phases of the cell cycle and are generally bound to p107 and p130. Interestingly, E2F6-8 function as atypical repressors independently of pocket protein association and their expression peaks in late S phase. E2F6 has been shown to inhibit transcription through association with Polycomb group (PcG) proteins (Attwooll et al., 2004; Ogawa et al., 2002). E2F1–E2F6 conserve dimerization domains with the DP family to form DNA-binding heterodimers. However, E2F7-8 lack the DP-binding domain but contain an E2F DNA-binding domain and are able to form homodimers and heterodimers (Van Den Heuvel and Dyson, 2008; Kent and Leone, 2019). Of note, high E2F expression in tumors has been linked to poor prognosis in cancer (Liu and Hu, 2020).

E2F1 is the best characterized member of the E2F family and it is frequently altered in human cancers (Hollern et al., 2019; McNair et al., 2018; Roelofs et al., 2020). Transcriptional regulation of cell cycle genes is not the only important process regulated by E2F1. It has also been shown to regulate apoptosis and senescence and to protect genome stability after DNA double-strand breaks. Furthermore, it is involved in the regulation of metabolism both under normal and pathological conditions (Denechaud et al., 2017; Dimri et al., 2000; Polager and Ginsberg, 2008).

1.3.2 Cyclin-CDK complexes

The cell cycle machinery has two essential protein families, namely Cyclin-dependent kinases (CDKs) and Cyclins. The formation of Cyclin-CDK complexes is necessary for the kinases to

be active and to orchestrate the advance of the cell through the different phases of the cell cycle. The main targets of these Cyclin-CDK complexes are RB pocket proteins, whose activity is inhibited by phosphorylation throughout the cell cycle.

In mammalian cells, Cyclins D and E mediate progression through G1/S phases. Upon mitogenic signaling, D-type cyclins assemble with CDK4 or CDK6 in early G1. However, Cyclin E reaches maximum expression at G1/S, followed by an increase in Cyclin A in the S phase. Both Cyclin E and A form protein complexes with CDK2, and Cyclin A can also interact with CDK1 (Ludlow et al., 1993). At the G2/M transition, Cyclin B levels peak, resulting in an activation of the Cyclin B-CDK1 complex and allowing the cell to advance towards mitosis. This oscillation in Cyclin expression and CDK activity allows the coordinated regulation of RB pocket proteins and, hence, the proper progression of the cell cycle (Giacinti and Giordano, 2006).

CDK levels remain relatively steady throughout the cell cycle and most regulation is post-translational. CDK activity is regulated by complex formation with Cyclin subunits, by phosphorylation, and by binding of CDK inhibitory proteins (CKI). The activity of CKI is a very important regulatory mechanism for pocket proteins throughout the cell cycle. CKI act directly upstream of CDKs to block their catalytic activity. CKI are grouped into two families: the CIP/KIP family (p21CIP1, p27KIP1 and p57KIP2) and the INK4 family (p16INK4a, p15INK4b, p18INK4c, and p19INK4d) (Besson et al., 2008). CIP/KIP members bind both Cyclin and CDK and disable its kinase activity. Therefore, the members of this family can inhibit any

Cyclin-CDK complex during the G1 phase. By contrast, INK4 members can bind only CDK4 and CDK6 in association with D-type Cyclins.

1.3.3 Role of RB proteins in cell cycle regulation

RB pocket proteins are cell cycle regulators that restrict the transcription of cell cycle genes, mainly through the control of the transcription factor E2F. The three RB pocket proteins regulate the expression of E2F-dependent genes. However, p107, RB and p130 perform their function differently by associating with protein complexes that vary throughout the cell cycle.

On the one hand, RB proteins inhibit the expression of E2F-regulated genes in two ways (Dagnino et al., 1995; Stevaux and Dyson, 2002), namely by directly binding and blocking the activation domain of E2F proteins or by recruiting transcriptional repressors., pocket proteins associate with chromatin remodeling factors through their LXCXE binding motif and recruit them to E2F-dependent promoters. RB proteins interact with chromatin remodeling enzymes such as SWI/SNF (BRG and BRM), histone deacetylases (HDAC1, 2 and 3), histone methyltransferases (Suv39h1 and 2) (Vandel et al., 2001), and Polycomb group proteins, among others (Dahiya et al., 2001). These interactions allow RB proteins to recruit and stabilize transcription repression complexes, thereby limiting the expression of genes necessary for cell proliferation.

On the other hand, p107 and p130 form a complex called DREAM that inhibit the activity of some of the E2F transcription factors. In turn, this DREAM complex is composed of E2F4/5, DP1/2,

p130/p107 and multi-vulval class B (MuvB). The MuvB complex is highly conserved throughout evolution. In mammals, this complex comprises the proteins LIN9, LIN37, LIN52, LIN54, and RBAP48 and its composition does not change during the different stages of the cell cycle. However, when it is part of the DREAM complex, MuvB acts as a transcriptional repressor in G0 and G1. In contrast, when not part of DREAM, MuvB acts as a transcriptional activator in S, G2 and M (Fischer and Müller, 2017) .

Multiple protein contacts allow pocket proteins to recruit corepressors or activators and chromatin remodelers with different pervasive effects on chromatin structure, including entire chromosomes. Although RB can influence gene transcription on a very broad scale, the role of pocket proteins in repressing chromatin during cell cycle progression is unknown (Talluri and Dick, 2012).

As the cell cycle progresses, RB pocket proteins are progressively phosphorylated by CDKs, which inhibit their transcriptional repressive function and allows the cell to advance through the cell cycle (Narasimha et al., 2014). These proteins have been shown commonly as the key negative regulator in the transition from G1 to S phase; however, they have also been described as players in other cell cycle stages (Henley and Dick, 2012). RB pocket proteins are found in quiescent cells or G0 phase, during G1 phase and at the end of G1, where they regulate G1/S checkpoint.

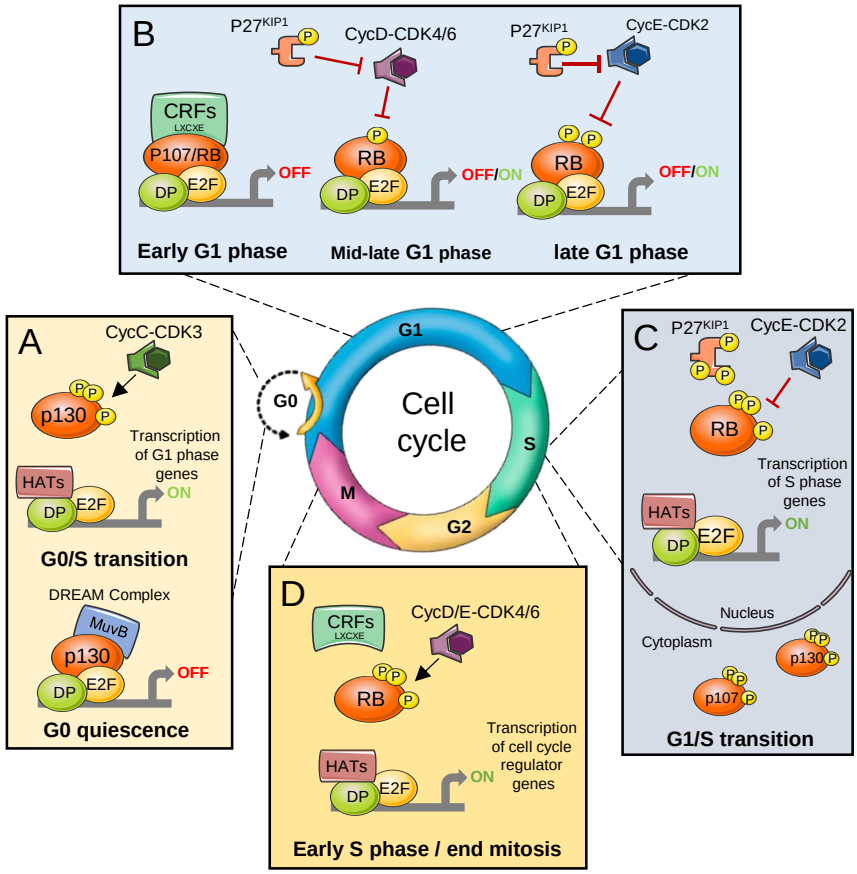

Figure 3. Cell cycle regulation by the RB pocket proteins. A. In G0, p130 and DREAM complex repress E2F target transcription. Upon mitogenic signals, the phosphorylation and inhibition of p130 by Cyclin C-CDK3 allows the cell to enter the cell cycle. **B.** As cells progress into G1, p107 and RB-E2F complexes replace p130. Chromatin remodeling factors (CRFs), such as histone deacetylases (HDACs), are recruited to the E2F promoters and mediate alterations at the chromatin, repressing E2F-mediated gene expression. RB phosphorylation is increased gradually by an increase on CDK activity as G1 phase progresses. **C.** At the G1/S transition, Cyclin-CDKs phosphorylate the RB pocket proteins, forcing their dissociation from E2F/DP heterodimers and allowing the transcription of E2F target genes through the S phase. The repressive heterochromatin state present in G1 are reversed by the recruitment of histone acetyltransferases (HATs). p130 and 107 protein complexes are exported to the cytoplasm. **D.** RB pocket proteins are

inactivated at the onset of the S-phase, remaining in this non-active state until their dephosphorylation at the end of mitosis.

The cells that have exited the cell cycle are in a quiescence state or G0 phase, which can be either temporary (quiescence) or permanent (terminal differentiation or senescence). In G0, RB pocket proteins remain in an unphosphorylated state. p107 is not expressed and RB expression is low, while p130 is the most expressed pocket protein and binds mostly to E2F4 to form the DREAM complex (Guiley et al., 2015). p130 contributes to cellular quiescence by repressing the transcription of RNA polymerase I and III, resulting in the reduction of rRNA and tRNA (Ciarmatori et al., 2001; Scott et al., 2001; Sun et al., 2007). Pocket proteins may also control the transition from G0 to G1 phase (Cobrinik, 2005). Under mitogenic stimuli, cells are prompted to enter the cell cycle and Cyclin C-CDK3 complexes phosphorylate p130 or RB proteins, thereby relieving this transcriptional repression, which in turn increases the RNA content and allows the G0–G1 transition. Therefore, entry into G1 is regulated analogously to entry into S phase, but it involves a different combination of Cyclin-CDK (Ren and Rollins, 2004) (Figure 3 A).

During G1 phase, the prevalence of p130-E2F4 complexes decreases, coinciding with an increase in p107 and RB expression. RB-E2F is the most predominant regulatory complex in the promoters that respond to E2F in G1 phase (Flemington et al., 1993; Helin et al., 1993; Hiebert et al., 1992b) (Figure 3 B). In the early G1 phase, the expression levels of p27KIP1 are high enough to inhibit Cyclin-CDK complexes. CDK kinase activity remains low and pocket proteins are in their hypo-phosphorylated form, thus

preventing the expression of E2F-dependent genes and the initiation of DNA synthesis (Sherr and Roberts, 1999). Some E2F target genes subject to this regulation are the E2F activators, cell cycle regulators such as cyclins A and E, and RB and p107 (Mulligan et al., 1998; Takahashi et al., 2000; Wells et al., 2000). The E2F target genes include constituents of the replication machinery such as DNA pol α and the proliferating cell nuclear antigen (PCNA), along with enzymes involved in nucleotide biosynthesis (Dagnino et al., 1995; Lavia and Jansen-Dürr, 1999).

Throughout G1 phase, pocket proteins are active and CDK activity is inhibited to prevent the cell from entering the S phase and replicating DNA prematurely. In this phase, the main repressor of CDK activity is p27KIP1. By inhibiting CDK activity, p27KIP1 keeps pocket proteins active in G1 (Sherr and Roberts, 1999). However, the pocket proteins themselves also contribute to this regulation. Like p27KIP1, p107 and p130 have a spacer region between pockets A and B and a domain at the N-terminus that allow them to bind and inhibit Cyclin A/E-CDK2 complexes (Lacy and Whyte, 1997; Woo et al., 1997). Unlike the p130 and p107 proteins, RB does not have a CDK inhibition domain (Castaño et al., 1998). However, RB can also repress Cyclin-CDK activity through the regulation of p27KIP1 itself. RB prevents the degradation of p27KIP1 by behaving as a protein contact platform that binds APC-Cdh1 and Skp2, which directs Skp2 for ubiquitin-mediated degradation (Binné et al., 2007). Furthermore, the binding of Skp2 to RB hinders its association with p27KIP1 (Wang et al., 2010). Skp2 is an adapter protein necessary for the degradation of p27KIP1 and

therefore its degradation increases the stability of p27KIP1 (Ji et al., 2004). Other studies have also related p107 to the degradation of Skp2 and the inhibition of CDK2 (Rodier et al., 2005; Sangwan et al., 2012).

Late G1 and entry into S-phase is controlled by the key G1/S checkpoint, which is dysregulated in most cancer cells (Gordon et al., 2018; Massagué, 2004). Pocket proteins, especially RB, play a key role in this regulatory mechanism (McNair et al., 2018). Of note, the central event in this restriction point is the separation of hyper-phosphorylated RB from E2F (Yao et al., 2008). The G1/S checkpoint is regulated by various feedback loops, which increase CDK activity and trigger an increase in the phosphorylation of pocket proteins, as well as proteolytic degradation of CDK inhibitors such as p27KIP1.

Towards the end of G1, pocket proteins are partially phosphorylated and inhibited, thereby allowing limited transcription of E2F-dependent genes, and slightly stimulating Cyclin E expression. Cyclin E-CDK2 complexes increases phosphorylation of RB, thereby leaving more E2F free and further increasing Cyclin E expression (Mittnacht, 1998b). At this point, inhibition by p27KIP1 is the most crucial obstacle to the full activation of this kinase complex (Sherr and Roberts, 1999). Finally, increasing the active Cyclin E-CDK2 complex causes phosphorylation of p27KIP1, resulting in its targeting for degradation, thereby allowing complete kinase activation and entry into S phase (Figure 3C).

When cells begin to progress through S-phase, Cyclin-CDKs phosphorylate pocket proteins, thus driving its separation from

E2F/DP heterodimers and allowing the transcription of E2F target genes through the S-phase. The repressive heterochromatin changes present in G1 are reversed by the recruitment of HATs, which acetylate histones H3 and H4, allowing the transcription of the genes required to complete the S-phase (Frolov and Dyson, 2004). p130 and 107 proteins and repressor E2F-DP complexes are exported to the cytoplasm (Chestukhin et al., 2002; Verona et al., 1997) (Figure 3C).

RB pocket proteins are inactivated at the onset of the S-phase and they remain in this non-active state until their dephosphorylation at the end of mitosis (Henley and Dick, 2012) (Figure 3D).

However, several studies demonstrate the resistance of some RB activity to Cyclin-CDK phosphorylation in the S-phase (Cecchini and Dick, 2011). Phosphorylated RB binds to E2F1 trough a specific domain to repress the transcription of pro-apoptotic target genes. This regulation is independent to another cell cycle regulatory functions of E2F. Therefore, the apoptotic function of E2F1 is suppressed while the cell cycle is active (Dick and Dyson, 2003). Furthermore, when DNA damage occurs, the cell cycle is halted in order to allow cells to repair the damage before continuing with DNA replication, and RB activation also plays a key role in regulating this mechanism. After DNA damage, RB is dephosphorylated to inhibit transcription, thereby stopping DNA replication (Frolov and Dyson, 2004; Markham et al., 2006; Ovejero et al., 2020).

p38 MAPK PATHWAY

Cells need to quickly sense, respond, and adapt to changes in their microenvironment to survive and maintain homeostasis. One of the

most important signaling cascades activated in response to environmental and intracellular stress is the p38 signaling pathway, which comprises members of the Mitogen-Activated Protein Kinase (MAPK) family. In eukaryotic cells, MAPK cascades show a high degree of conservation throughout evolution since they play a key role in the regulation of several aspects of the cellular physiology by converting extracellular signals in a broad range of cellular responses.

Three major MAPK cascades have been defined in mammalian cells. The ERK1/2 pathway is activated by growth factors and mitogens and it promotes cell division and differentiation. In contrast, the Jun N-terminal kinase (JNK) and p38 pathways are activated typically by environmental and genotoxic stresses and are thus also called as Stress-Activated Protein Kinases or SAPKs. The JNK and p38 signaling pathways show a certain degree of functional redundancy. However, the crosstalk between them and their implications in cell physiology regulation depends on the cellular type, tissue, and organism.

The MAPK pathways are organized in a three-tiered module of protein kinases. On top, MAPK kinase kinases (MKKKs or MAP3Ks) are activated downstream from cell surface receptors: Once activated, the MAP3Ks directly phosphorylate and activate MAPK Kinases (MKKs, MEKs, or MAP2Ks), which in turn phosphorylate and activate MAPKs at the bottom. Upon activation, MAPKs phosphorylate specific substrates on serine or threonine residues followed by a proline, leading to modulation of diverse physiological processes (Cargnello and Roux, 2011) (Figure 4).

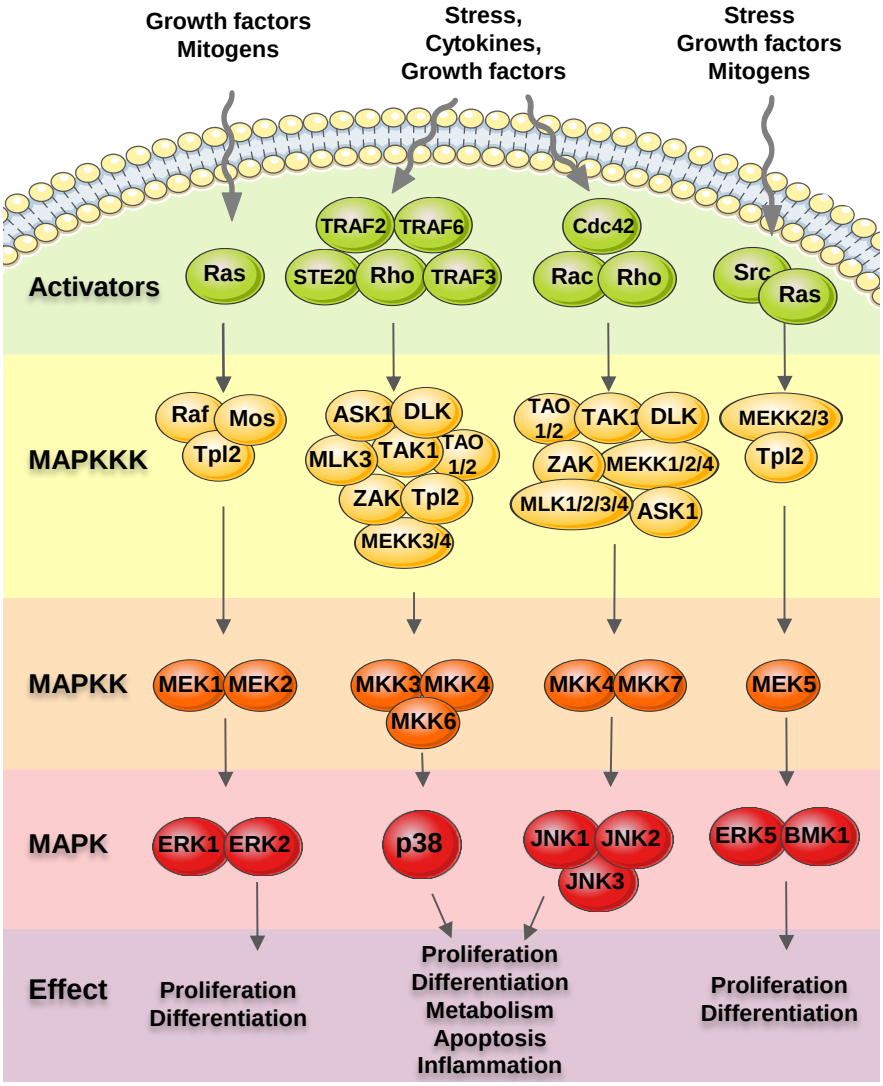

Figure 4. Overview of the MAPK pathways. ERK, JNK, and p38 signaling pathways integrate different types of stimuli to trigger diverse cellular responses. MAPK signaling cascades are organized into three modules. MAPKs are phosphorylated and activated by MAPK-kinases (MAPKKs), which in turn are phosphorylated by MAPKK-kinases (MAPKKKs). MAPKKKs are activated by interaction with the family of small GTPases or other protein kinases, associating the MAPK module (with cytosolic and nuclear functions) to cell surface receptors or external stimuli.

The p38 MAPK family includes four distinct isoforms encoded by different genes: p38α (MAPK14), which comprises different splicing variants: p38β (MAPK11); p38γ (MAPK12); and p38δ (MAPK13) (Cuenda and Rousseau, 2007; Cuenda and Sanz-Ezquerro, 2017). p38 MAPK family members are divided in two groups based on their similarity and tissue distribution. p38α and p38β are ubiquitously expressed, while p38γ and p38δ are differentially expressed depending on the tissue type. Remarkably, p38α is the best characterized isoform because of its high abundancy in most of cell types and, thus, high proportion of the published literature refers to this isoform. Some studies have described the functional redundancy between the p38 family members when they were genetically deleted, observing that the lack of one isoform can usually be complemented by the function of the other isoforms (Sabio et al., 2005). In this thesis we focus on the study of p38α.

2.1 Activation and regulation of p38 MAPK

The p38 MAPK pathway is activated by a wide range of stress types from external and intracellular stresses to pathologies such as infection or cancer, as well as by non-damaging processes, such as cell differentiation, but that cause a certain degree of stress. These diverse stress stimuli include changes in osmolarity, heat shock, hypoxia, oxidative stress, genotoxic and DNA-damaging agents (UV and γ-irradiation, cisplatin, doxorubicin etc.), inflammatory cytokines, PAMPs (pathogen-associated molecular patterns), and DAMPs (danger-associated molecular patterns)(Cuadrado and Nebreda, 2010; Han et al., 2020; Hotamisligil and Davis, 2016). After detecting environmental stress, the cell deploys a complex signaling

cascade upstream of the p38 MAPK pathway, where the activation of MAPKKKs involves phosphorylation by STE20 family kinases and association with small GTP-binding proteins of the Rho family, together with ubiquitination-based mechanisms. Due to these regulatory mechanisms, cells are able to respond to many different external signals, facilitating both signal fine-tuning and cross-talk with other pathways (Cuevas et al., 2007). A wide variety of MAP3Ks have been shown to orchestrate p38 activation, including ASK1 (apoptosis signal-regulating kinase 1), DLK1 (dual-leucine-zipper-bearing kinase 1), TAK1 (transforming growth factor β-activated kinase 1), TAO (thousand-and-one amino acid) 1 and 2, TPL2 (tumor progression loci 2), MLK3 (mixed-lineage kinase 3), MEKK (MAPK/ERK kinase kinase) 3 and MEKK4, and ZAK1 (leucine zipper and sterile-α motif kinase 1). Consequently, the signaling events that take place in MAP3K are rather complex. Indeed, the diversity of MAP3Ks and their regulation provide cells with a plethora of mechanisms that respond to diverse stimuli (Cuevas et al., 2007) (Figure 4).

Activation of MAP2K occurs upon phosphorylation of two conserved Ser and Thr residues by diverse MAP3Ks. The activation of p38 by MAP2K depends on the cell type and the stimulus (Cuadrado and Nebreda, 2010). The MAP2Ks responsible for phosphorylating p38 are MKK3 and MKK6. The latter is able to phosphorylate all the p38 family members, whereas the former activates the α, γ, and δ isoforms, but not β. Both MAP2Ks are highly specific for p38 MAPKs (Cuenda and Rousseau 2007; Remy et al. 2010). Exceptionally, ultraviolet radiation has also been shown to

activate p38 through JNK activators such as MKK4 (Zhang and Bowden, 2012).

The full activation of p38 requires the dual phosphorylation of Thr and Tyrosine (Tyr) on the Thr-Gly-Tyr motif that is a flexible motif located on the activation loop found on the kinase subdomain VIII (Doza et al., 1995). Dual phosphorylation at these two residues alters the folding of p38 by stabilizing the activation loop in a more open conformation and causing rotation between the two major lobules, which allows for substrate recognition and increases the activity of the kinase (Coulthard et al., 2009).

A huge number of substrates are phosphorylated by p38 to regulate broad range physiological mechanisms. So far a complete characterization of the p38 phospho-proteome has not been performed (Trempolec et al., 2013), but more than 100 proteins have been identified as substrates of p38α (Han et al., 2020). Although, several studies have reported p38 phosphorylation sites non-proline-directed (Reynolds et al., 2000), most known p38 substrates are phosphorylated at Serine or Threonine sites followed by a Proline residue. Of note, this Ser/Thr-Pro motif is particularly common in most mammalian proteins, therefore specific mechanisms may operate to ensure proper MAPK substrate recognition and signaling exclusivity. Some p38 targets have a common region of interaction called the D domain, composed of several basic residues that interact with specific acidic residues of p38 (Biondi and Nebreda, 2003; Tanoue et al., 2000, 2001). Substrate concentration, availability, interacting partners or subcellular localization are other factors that influence substrate specificity.

p38 phosphorylates both cytoplasmic and nuclear proteins. Many of these proteins susceptible to phosphorylation by p38 are involved in transcription, chromatin remodeling, apoptosis, endocytosis, mRNA stability, translation, protein degradation and localization, cell cycle, endocytosis, metabolism, cell migration or cytoskeleton dynamics (Canovas and Nebreda, 2021). Upon activation, p38 is translocated from the cytoplasm to the nucleus to target diverse proteins including transcription factors, chromatin remodeling enzymes, protein kinases and RNA-binding proteins. The molecular mechanism by which p38 is translocated inside the nucleus is not fully understood as MAPKs have neither nuclear localization nor nuclear export motifs. However, several studies in yeast revealed that the p38 homolog known as Hog1 required phosphorylation at the Thr-Gly-Tyr activation motif in order to translocate to the nucleus. (Ferrigno and Silver, 1999; Ferrigno et al., 1998). Subsequent studies in mammalian cells showed that p38 also requires the phosphorylation of the Thr-Gly-Tyr sequence for its translocation inside the nucleus (Gong et al., 2010). It is then transported to the nucleus through the association with β-like importins and its transport is mediated by microtubules and dyneins (Ferrigno and Silver, 1999; Ferrigno et al., 1998). Just like Hog1 nuclear export in yeast, p38 also requires dephosphorylation, which takes place in association with MK2, a known p38 substrate (Ben-Levy et al., 1998).

The substrates of p38 are highly heterogeneous, ranging from transcription factors, DNA binding proteins and structural protein to

regulatory proteins and kinases, which spread the signaling pathway regulating different cellular processes.

Finally, the mechanisms that regulate the termination of p38 signaling are key to the maintenance of homeostasis and sustained hyper-activation of p38 is usually detrimental to the cell. p38 signaling ends with its inactivation through the removal of the phosphates from the Thr-Gly-Tyr motif (Ferreiro et al., 2010a; Ferrigno et al., 1998). Generic phosphatases such as PP2A and PP2C (e.g., Wip1) have been described to remove the Thr phosphate on the activation motif. The Tyr residue is dephosphorylated by STEP (striatal enriched tyrosine phosphatase), and HePTP (haematopoietic protein tyrosine phosphatase). Both thr and tyr phosphatases generate monophosphorylated p38 variants that are up to 20 times less active (Zhang et al., 2008). Stress-activated p38 upregulates the gene expression of several members of the DUSP/MKP (dual-specificity phosphatases/MAPK phosphatases) family (Ferreiro et al., 2010a). DUSP/MKPs interact with p38 through specific docking domains and remove phosphate groups of both phosphotyrosine and phosphothreonine residues located in the activation motif. It should be noted that several reports show that stress signals known to activate MAPK signaling orchestrate the up-regulation of MPK in order to limit the extent of MAPK activation (Owens and Keyse, 2007). DUSP activation generate a negative feedback loop that can lead to asynchronous fluctuations and cellular heterogeneity in p38 activity. This regulatory process is crucial for pro-inflammatory gene expression (Tomida et al., 2015) and stress-induced cell death (Miura et al., 2018).

Although p38 activity is regulated mostly by phosphorylation and dephosphorylation events, additional regulatory mechanisms are involved in the control of the pathway, including the association with scaffolding proteins, proteolysis, other posttranslational modifications such as acetylation, and subcellular compartmentalization of p38 pathway components (Cuadrado and Nebreda, 2010).

2.2 Physiological and cellular functions of p38

Cellular responses are largely determined by the intensity and dynamics of p38 pathway signaling (Purvis and Lahav, 2013). The recent development of KTR (Kinase Translocation Reporter) technology has allowed the study of the dynamics of ERK, JNK and p38 MAPK activity simultaneously in single living cells (Regot et al., 2014). In the same way that p38 can be activated by a wide variety of stimuli and regulate the activity of different substrates, it also triggers many cell responses. Deregulation of the p38 pathway is involved in the loss of cellular homeostasis, resulting in the development of a range of pathologies, such as cancer and metastasis, atherosclerosis, inflammatory states, cardiovascular dysfunctions and Alzheimer's disease, among others (Canovas and Nebreda, 2021; Cuenda and Rousseau, 2007). To maintain cellular homeostasis, p38 not only orchestrates cellular responses to different environmental and genotoxic stresses, but also regulates a wide range of biological processes, ranging from immune responses and inflammation to proliferation, differentiation, and migration.

Many of these biological processes regulated by p38 have been clarified with the study of p38 knockout mice. p38α knockout mice do not survive during embryonic development due to placental morphological defects (Mudgett et al., 2000), indicating the high biological relevance of this isoform (Adams et al., 2000). p38β, p38γ and p38δ knockout mice do not show defective embryonic development. However, p38δ knockout mice exhibit greater glucose tolerance and increased insulin exocytosis through PDK1 regulation. The p38δ isoform therefore plays a key role in the regulation of glucose homeostasis (Cuenda and Nebreda, 2009; Sumara et al., 2009). In addition, p38δ-deficient mice are resistant to the development of TPA (12-O-Tetradecanoylphorbol-13-acetate) induced skin papilloma (Schindler et al., 2009). This observation is consistent with the key role of p38δ in the differentiation and survival of keratinocytic cells (Efimova et al., 2004).

Interestingly, these physiological responses depend on the nature of the signal that activates p38 and the cellular context. For instance, in a healthy physiological context, p38 shows antitumor properties; however, in a carcinogenic context, it favors tumor development and promotes metastasis (Martínez-Limón et al., 2020). Similarly, p38 activates cell type-specific anti-inflammatory processes that are important in inhibiting inflammatory responses and preventing tissue damage (Arthur and Ley, 2013). On the contrary, the activation of p38 has been involved in the activation of the immune response under pathogenic stimuli or may even be implicated in diseases such as rheumatoid arthritis (Gupta and Nebreda, 2015). The original motivation to treat cancer and inflammatory diseases led to the

production of potent p38 inhibitors with positive pharmacokinetic properties. These inhibitors are in different phases of clinical and preclinical studies to treat various diseases, ranging from cancer, inflammatory diseases and Alzheimer's to even Covid19 (Canovas and Nebreda, 2021).

It should be noted that p38 regulated the complex physiological processes through the coordination of essential cellular functions like the decision to survive, the regulation of gene expression and the control of cell cycle (Kyriakis and Avruch, 2012).

2.2.1 Control of cell survival by p38

Cellular survival/death decisions in response to diverse stress stimuli are an essential cellular function. p38 activation plays a dual role in these decisions, as its activation is associated with cell survival or death depending on the duration of stimulus, as well as on cell type. Low p38 activation has been linked to a cell survival response, whereas sustained activation has an effect on apoptosis, senescence, and terminal cell differentiation (Puri et al., 2000).

p38 is involved in many cell viability processes, including autophagy. MK2 and p38 phosphorylate key autophagy activators such as lysosomal LAMP2A, Beclin-1 and ULK1 (Li et al., 2017; Slobodnyuk et al., 2019; Wei et al., 2015). In addition, p38 can promote pro-survival processes in response to metabolic alterations by activating of the transcription coadaptor KAP1 (also known as TRIM28), which decrease mitochondrial oxidative phosphorylation, by increasing β-oxidation of fatty acids (Cheng et al., 2016) and by limiting the stress of the endoplasmic reticulum (Soustek et al.,

2018). In addition, p38 controls other survival mechanisms modulating alternative splicing through the phosphorylation of hnRNPA1 by MNK1/2 (Guil et al., 2006) or the phosphorylation of SKIIP by p38 (Carbonell et al., 2019). There is evidence that p38 regulates NELFE105 and RBM7 through MK2 phosphorylation (Bugai et al., 2019), thereby allowing a RNA polymerase II transcriptional response, including genes required for telomere maintenance or DNA repair. p38 also facilitates cell division and survival by inducing anti-apoptotic inflammatory signals or by indirect regulation of survival genes (Thornton and Rincon, 2009)

In contrast, higher and sustained activity of the p38 pathway generally induces cell death. p38 triggers apoptosis through transcriptional and post-transcriptional mechanisms. It phosphorylates and activates some pro-apoptotic proteins of the Bcl-2 family such as BimEL (Cai et al., 2006). At a transcriptional level, p38 up-regulates several apoptotic genes, such as FOXO3a transcription factor. This gene up-regulation, together with the later induction of BimEL expression, has been established as a novel apoptotic mechanism (Cai and Xia, 2008). In addition, p38 activates and stabilizes the p53 protein which in turn induces the expression of pro-apoptotic Bcl-2 proteins and simultaneously represses anti-apoptotic proteins (Phong et al., 2010). p38α also sensitizes cells to apoptosis via both the up-regulation of proapoptotic proteins (as Bax and Fas) and down-regulation of survival pathways. Moreover, p38 is a strong activator of pathogen-induced necrosis triggered by alterations of the mitochondrial membrane (Gräb and Rybniker, 2019).

2.2.2 Regulation of gene expression by p38

The study of whole genome in mouse embryonic fibroblasts (MEFs), comparing wild- type versus p38 K/O, have revealed that p38 coordinates the expression of more than 60% of the early-induced genes upon different stress stimuli. In addition, transcriptome analysis shows that among the genes induced by p38, transcription factors are abundant. This observation thus indicates that p38 regulates a wide program of gene expression for long-term adaptation to stress (Amat et al., 2019; Ferreiro et al., 2010a).

In response to stress, the induction of p38-dependent gene expression is achieved by regulation of mRNA biogenesis. p38 is recruited to stress-responsive loci by binding to specific transcription factors, and it allows the recruitment of the RNA Pol II machinery to induce transcription initiation (Chow and Davis, 2006; Edmunds and Mahadevan, 2004; Ferreiro et al., 2010b). Moreover, p38 phosphorylates various transcription factors and chromatin-remodeling enzymes, regulating its stability, localization or its interaction with DNA and other regulatory proteins (Han et al., 2020). For instance, p38 phosphorylates BAF60c, a subunit of the SWI/SNF complex, that enables chromatin remodeling and transcriptional activation of muscle-specific promoters (Forcales et al., 2012). The transcriptions factors targeted by p38 include TF1, ATF2, ATF6, SAP1, CHOP, p53, MEF2C, MEF2D and MEF2A (Cuadrado and Nebreda, 2010). Moreover, several kinases downstream of p38 like MSK1/2 phosphorylate other transcription factors such as CREB, ATF1, NFκB, STAT1 and STAT3 (Indovina et al., 2013; Wiggin et al., 2002; Zhang et al., 2001, 2004), as well as the nucleosomal

proteins histone H3 and high mobility-group 14 (HMG-14) (Arthur, 2008).

In addition to transcriptional processes, p38 also regulates mRNA stability and translation (Cargnello and Roux, 2011; Tiedje et al., 2014), through MK2 and MK3 kinases activated downstream of p38 (Sandler and Stoecklin, 2008). p38 also acts on some mRNAs through the regulation of the RNA binding protein HuR (Farooq et al., 2009; Gaestel, 2016; Lafarga et al., 2009). Finally, p38 activation regulates protein synthesis, through kinase MNK, which catalyzes the phosphorylation of eukaryotic initiation factor 4E (EIF4E) (Lawson et al., 2013; Reyskens and Arthur, 2016).

2.2.3 Regulation of cell cycle progression by p38 MAPK

The ability of p38 to regulate cell proliferation is highly relevant for the maintenance of cell homeostasis. As mentioned above, the decision to proliferate or trigger cell cycle arrest depends on the duration and intensity of p38 signaling, as well as tissue specificity.

p38 can favor the proliferation of certain cell types, such as hematopoietic cells and some cancer cell lines (Wagner and Nebreda, 2009). In the context of cancer, this kinase was originally described as a tumor suppressor, but there are several publications supporting its function as tumor promoter. Despite extensive studies, a clear picture of the role of p38 as a regulator of the cell cycle in tumorigenesis is still missing (Martínez-Limón et al., 2020).

Activation of the p38 pathway by stress stimuli involves arresting cell proliferation to trigger the appropriate adaptive response and allow for the repair of any stress-induced damage (Duch et al., 2012).

p38 regulates cell cycle progression through checkpoints activation in both G2/M and G1/S phases of the cell cycle (Barnum and O'Connell, 2014).

Regarding the regulation exerted by p38 in the G2/M transition, it has been described mostly in the context of the cellular response to DNA damage. DNA damage stimuli are detected by the ATM/ATR protein kinases, which trigger the activation of p38 via MKK3/6 (Raman et al., 2007). p38 activation stimulate p53 and promotes the transcription of GADD45α, which binds to the Cyclin B-CDK1 complex to halt the cell cycle in G2/M phase (Jin et al., 2002). Moreover, p38 inhibits Cdc25B phosphatase activity through MK2, also resulting in a delay in G2/M phase, independently of p53 activity (Cannell et al., 2015; Donzelli and Draetta, 2003; Reinhardt et al., 2007). In addition, in yeast it has also been shown that Hog1, the homologue of p38, delays M phase exit when cells are stressed during metaphase (Tognetti et al., 2020).

Exposure to diverse stress stimuli that activate p38 MAPK pathway signaling also triggers the stimulation of the G1/S checkpoint. Activation of p38 leads the downregulation of Cyclin D1, which is crucial for S phase transition. Cyclin D1 downregulation is reached by down-regulating its expression (Bollaert et al., 2019) and promoting its ubiquitin-dependent degradation (Thoms et al., 2007). Moreover, p38 is able to activate p53 tumor suppressor both directly or indirectly through HBP1 (Kishi et al., 2001), which promotes the upregulation of cell cycle negative modulators such as p21CIP1/WAF1, GADD45 and 14-3-3σ proteins (Ho and Benchimol, 2003; Stramucci et al., 2018).

In addition, p38 also promotes G1 / S cell cycle arrest by directly or indirectly activating the CKI p21CIP1 (V. Lafarga et al., 2009) and p27KIP1 (Swat et al., 2009) in response to different stimuli. In contrast, p57KIP2 protein levels, intracellular location, or stability remain constant under stress stimuli. However, phosphorylation of p57KIP2 at T143 by p38 increases its affinity towards CDK2 and inhibits it more effectively, resulting in a transient delay of the cell cycle in the G1 phase. Cells deficient in p38 or p57KIP2 fail to properly arrest at G1 and display a reduction of viability under stress stimuli. Therefore, the phosphorylation of p57 by p38, which inhibits CDK activity, constitutes an important mechanism for cell survival under various stresses (Joaquin et al., 2012).

2.2.4 Regulation of RB by p38

As mentioned above, under stress conditions, p38 regulates key components of the cell cycle machinery, such as CDK inhibitors, p21CIP1, p27KIP1, and p57KIP2. The complex regulation of the cell cycle upon stress and the fact that p57KIP2 knockout cells still show a certain delay in cell cycle indicates that these G1 regulatory mechanisms are not the only ones present in the cell.

An essential mechanism of regulation of the cell cycle under stress stimuli by p38 is the inhibition of the transcription of E2F-dependent genes necessary for the progression of the G1 to S phase of the cell cycle. p38 phosphorylates RB at S249 / T252 residues (Figure 5A), inhibiting the expression of E2F-regulated genes (Gubern et al. 2016). The *in-silico* predictions showed a marked increase in affinity when these residues located in the N-terminal region of RB were

phosphorylated. Based on these modeling predictions, *in vivo* and *in vitro* experiments demonstrated that, unlike phosphorylations at the C-terminus and pocket region sites, which disrupt their interaction with E2F, phosphorylation at these N-terminus S249 / T252 sites increases this binding of RB-E2F. The phosphorylated RB at S249 / T252 sites by p38 upon stress stimuli or the mutation of these two sites in phosphomimetic residues, such as glutamic acid (RB S249E / T252E), favored interaction between RB and E2F. In contrast, the mutation of S249 and T252 in non-phosphorylatable residues, such as alanine (RB S249A / T252A), desensitized the regulation of RB by p38. Phosphorylated RB at S249 / T252 sites and the phosphomimetic mutant make RB unresponsive to its inhibition by CDK and improve its affinity for the E2F transcription factor (Figure 5 B), thus blocking E2F-mediated gene expression (Figure 5 C) and halting cell-cycle progression towards S phase (Figure 5 D) (Gubern et al., 2016; Joaquin et al., 2017).

This regulation mechanism of RB activity by p38 has important biological relevance in the cell cycle blocking, evading defective proliferation and allowing the cells develop the proper response to adapt to stress stimuli.

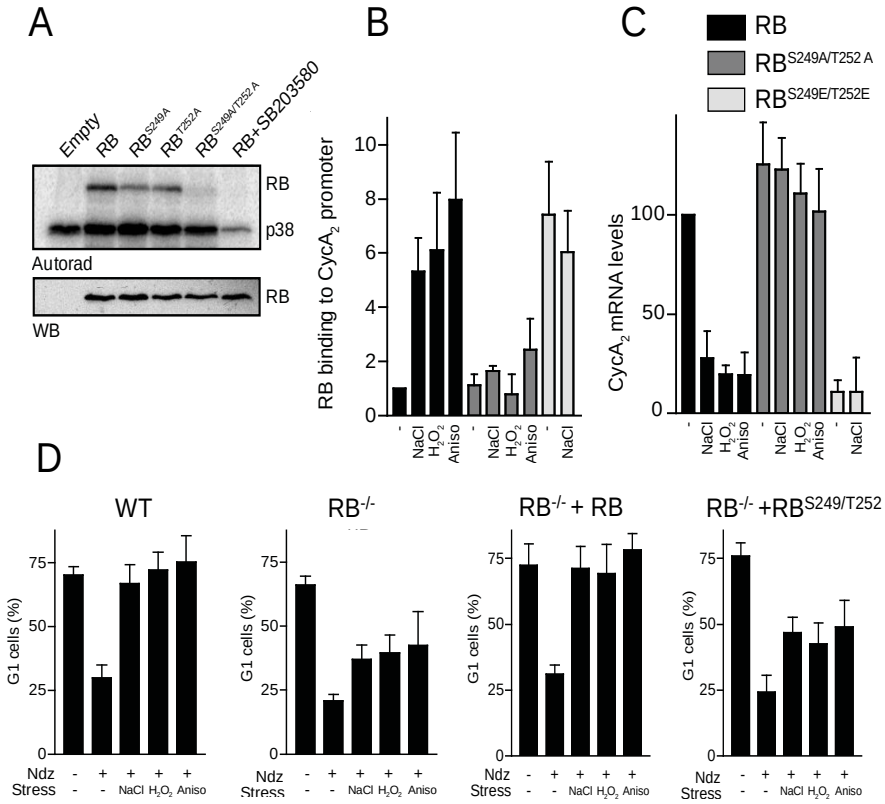

Figure 5. S249/T252 phosphorylation of RB by p38 increases binding between RB-E2F, repress cell cycle genes expression and delays the cell cycle in G1. A. p38 phosphorylates RB at S249 and T252. **B**. The phosphorylation in these two sites by active p38 under different stress conditions increase the recruitment of RB to the CycA2 promoter in wild-type RB or RB S249E/T252E, but not in RB S249A/T252A cells. **C.** CycA2 downregulation upon stress is showed in RB-/- MEFs transfected with wild-type RB or RB S249E/T252E, but not with RBS249A/T252A. **D.** Stress-induced G1 delay in RB WT MEF cells but not in RB-/- MEFs. RB-/- MEFs transfected with RB recover the wild type phenotype but not RB-/- MEFs transfected with RB S249A/T252A. MEFs were stressed with 100 mM NaCl, 400 μM H_2O_2 or 25 ng/ml Anisomycin (Aniso) as indicated. Nocodazole (Ndz) was added to trap the cells at the G2/M transition. Adapted from Gubern et al., 2016.

RB PROTEIN IN A CANCER CONTEXT

As mentioned before, alterations in the functions of RB proteins are directly related to the loss of negative regulation of the cell cycle, favoring deregulated cell proliferation and tumor development.

3.1 Dysfunctional RB functions lead to cancer phenotype

Components of the RB regulatory machinery act as tumor suppressors. Mutations in components of RB pathway occur frequently indicating that disabling "the RB pathway" may be crucial for the formation of tumor cells. RB function disappears in most human cancers contributing to deregulate a diversity of cellular functions, including cell proliferation, differentiation, senescence, cell death, and genome stability highlighting the importance of tumor suppressor function of RB (Khidr and Chen, 2006; Knudsen et al., 2020; McBrayer et al., 2018; Vélez-Cruz and Johnson, 2017).

Extensive studies of the genome and transcriptome of 601 genes in 91 primary glioblastoma tumors have revealed that components of the RB-pathway are altered in about 80% of tumor samples (McLendon et al., 2008). The RB pathway, whose components are inhibitors and activators of CDK, the pocket proteins, and the E2F-family transcription factors, plays key roles in the regulation of cell cycle progression and cell death (Schaal et al., 2014). Every component of the RB pathway that activates cell cycle progression is subject to oncogenic upregulation and the cell cycle repressors are subject to mutational inactivation, thus evidencing that the whole pathway is critical in cancer development.

RB1 gene mutations are infrequent and the mutation rate is variable between tumor types, being highest in retinoblastoma, osteosarcoma, and small-cell lung cancer (SCLC) (Bhateja et al., 2019; Thomas et al., 2001; Wu et al., 2020). These mutations directly affect RB function by either suppressing its expression or by producing a nonfunctional protein (Knudsen and Wang, 2010). Remarkably, although some cancers harbor RB mutations, it is much more frequent to find tumors with wild-type RB1 alleles but impaired function, due to alterations in genes coding for upstream RB regulators. These alterations in the RB pathway range from inactivation by mutations, deletions, or epigenetic silencing of CDK inhibitor genes (such as the p16INK4A locus) to upregulation of Cyclins or CDKs, Cyclin D and CDK4 being the most commonly overexpressed (Dahlstrand et al., 2005; Gladden and Diehl, 2005). This scenario results in RB inactivation by chronic hyperphosphorylation. Hence, oncogenesis usually entails either complete loss of RB expression or, more commonly, its inactivation by hyperphosphorylation (Beroukhim et al., 2010; Otto and Sicinski, 2017).

3.2 S249/T252 phosphorylation of RB by p38 suggests a new cancer therapeutic strategy

Since the discovery of RB more than two decades ago, and due to its importance in the development of most human cancers, considerable effort has been channeled into elucidating the role of the RB pathway in cancer, with high expectations of pharmacological intervention. However, despite the great interest and numerous studies dedicated to the RB pathway in the development of human

tumors, a large number of specific drugs targeting this pathway has not been found. Surprisingly, the discovery of drugs that inhibit CDK inhibitor drugs has progressed dramatically over the last decade. Dual selective CDK4,6 inhibitors have demonstrated robust clinical activity with manageable toxicity. Given their efficiency and safety profile, Palbociclib, Abemaciclib, and Ribociclib, approved by the U.S. Food and Drug Administration for the treatment of hormone receptor-positive (ER+) metastatic breast cancer, may also offer benefits in other tumor types, including lung, prostate and Ovary cancer (Sánchez-Martínez et al., 2019). To date, these are the only commercially available cancer drugs that target the RB pathway by specifically inhibiting the activity of Cyclin-CDK4,6 (Otto and Sicinski, 2017). In patients with ER+ breast cancer, CDK inhibitors improve the arrest of tumor growth in patients treated with hormone therapy, but these drugs are relatively new, and their therapeutic potential should be optimized. Despite the obvious benefits of the use of these CDK inhibitors in cancer, undesirable effects such as increased toxicity and side effects have also been reported when they are used in combination therapies with hormonal treatment or in patients resistant to treatment. In addition, subset studies of ER+ breast cancer patients in clinical trials so far do not reveal clear populations of patients who benefit from combination therapy, so we cannot predict in detail which patients may benefit from these drugs (Vijayaraghavan et al., 2018). These negative effects, added to the fact that these inhibitors are the only available drugs targeting the RB pathway, demonstrate that for the clinical success is necessary the rational design of combination therapies, determine patient selection

and define new therapeutic targets for the RB pathway (Sánchez-Martínez et al., 2019).

The new regulatory mechanism of RB activity by p38 opens the possibility to development a new type of anticancer drugs. The development of compounds capable of promoting the association of E2F transcription factors with the N-terminal region of RB, thereby mimicking the phosphorylation of RB by p38 at residues S249 / T252 is really promising (Joaquin et al., 2017). The phosphomimetic mutant RB S249E / T252E that mimics RB phosphorylation by p38, increased its affinity for E2F. This mutant arrested cells in G1 phase and could restrict cell growth in three cancer cell lines with high CDK activity (MCF7, PK9 and 235J breast, pancreatic and bladder cancer cell lines respectively) (Figure 6A). Of note, RB S249E / T252E mutant reduced tumor size in a mouse xenograft model (Figure 6B), suggesting that phosphorylated RB at the S249 / T252 sites acts as a super-repressor preventing cancer cell proliferation (Figure 6C) (Gubern et al., 2016).

Furthermore, RB phosphorylated at S249 / T252 promotes tumor immunity through a mechanism independent of cell cycle regulation. Programmed death-1 (PD-1) and its ligand PD-L1 are two key molecules in immune regulation. Aberrant PD-L1 expression is a common feature in most human cancers, triggering evasion of immune surveillance. PD-L1 interacts with its PD-1 receptor on activated T cells, promoting apoptosis of T cells and, thus, immune evasion of cancer. PD-L1 expression is, in turn, regulated by the p65 protein, a transcription factor of the nuclear factor-kB (NF-kB) family. Apart from the interaction with E2F, RB interacts with other

transcription factors such as the p65 protein. The interaction of RB with p65 is dependent on RB phosphorylation at residues S249 / T252, which represses the expression of p65-dependent genes such as PD-L1. In fact, the expression of an RB-derived phosphomimic peptide S249 / T252 suppresses the up-regulation of PD-L1 induced by radiation therapy and increases the therapeutic efficacy of radiation *in vivo* (Jin et al., 2019).

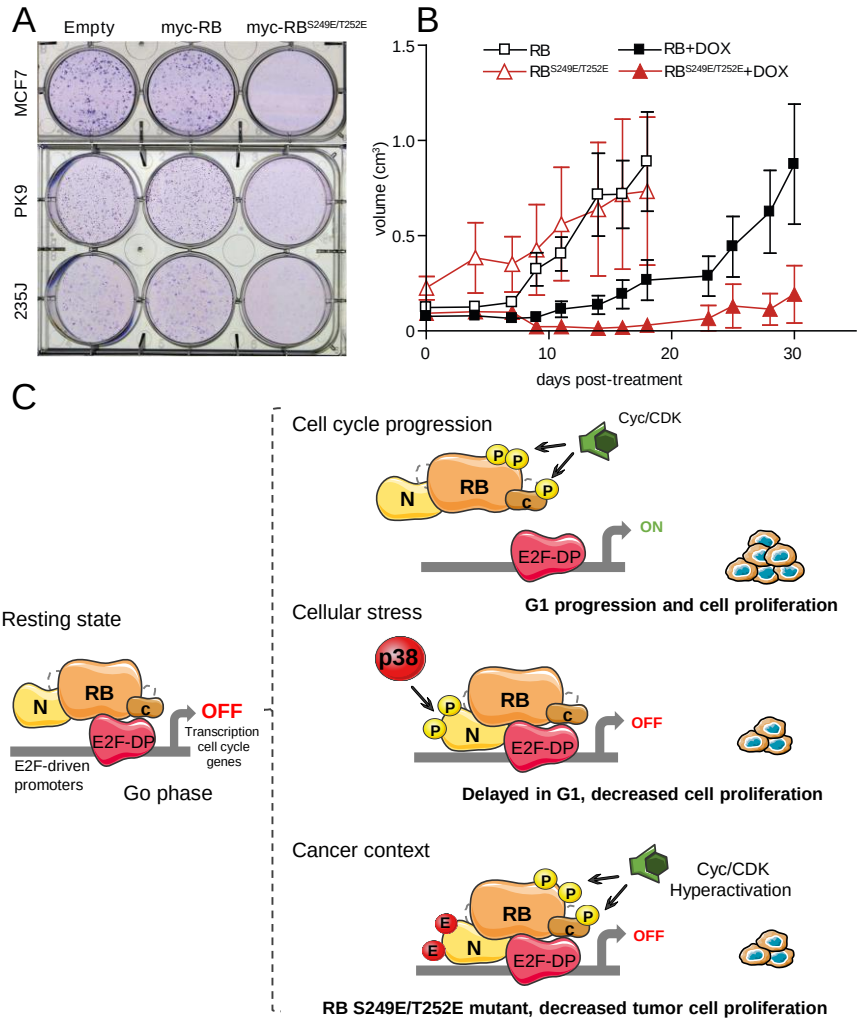

Figure 6. RB S249E/T252E mutant reduces cancer cell lines proliferation and tumor growth. A. RB S249E/T252E impairs colony formation of MCF7, PK9, and

235J cancer cell lines. **B.** RB S249E/T252E prevents tumor formation in a tumor xenograft mouse model. **C.** Scheme about S249/T252 phosphorylation of RB by p38. Adapted from Gubern et al., 2016.

The development of compounds that mimic the effect of the phosphorylation at RB S249 / T252 residues is a promising antitumor strategy because these compounds will inhibit tumor growth and are also likely to improve immune efficacy.

3.3 The challenge of using RB as a therapeutic target.

Restoration of tumor suppressor function has proven challenging as a therapeutic strategy (Morris and Chan, 2015). The drug-ability of tumor suppressor proteins is not usually feasible using the standard mechanisms used for cancer therapies because tumor suppressors are not usually cell surface proteins or enzymes and therefore they cannot target antibodies or enzyme inhibitors (Lee et al., 2018). This is why therapies tend to be directed towards improving the expression of these proteins for example, introducing encapsulated tumor suppressor messenger RNA (mRNA) (Islam et al., 2018), blocking the function of their inhibitors (such as CDK inhibitors), stabilizing the protein or inhibiting the degradation of the tumor suppressor protein (Kogan and Carpizo, 2016; Surget et al., 2014).

Currently there is no drug that acts directly on RB. In this regard, only the CDK inhibitors already mentioned are approved for clinical use. Recent studies have shown that chemotherapeutics and small molecule inhibitors targeting DNA damage checkpoints (e.g., CHK) and chromosome segregation (e.g., PLK1), exhibit similar results to CDK inhibitors (Kogan and Carpizo, 2016). However, no molecule is known to increase the activity of RB directly. Mimicking the

phosphorylation at S249/T252 sites of RB can be exploited to develop new-targeted therapies to improve current therapeutics strategies. Many human tumors with high Cyclin-CDK levels still carry a functional RB gene, and therefore, might benefit from such compounds capable of promoting E2F binding to RB (Gubern et al., 2016; Joaquin et al., 2017).

DRUG DISCOVERY

Drug discovery is the process by which new potential drugs are identified for therapeutic applications. This process is long and expensive, which involves a wide range of scientific disciplines, including biology, computational and medicinal chemistry, toxicology, and pharmacology.

In the past, the drug discovery involved recognizing the active ingredient from traditional remedies or by unexpected discovery. Nowadays, the most widely used approach is to study how a disease is regulated at the molecular and physiological level and to modulate specific therapeutic targets such as proteins based on this knowledge. Once the involvement of a target protein in a specific disease is discovered and validated (fundamental research), drug discovery begins. Early drug discovery is the first stage of this process and consists of identifying candidate molecules that show proper effectiveness, safety, and pharmacokinetic profiles in *in vitro* and *in vivo* models (Sinha and Vohora, 2017).

Early drug discovery process is divided into three different phases (Figure 7):

(1) Hit Finding (HF): discovery of new chemical starting points (Hits). These hits modulate the target and/or the phenotype of interest usually with potency in the micro-molar range. There are several processes to perform HF: through virtual screenings (computational drug screening based on known molecular structures and drugs), knowledge based design (consist on preselect a smaller subsets of molecules that are likely to have activity at the target based on previous knowledge, literature or patent) and HTS (large compound libraries screening to find activity on the target or phenotype of interest.). Validation of these hits in an orthogonal assay is strongly recommended. The orthogonal assay aims to validate the hits through a different assay than the one used to select the compounds that uses another technology and it is closer to the target physiological condition.

(2) Hit to Lead (H2L): Hit refinement and Lead nomination. Process during which medical chemistry teams synthesize specific compounds with similar structures or small series of drugs, with the goal of testing them and understanding the structure-activity relationship. The "hit to lead" phase end with a group of compounds (the lead series) which has proper properties such as selectivity, pharmacokinetics, or bioactivity. These properties can then be further improved by medicinal chemistry in a lead optimization process (Keseru and Makara, 2006).

(3) Lead Optimization (LO): This phase consists in improve Leads to get candidate for its entry in pre-clinical regulatory phase. Selected candidate selectively binds to the target site, elicits the desired functional response (*in vivo* and *in*

vitro), and has adequate bioavailability and biodistribution. It is expected that these candidates will safely elicit the appropriate response in humans according to the efficacy, toxicology and safety studies previously carried out.

Once the candidate molecules are defined, the preclinical regulatory phase begins followed by human clinical trials.

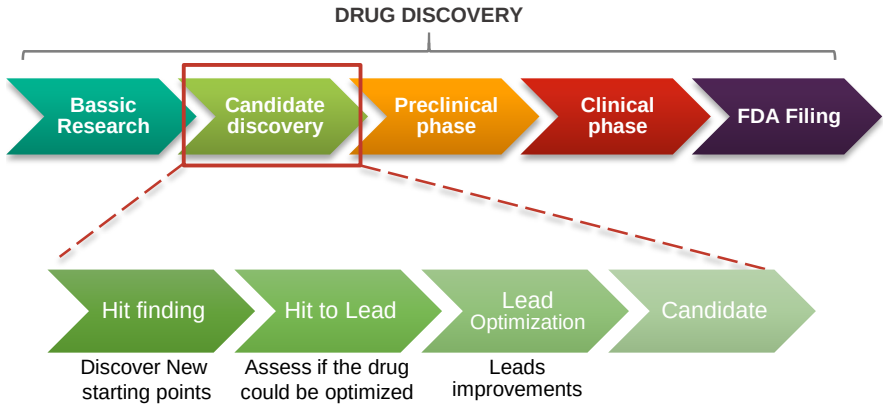

Figure 7. Schematic representation of different phases of Drug discovery process. The drug discovery process ranges from basic research to FDA filing through discovery candidate and the preclinical and clinical phases. The discovery of candidates in turn is divided into hit finding, hit to lead, lead optimization until the candidate is reached to move to the preclinical phase.

4.1 High-throughput screening

High-throughput screening (HTS) is one of the main technological breakthroughs in drug discovery. HTS technology consists of the use of automated equipment to rapidly test thousands or millions of compounds to detect biological activity at molecular or cellular level, in a determined signaling pathway or in a model organism (Schneider, 2018).

A wide variety of assay formats can be implemented in drug discovery and, but they generally fall into two approaches: target based and phenotypic assays.

Phenotypic screening is a type of assay used to identify compounds that alter the phenotype of a cell or organism in the desired way. Cell-based phenotypic screening has proven to be very useful in reproducing relevant biological conditions. These systems tend to be methodologically complex or make HTS difficult. However, advances in cellular, molecular and bioinformatics technologies such as super-resolution microscopy, flow cytometry or rapid bioinformatics analysis are solving many obstacles in this field (Aulner et al., 2019).

Target-based assays consist of the use of methods to direct drugs to defined molecular targets. Advances in genetics and molecular biology allow the identification of genes involved in diseases. In addition, currently, human genome sequencing and advances in genomics have increased the number of molecular targets available for drug discovery. Target based assays is divided in two categories biochemical and cell-based assays. The advantage of target-based assays is that they tend to be methodologically simpler than phenotypic approaches. Crystallography, molecular modelling, biochemistry, binding kinetics, pharmacology, genomics, and mutational analysis are some techniques used to facilitate the understanding of the interaction between a drug and its target and the finding of future generations of drugs. In contrast, optimizing compounds without a known target, as the case with a phenotypic approach, can be challenging (Croston, 2017). There are two main

target-based assay formats: biochemical and cell-based assays. The former involves the use of an *in vitro* systems and provide direct information on the nature of the molecular interaction, they tend to have a higher tolerance to solvents, thus allowing the use of higher concentrations of drugs. In contrast, the cell-based assays require complex protocols, with multiple steps (remove medium, wash step, cell lysis etc.) until the readout is done. However, they more closely mimic *in vivo* conditions and can be adapted for targets that are not suitable for biochemical assays, such as those involving signal transduction, transcriptional activity, membrane transport, cell division, or cytotoxicity pathways (Hemmilä and Hurskainen, 2002).

The nature of the entities tested by HTS is diverse, with small chemical molecules being the most common compounds selected. Other substances, such as chemical mixtures, natural product extracts, oligonucleotides, and antibodies, can also be screened.

HTS technology allows quick and efficient screening of large compound libraries at a rate of thousand compounds per day or per week, thus speeding up the drug discovery process. Given that HTS generally aims to analyze many compounds per day, relatively straightforward assay designs compatible with automation, robot-assisted sample handling, and automated data processing are critical parameters to consider in the planning of HTS. In the development of high-quality assays, which are usually based on biochemistry and cell biology knowledge, there is a clear tendency to mechanize the process. Homogeneous assay principles and sensitive detection technologies have enabled the miniaturization of assay formats,

which allows for a significant reduction in reagent use and cost per data point (Attene-Ramos et al., 2014).

HTS is routinely applied in pharmaceutical and biotechnology companies to detect compounds with pharmacological and/or biological activity. HTS assays are usually performed in microplates in 96-, 384-, or 1536-well formats. The traditional HTS tests each compound of a compound library at a single concentration, most commonly 10 μM (Attene-Ramos et al., 2014).

The statistical parameters used to regulate the quality of HTS include the calculation of standard deviations, coefficient of variation (CV) and signal to noise (S/N) or signal to background (S/B) ratio. However, S/N and S/B do not consider the dynamic range between the signal to background (low control) and the maximum (high control) signal, or the variability of the sample. Thus, a more consistent quality statistical parameter is by the "Z´ Factor" equation.

$$Z' = 1 - \frac{(3(SD\ of\ high\ control) + 3(SD\ of\ low\ control))}{[Mean\ of\ high\ control - mean\ of\ low\ control]}$$

Where SD is the standard deviation and the maximum possible value of Z is 1. This equation considers that the quality of an assay is reflected in the variability of the high and low controls, and the separation between them. For biochemical assays, a Z´ value greater than 0,4 denote a high-quality assay and less than 0,4 is consider inacceptable. A higher threshold 0,4 is typically consider suitable for cell-based assays (Zhang et al., 1999).

Typically, the HTS process is made up of several stages (Figure 8). Once the therapeutic target associated with a certain disease has

been identified or the phenotypic assay to be carried out has been selected. The first step is the development and optimization of the assay to detect the active molecules. The assay is then adapted for HTS by using state of the art dispensers, pipettors, readers and automation. In this phase, the proposed HTS assay is tested, using positive and negative controls, to determine the robustness of the assay (Z) followed by pilot screen.

The assay is then developed and optimized for HTS. In this phase, the proposed HTS assay is tested using positive and negative controls to determine the Z 'of the assay. The assay should use the HTS protocol, including robotics and plate readers where appropriate. When Z 'is constantly greater than 0.4, the pilot phase begins.

The pilot assay is carried out on a small scale in which some compounds are tested using the HTS protocol. In this phase, all aspects of the screening are assayed, including data analysis. The set of compounds for the pilot test can be a specific library (e.g. a set of drugs) or the first plates of the whole library. When the value of Z ' is greater than 0.4, it is considered that the pilot test has concluded successfully (Iversen et al., 2006).

The next phase is the Primary Screening, where the complete library of compounds is screened. In this round, several bioactive compounds called hits, are identified. These hits are “Cherry Picked” or retested to verify their activity by using the same assay (Confirmation). At this point, it is advisable for a better validation of hits to use an orthogonal test. This test is different from the one used

to select compounds and it is based on a different technology and / or is closer to the target physiological condition.

All results obtained together with a first evaluation run by a Medicinal Chemist and/or Computational Chemist, are considered to prioritize/discard frequent hitters or compounds not interesting due to several reasons.

Dose response experiments are then run to determine the potency of drugs using the IC50/EC50 or pIC50/pEC50 parameters. The concentration of compound that inhibits (IC50) or activates (EC50) 50% of the response is defined as compound potency. The pIC50 represents the IC50 / EC50 value on a logarithmic scale (it is the negative logarithm of the IC50 value). Finally, the medicinal chemist will prioritize remaining chemical series based on purity, novelty, structure-activity relationships, possibility of optimization, etc. and will confirm the activity of the selected chemical series using a resynthesized new batch.

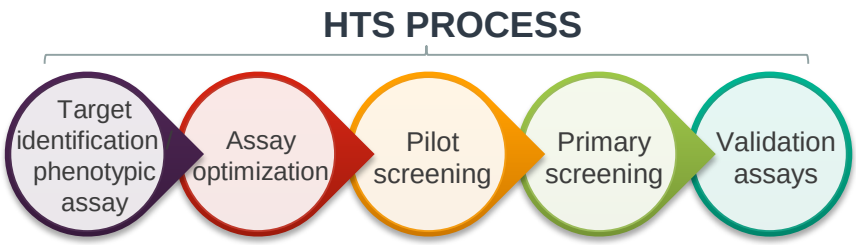

Figure 8. Schematic representation of different phases of HTS process. HTS consist on different phases such as target identification or selected phenotypic assay, assay optimization, pilot screening, primary screening, and validation assays.

For this Ph.D. thesis, we optimized a cell-based HTS assay that monitors RB activity. This assay allowed us to identify compounds

capable of enhancing the tumor suppressor capacity of RB, making RB a potential therapeutic target in the cancer therapy.

OBJECTIVES

The main goal of the present thesis was the identification of molecules capable of mimicking the effect of RB N-terminal phosphorylation, as a possible therapeutic target in cancer treatment.

Specifically, the main objectives of this Ph.D. were:

1. To characterize the RB N-terminal and E2F1 minimal binding region.
2. To set up a cell-based assay to monitor RB activity amenable for HTS (high-throughput screening) assay.
3. To optimize and automatize a cell-based high-throughput screening (HTS) assay for drug discovery.
4. To perform pilot HTS assays to identify compounds that regulates RB activity.
5. To analyze and characterize the hits obtained in the HTS.
6. To perform a large-scale screening monitoring RB activity for developing new drugs to treat cancer diseases

EXPERIMENTAL PROCEDURES

Cell culture

HEK293T, NIH-3T3, MCF7, PK9 and 235J cell lines were maintained in complete medium (Dulbecco's modified Eagle's medium DMEM (41965-062, Invitrogen) containing 10% fetal calf serum (F7524, Sigma-Aldrich), supplemented with 1mM sodium pyruvate (11360-039, Invitrogen), 100U/ml penicillin/streptomycin (15140-122, Invitrogen) and cultured in a 5% CO2 humidified incubator at 37°C. The experiments have been performed with cells at low passage and have been passed every 24-48 hours to ensure that they are actively dividing and that they have the appropriate cell density at the time of the experiment with ≥ 90% viable cells. The counting of the cells for the experiments was carried out using the Countess II Automated Cell Counter equipment (Applied biosystems).

RB transcriptional activity assay

The principle of this assay is based on a luciferase reporter assay, that needs the co-transfection of three plasmids: E2F-Luc (luciferase coding sequence cloned under the control of a promoter region containing several E2F consensus binding sites), HA-E2F (E2F coding sequence with HA tag, expressed under the control of CMV promoter) and Myc-RB or GFP-RB (RB coding sequence with Myc or GFP tag, expressed under the control of CMV promoter). In parallel, a control for transfection efficiency with a plasmid encoding the green fluorescent protein (pEGFP) was included and analyzed by fluorescence microscopy and flow cytometry, reaching 98% of transfection efficiency. This assay has been adapted to test

compounds with a putative effect on E2F-RB interaction, in HEK293T cells.

This assay has undergone subtle modifications in the different drug discovery platforms (Innopharma, in CDRD and, finally, in IRB and FIMM) in which it has been carried out.

Innopharma assay conditions: 30.000 cells/well were seeded in 384 well-plate in complete DMEM medium with 2% FBS. 24 hours later, cells were co-transfected with Fugene 6 (Promega) and seeded in DMEM supplemented with FBS CS using E2F-luc, HA-E2F1, Myc-RB and pEGFP plasmids (0.5:1:4:4 plasmids proportion) 0.1 μg/well DNA in total and cells were incubated overnight at 37ºC and 5% CO2. pEGFP was included as a transfection efficiency control that was visualized in the Operetta High Content System (Perkin Elmer). The transfection medium was removed, and cells were incubated in complete DMEM medium to allow maximum expression of the plasmids. Cells were treated with the different libraries of compounds at 1 or 10 μM, Anisomycin at 50 μM as a positive control or DMSO (Vehicle) as a negative control for 4 hours. Cells were lysed with cell culture lysis reagent (E1500, Promega) for 15 min. Then, Luciferase Reporter Assay reagent (E1500, Promega) was added, mixed, and incubated 5 min. The luminescence was detected using in Tecan Infinite M1000Pro (0.5 sec/read).

CDRD assay conditions: Cells were transfected with E2F-luc, HA-E2F1, GFP-RB plasmids (1:1:1/4 plasmids proportion) in bulk using PEI reagent. After 48h transfected cells were harvest, wash and resuspend in HBSS medium. Then cells were seeded at 10,000 cells/

20 µl/well in plates preprinted with the compounds at 10µM, H_2O_2 at 1mM as a positive control or DMSO (Vehicle) as a negative control and they were incubated 2 hours at 37ºC. Finally, the addition of 20 µL of Bright-Glo detection reagent (E2610, Promega) per well, incubated at RT for 5 minutes and read on Varioskan (0.5 sec/read).

IRB and FIMM assay conditions: Cells were transfected with E2F-luc, HA-E2F1, GFP-RB plasmids (1:1:1/4 plasmids proportion) in bulk using LTX plus reagent (15338100, Thermo Fisher). After 48h transfected cells were harvest, the cells were frozen in FBS 10% DMSO for later use. Transfected cells were thawed, centrifuged at 1000 rpm to remove the supernatant, and resuspend in Opti-MEM (31985070, Gibco) with 2%FBS. Then cells were seeded at 12,500 cells/ 25 µl/well in plates preprinted with the compounds at 10 µM, hits compounds in previous screenings at 10 µM as a positive control or DMSO (Vehicle) as a negative control and they were incubated 4 hours at 37ºC. Finally, the addition of 6.25 µL of One-Glo detection reagent (E2610, Promega) per well, incubated at RT for 30 minutes and read on EnVision (PerkinElmer) (0.5 sec/read).

Cytotoxicity assay

The CellTiter-Glo® detection kit was used in drug discovery platforms to determine viability of cells in culture by quantifying the amount of ATP present, indicating the presence of metabolically active cells. This assay was used to determine the cytotoxic effect of the positive compounds detected in the screenings. Cell were seeded in the 384 wells. The cells were seeded in the 384 wells/plate in the same way that they were seeded for the screening of compounds in

the RB activity assay, that is, at Innophama the cells were seeded and treated with the compounds for 4 hours and at CDRD the cells were seeded with pre-printed compounds and incubated for two hours. In the two HTS platforms, the dose response of the drugs was performed to determine the IC50 of the cytotoxic effect. 25μL of reagent was added on the wells, mixed 2 min with orbital shaker to induce cell lysis and incubated 10 min at room temperature. Finally, the luminescence was read with Tecan Infinite M1000Pro or Varioskan respectively (0.5 sec/read).

Nonspecific transcription inhibition assay

HEK293T cells were transfected with doxycycline-inducible GFP-RB vector (pLVX-GFPRB) using LTX plus reagent for 6 hours, after a culture medium change to complete DMEM, cells were incubated for 24 hours at 37ºC. Cells were treated with 10 μM drugs for 1 hour and the GFP-RB expression was induced over nigh with doxycycline. GFP expression were measured by flow cytometry.

Nonspecific luminescence inhibition assay

HEK293T cells were transfected with doxycycline-inducible GFP-RB vector using LTX plus reagent for 6 hours, after a culture medium change to complete DMEM, cells were incubated for 24 hours at 37ºC. Cells were treated with 10 μM drugs for 4 hours and luminescence was measured with Ensight PerkinElmer luminometer.

Colony formation assay

PK9, MCF7 and 235J tumor cell lines were seeded in a low density and treated with the different drugs in a dose response

(performed by diluting each compound 1:2 over 5 points starting at 10 μM) for 4 days, the colonies were stained crystal violet solution (0.5g crystal violet, 1% methanol, 87% formaldehyde diluted in PBS phosphate-buffered saline 1x) for 30 minutes, washed with water and left inverted until dry. Colony area occupancy was measured with ImageJ-plugin ColonyArea software (Guzmán et al., 2014).

Cell cycle assay

HEK293T cells were treated with the drugs at 10 μM or Anisomycin at 150 μM as a positive control and 1 hour later 10 ng/μL of nocodazole were added in each well to inhibit the microtubules formation and arrest the cell cycle in G2/M phase. Cells were incubated overnight at 37ºC. Then, cells were collected in tubes, centrifuged at 1200 rpm 5 min and the supernatant was discarded. Then PBS was added to wash. Cell were collected by centrifugation at 1200 rpm 5 min, were fixed adding cold Ethanol 70% and were incubated overnight at -20ºC. Next day, cells were centrifuged at 4000-5000 rpm and washed with cold PBS to remove the ethanol. After, cells were centrifugated at 5000 rpm to discard the PBS, the cells pellets were resuspended in working solution (200 μg/mL RNAsa, 20 μg/mL Propidium Iodide in PBS 1x) and were incubated at room temperature for at least 1h followed by FACS analysis. The stained cells were acquired on an FACSCalibur flow cytometer (Becton Dickinson) using CellQuest and flowJo software.

CDK2 Immunoprecipitation (IP) assay

HEK293T cells were washed with cold PBS and scraped into IP/Lysis buffer (10 mM Tris HCL pH 7.5, 1% NP40, 2 mM EDTA,

50 mM NaF, 50 mM b-glycerophosphate, 1 mM Sodium Vanadate, supplemented with the protease inhibitors 1mM PMSF, 1 mM Benzamidine, 200 µg/ml Leupeptine and 200 µg/ml Pepstatine). The lysates were cleared by microcentrifugation. For the IP assays, 10% of the total lysate was reserved as input. The lysate remaining were incubated with 50 µl sepharose-protein A beads (GE Healthcare, 50% slurry equilibrated in IP buffer) coupled to CDK2 specific antibody (anti CDK2 mAB, Sc-163, Santa Cruz biotechnology) overnight at 4°C. The formed protein complexes were immunoprecipitated by centrifugation and washed three times with IP buffer. Input and IP samples were subjected to PAGE–SDS and western blotting.

***In vitro* CDK2 and CDK4 Kinase assay**

The reactions were carried out in kinase assay buffer (50 mM Tris–HCl pH 7.5, 10 mM MgCl2, 2 mM DTT). Approximately 0.05 µg/reaction of purified CDK2 (CDK2 protein was immunoprecipitated and purified from HEK293T) and CDK4 (human active CDK4/Cyclin D1, C0620-10UG Sigma Aldrich) were incubated with 10 µM of the drugs and 1µg/reaction of histone 1 (H1, HIST-RO, Sigma Aldrich) as a non-specific substrate of CDK in the presence of 1 µCi/assay of radiolabeled 32P-γ-ATP (3000 Ci/mmol, Perkin-Elmer) in a final volume of 20 µl/assay for 30 minutes at 30 °C. Reactions were stopped by adding 5X SB (250 mM Tris–HCl pH 6.8, 0.5 M DTT, 10% SDS, 20% glycerol, 0.5% Bromophenol Blue) and boiling at 100 °C for 5 minutes. Phosphorylated proteins were analyzed using SDS-PAGE and were transfer blotted onto a PVDF membrane followed by autoradiography and performed a western

blot with CDK specific antibodies (anti CDK4 and CDK2 mAB, sc-70832 and Sc-163, Santa Cruz) as a loading control.

Sample preparation and Western blot

HEK293T cells were treated with 10 μM of the drugs or with 150 μM of Anisomycin as positive control for 1 hour. Cells were washed with cold PBS and scraped into lysis buffer (10 mM Tris HCL pH 7.5, 1% NP40, 2 mM EDTA, 50 mM NaF, 50 mM b-glycerophosphate, 1 mM Sodium Vanadate, supplemented with the protease inhibitors 1 mM PMSF, 1 mM Benzamidine, 200 μg/ml Leupeptine and 200 μg/ml Pepstatine). The lysates were cleared by microcentrifugation. Samples were subjected to PAGE–SDS and western blotting.

Real Time (RT)-PCR mRNA analysis

Total RNA was purified from HEK293T cells using the RNeasy kit (Qiagen) according to the manufacturer's instructions. The reverse transcriptase Superscript kit (Invitrogen) was used to convert 100 ng of RNA to cDNA following the commercial protocol. cDNA was analyzed by real-time PCR using a DNA Biosystems ViiA7 sequence detector (Thermofisher) and the SYBR Green kit (Applied Biosystems). Real-time PCRs were performed in triplicate and were normalized using the GAPDH mRNA levels. Primers for qPCR assay were designed so that their annealing temperature was 60ºC, producing single amplification products in the range of 60-200 base pairs long. Primer pairs used for qPCR analysis are listed in Table 2.

Expression and purification of recombinant proteins

GST-Tagged proteins purification: Competent BL21 *Escherichia coli* bacteria, previously transformed with the plasmids that express the interest protein, were grown in LB medium with the appropriate selective antibiotics at 37°C until they reached an optical density (OD) about 0.4-0.6 at 600nm. At this point, GST-tagged proteins expression was induced for 6 hours by adding 1 mM IPTG and switching the culture temperature to 25°C. After induction, cells were collected by centrifugation and resuspended in 1/50 volume of STET 1X buffer (100 mM NaCl, 10mM Tris–HCl pH 8.0, 10mM EDTA pH8.0, 5% Triton X-100 supplemented with 2 mM DTT and the 1 mM PMSF, 1 mM Benzamidine, 200 mg/ml Leupeptine and 200 mg/ml Pepstatine). Cells were lysed by ice-cold sonication and cleared by high speed centrifugation. GST-tagged proteins were pulled down from supernatants with 300 µl of gluthatione-sepharose beads (GE Healthcare, 50% slurry equilibrated with STET) by mixing 45 min at 4°C. The gluthatione-sepharose beads were collected by brief centrifugation and washed four times in STET buffer and twice in 50 mM Tris-HCl pH 8.0 buffer supplemented with 2 mM DTT. The GST-fused proteins were then eluted in 200 µl of 50 mM Tris-HCl pH 8.0 buffer supplemented with 2 mM DTT and 10 mM reduced gluthatione (Sigma) by mixing for 45 min at 4ºC and stored at -80°C.

Histidine-Tagged proteins purification: Competent BL21 *E. coli* bacteria, previously transformed with the plasmids that express the protein of interest, were grown in LB medium with the appropriate selective antibiotics at 37°C until they reached an optical density

(OD) about 0.4-0.6 at 600nm. At this point, Histidine-tagged proteins were induced overnight by adding 1 mM IPTG and switching the culture temperature to 18°C. After induction, cells were collected by centrifugation and resuspended in 1/50 volume of Sonication buffer (100 mM NaCl, 20mM Tris–HCl pH 8.0, supplemented with 1 mM PMSF, 1 mM Benzamidine, 200 mg/ml Leupeptine and 200 mg/ml Pepstatine). Cells were lysed by ice-cold brief sonication and cleared by high speed centrifugation. Histidine-tagged proteins were pulled down from supernatants with 300µl of TALON® Metal Affinity Resin (635501 Clontech, 50% slurry equilibrated with Sonication buffer) by mixing 45 min at 4°C. The TALON Metal Affinity beads were collected by brief centrifugation and washed six times in sonication buffer. The Histidine-fused proteins were then eluted in 200 µl of elution buffer (20mM Tris pH 8, 100mM NaCl, supplemented with 250mM Imidazole) and stored at -80°C.

To avoid artifacts generated by the buffer in interaction assays, the eluates of the samples were passed through desalting columns (28918008, PD MidiTrap G-25 Columns from GE Healthcare) and proteins were eluted in PBS following manufacturer's instructions.

Surface plasmon resonance protocol

The protein-protein interaction was studied by surface plasmon resonance (SPR) using a Biacore X100 system (GE Healthcare).

CM7 chip was used and prime with running buffer (PBS 1x). A manual run was used to fix a stable baseline with a flow rate of 5 µl/min. To activate the carboxymethyl surface to reactive esters of the chip, a solution mixture comprised equal part of 100 mM NHS and

400 mM EDC was used. Purified His-E2F protein was immobilized by amino coupling on the activated CM7 chip. His-E2F was immobilized in the channel 2 of the chip and purified recombinant GST protein was immobilized in the channel 1 to use as a reference channel. The N-Hydroxysuccinimide esters on the chip reacted with the amines on the E2F to form covalent links. 1 M ethanolamine hydrochlorid adjusted to pH 8.5 with NaOH was used to deactivated unreacted NHS-esters. Serial dilutions (concentration range, from 0.75 μM to 12 μM) of the GST-RBN WT protein were prepared using the running buffer (PBS, 0.05% tween and 0.1% DMSO) and the drugs at 10μM were added in this dilution mixtures. We used the phosphomimetic GST-RBN S242E/T249E mutant as positive control and GST-RBN S242A/T249A protein as negative control. Samples (GST-RBN protein with drugs) were injected from low to high concentration on the chip with immobilized E2F. The DMSO concentrations (0.1%) were maintained constant in all sample mixes. PBS supplemented with 0.05% Tween was used to regenerate the system. The obtained sensograms based on the changes in the refraction index caused by the protein interactions were analyzed using Biacore T200 evaluation software. The equilibrium constants (KD) were calculated by affinity analysis.

Binding assays

Derived GST-RB proteins were not eluted from the beads in the purification process. These GST-RB beads were washed three times with IP buffer (10 mM Tris HCL pH 7.5, 1% NP40, 2 mM EDTA, 50 mM b-glycerophosphate, 1 mM Sodium Vanadate, supplemented with the protease inhibitors 1mM PMSF, 1 mM Benzamidine, 200

µg/ml Leupeptine and 200 µg/ml Pepstatine) by centrifugation 2000 rpm 1 min. For the binding assays, 10% of the total protein extracts was reserved as input. These GST-RB proteins were incubated with eluted derived His-E2F1 proteins together with drugs at 10 µM overnight at 4ºC in a final volume of 500 µL per condition with IP buffer. The glutathione beads bound to derived GST-RB proteins were pulled down by centrifugation. The co-precipitation with derived His-E2F1 proteins was analyzed by western blot.

Antibodies

The antibodies used are as follows: Anti-phospho-p38 MAPK (Thr180/ Tyr182) (9215S) and total p38α antibody, (9218S) from cell signaling. Anti-E2F1 (sc-251), anti-RB (sc-50) and anti-CDK2 (sc-163), were from SantaCruz. Anti-phospho S249-RB (ab4788, Abcam). Anti-RB (554136) was from BD Pharmingen. Anti-tubulin (S9026) was from Sigma. Anti-GST antibody was from GE Healthcare. Horse Radish Peroxidase-conjugated anti-rabbit and anti-mouse antibodies and the Enhanced Chemiluminiscence kit were from GE Healthcare.

Plasmids

The following plasmids were used. pCDNA3 (Invitrogen), pGL2-E2F-luc and pRC-HA-E2F1 were provided by Dr. Tauler (UB, Barcelona) (Real et al., 2011). pEGFP-N1 (6085-1, Addgene). pPGL3 (E1751, Addgene). pCDNA3-Myc-RB was described before (Gubern et al., 2016). GFP-RB FL was from #16004, Addgene. pCDNA3-GFP-RB were PCR amplified with the oligos described in

the table 2 and using the full-length pETM11-E2F1 as a template. PCR products were cloned into the *BamHI/EcoRV* sites of pETM11.

pLVX-TetOne-Puro was from 631849, Clontech. pLVX-GFP-RB was PCR amplified with the oligos described in the table 2 and using the pCDNA3-GFP-RB plasmid as a template. PCR products were cloned into the AGEI/BamHI sites of pLVX-TetOne-Puro.

pGEX2TK-RB (human) was provided by Dr. Mayol (IMIM, Barcelona) (Qin et al., 1992). pGEX4T1-RBN (aa 1-379) was described before (Gubern et al. 2016). The GST-RBN S242E/T249E and S242A/T249A mutants were generated from pGEX4T1-RBN using the New England Biolab Mutagenesis kit, following the manufacturer's instructions, and primers described in the table 2.

pETM11 was obtained from EMBL (Dümmler et al., 2005). pETM11-E2F1 was obtained by PCR amplification of E2F1 using pRC-HA-E2F1 as a template, the primers described in table 2 and it was cloned into the *Nco1/Not1* sites of pETM11. His-E2F1 fragments were PCR amplified with the oligos described in the table 2 and using the full-length pETM11-E2F1 as a template. PCR products were cloned into the *Nco1/Not1* sites of pETM11. pETM11-E2F1-ΔFQISL, pETM11-E2F1-4A and pETM11-E2F1-DQIRD mutants were obtained by directed mutagenesis of pETM11-E2F1 using the New England Biolab Mutagenesis kit, and the primers described in the table 1.

pGEX6P1 was from GE Healthcare. pGEX6P1-RBN (aa184-330) was produced by PCR amplification with the oligos described in the

table 1 using the pGEX4T1-RBN as a template. PCR product was cloned into the *BamHI/HindIII* sites of pGEX6P1.

Table 1. Primer pairs used for cloning.

pETM11-E2F-1	F_E2F1 FL	TCTCTCCCATGGCCTTGGCCGGGGCCCCT
	R_E2F1 FL	TCTCTCGCGGCCGCTCAGAAATCCAGGGGGGTGAG
pETM11-E2F-1	F_fragm #1	TCTCTCCCATGGCCTTGGCCGGGGCCCCT
	R_fragm #1	TCTCTCGCGGCCGCTCAGCCGACGCCCACTGTGGTGTG
pETM11-E2F-1	F_fragm #2	TCTCTCCCATGGCCTTGGCCGGGGCCCCT
	R_fragm #2	TCTCTCGCGGCCGCTCACTCCTCAGGGCACAGGAAAAC
pETM11-E2F-1	F_fragm #3	TCTCTCCCATGGCGCCGGGGGAGAAGTCACGCTAT
	R_fragm #3	TCTCTCGCGGCCGCTCACTCCTCAGGGCACAGGAAAAC
pETM11-E2F-1	F_fragm #4	TCTCTCCCATGGGACGGCTTGAGGGGTTGACC
	R_fragm #4	TCTCTCGCGGCCGCTCAGAAATCCAGGGGGGTGAG
pETM11-E2F-1	F_loop-TD	TCTCTCCCATGGCGACCGTAGGTGGGATCAGCCCT
	R_loop-TD	TCTCTCGCGGCCGCTCAGAAATCCAGGGGGGTGAG
pETM11-E2F-1	F_CCMB	TCTCTCCCATGGGACGGCTTGAGGGGTTGACC
	R_CCMB	TCTCTCGCGGCCGCTCACTCCTCAGGGCACAGGAAAAC
pETM11-E2F-1	F_ΔFQISL	AAGAGCAAACAAGGCCCG
	R_ΔFQISL	GTTCTCCGAAGAGTCCAC
pETM11-E2F-1	F_4A	GATCTCCCTTGCAAGCGCACAAGGCCCGATCGATGTTTTC
	R_4A	TGAAAGTTTGCCGAAGATGCCACGGCTTGGAGCTGGGT
pETM11-E2F-1	F_DQIRD	CCGCGATAAGAGCAAACAAGGCCCG
	R_DQIRD	ATCTGATCGTTCTCCGAAGAGTCCAC
pCDNA3GFP-RBFL	F_GFP-RB	CATCATGGATCCATGGTGAGCAAGGGCGAGGAG
	F_GFP-RB	CATCATGATATCGAACTGCTGGGTTGTGTCAAA
pLVX-GFP-RB	F_RB	TCTCTCACCGGTATGGTGAGCAAGGGCGAGGAG
	R_RB	TCTCTCGGATCCATACAGTCACATCTGTGAGAG
pGEX4T1 RBNAA	F_RBNAA	CGAGCACCCAGGCGAGGTCAGACC
	R_RBNAA	AGGTGCACCATTAATGGGTATAACAGCTG
pGEX4T1 RBNEE	F_RBNEE	CGAGAACCCAGGCGAGGTCAGAAC
	R_RBNEE	AGGTTCACCATTAATGGGTATAACAGCTG
pGEX4T1 RBN	F_184-330	TCTCTCGGATCCGAAATAAATTCTGCATTGGTG
	R_184-330	TCTCTCAAGCTTTTAATCTTTATTTTTAAGATA

Table 2. Primer pairs used for qPCR analysis.

BRCA1	F_hBRCA1	GGAGGCCTTCACCCTCT
	R_hBRCA1	CTTCAACGCGAAGAGCAGATA
CycA2	F_hCycA2	TATCCTCGTGGACTGGTTAG
	R_hCycA2	CTGACATGGAAGACAGGAA
CycE1	F_hCycE1	CCCATCATGCCGAGGGA
	R_hCycE1	CTGGAGCGAGCCGAGAA
E2F-1	F_hE2F1	GACCTCGAAACTGACCATCA
	R_hE2F1	GGTCTCATAGCGTGACTTCTC
GAPDH	F_hGAPDH	CGTGGAAGGACTCATGACCA
	R_hGAPDH	CAGTCTTCTGGGTGGCAGTGA

RESULTS

1. Characterization of the RBN-E2F1 minimal interaction region

The prevailing cancer drug discovery strategy has been based on designing inhibitors for oncogenic targets, therapeutically targeting proteins that are more active than normal, or selecting an oncoprotein and designing drugs that inhibit its function. Today, tumor suppressor targets remain an underexplored area in cancer treatments, because is more difficult to repair the loss of function of a tumor suppressor protein.

Phosphorylation of the RBN domain at residues S249 and T252 stimulates a conformational change in RB that promotes an increase in its affinity towards E2F1. The increase in the affinity of RB-E2F1 interaction inhibited the E2F-dependent genes expression and delayed the cell cycle. Moreover the phosphomimetic RB mutant reduced cell proliferation, both in tumor cell lines and in a mouse xenograft model (Gubern et al., 2016). The dominant role of this mechanism over CDK activity opened up new possibilities to consider RB as a target of chemical compounds to restrict the proliferation of cancer cells (Joaquin et al., 2017).

In this scenario, it was proposed to identify molecules that increase the interaction between RB and E2F1 as a possible antitumor therapeutic strategy. Our first approach consisted of performing i*n silico* predictions of possible compounds that increase the affinity between RB and E2F RB. Although we knew that the N-terminal region of RB interacted with E2F1, for an *in-silico* drug screening it was required to decipher the tertiary

structure of the interaction by nuclear magnetic resonance (NMR). By binding assays, we determined the minimal regions of E2F1 and RBN that are involved in the interaction to facilitate NMR analyzes.

1.1 E2F1 interacts with RB by its CC-MB domain.

To determine the minimum interaction region of E2F1 that binds to the N-terminal region of RB, we produced different protein fragments of E2F1, and tested which of these versions interacted with RBN *in vitro* (Figure 9A). Purified GST-RBN protein not eluted from the glutathione beads was incubated with eluted derived His-E2F1 protein versions, as well His-E2F1 as positive control, overnight at 4ºC. GST-RBN protein bound to beads was pulled down by centrifugation and the co-precipitation with derived His-E2F1 proteins was analyzed by western blot (Figure 9B).

E2F1 fragments #2, #3 and #4, which contain a common CC-MB region (200-301 aa), bound to RBN. The E2F1 fragments #1 and loop+TD, whose sequence did not contain the CC-MB region, did not co-precipitate with RBN. Of note, the E2F1 CC-MB region was sufficient to interact with RBN

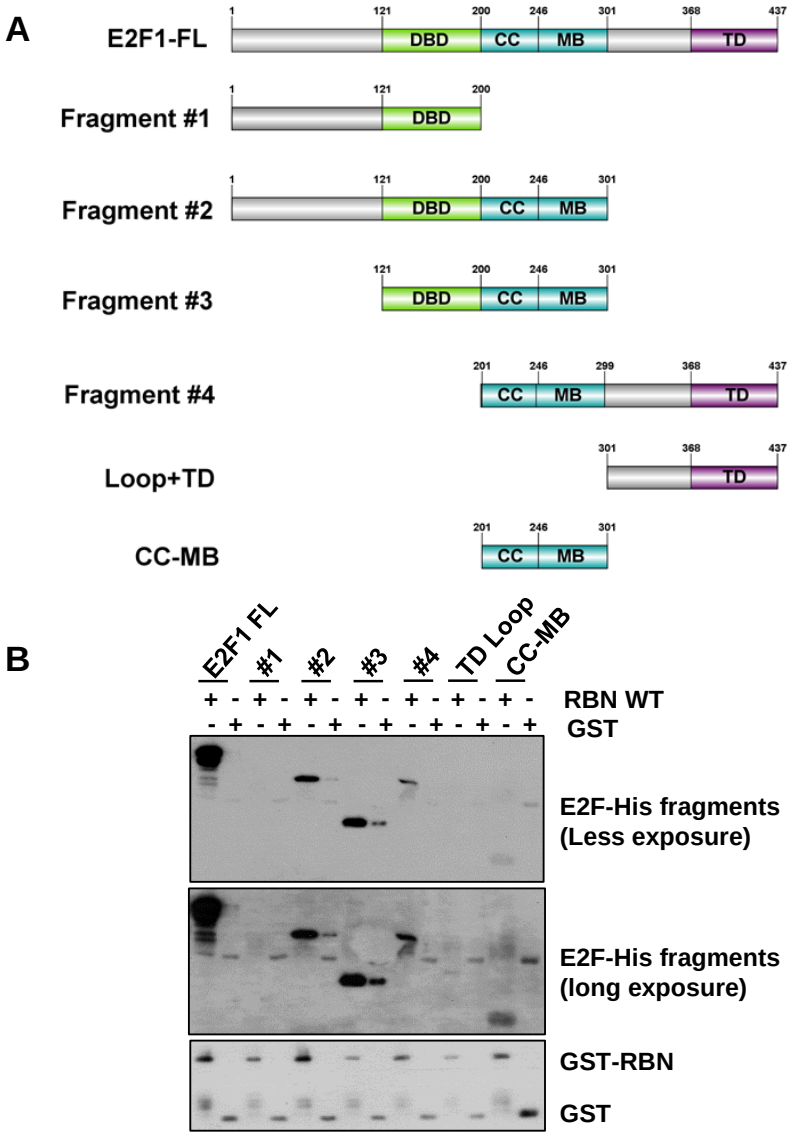

Figure 9. The CC-MB domain of E2F1 is sufficient to interact with RBN. A. Schematic representation of the different E2F1 fragments produced and tested in the RBN-E2F1 interaction assays. **B**. RBN interacts with fragments #2, #3, #4 and CC-MB domain of E2F1. GST-RBN (1-379 aa) was incubated with the different His-E2F1 fragments. All proteins were purified from *E. coli*. Empty GST was incubated with His-E2F1 fragments as a negative control. GST and GST-RBN was pulled-down using Glutathione Sepharose beads and the co-precipitation of the E2F1 fragments was analyzed by western blotting.

1.2 The ^{282}FQISL^{286} sequence of E2F1 and the charge of adjacent amino acids are required for the binding of RBN-E2F1.

A recent report has shown that a 21 amino acids fragment of the RB N-terminal domain containing S249/T252 was sufficient to bind to p65 and inhibit the NF-kB transcriptional activity. Similarly, RBN interacted with a small region of p65 that contained an evolutionally conserved FxxxV/L (^{161}FQVTV^{165}) motif (Jin et al., 2019). Moreover, the authors demonstrated that binding of RBN with p65 increased when RBN is phosphorylated at residues S249 / T252 due to the charge difference in the region of interaction. Surrounding the FxxxV/L motif of p65 there are basic (positively charged) amino acids that facilitate interaction with the phosphorylated (negatively charged) RBN form. Indeed, whereas binding with p65 increased with an RB phosphomimetic mutant, it was reduced in a RBN non-phosphorylatable mutant. Furthermore, mutation of the arginine residues (positively charged) surrounding FxxxV/L of p65 to alanine (neutral amino acid) or aspartic (negatively charged) residues increased its binding with RBN (Jin et al., 2019).

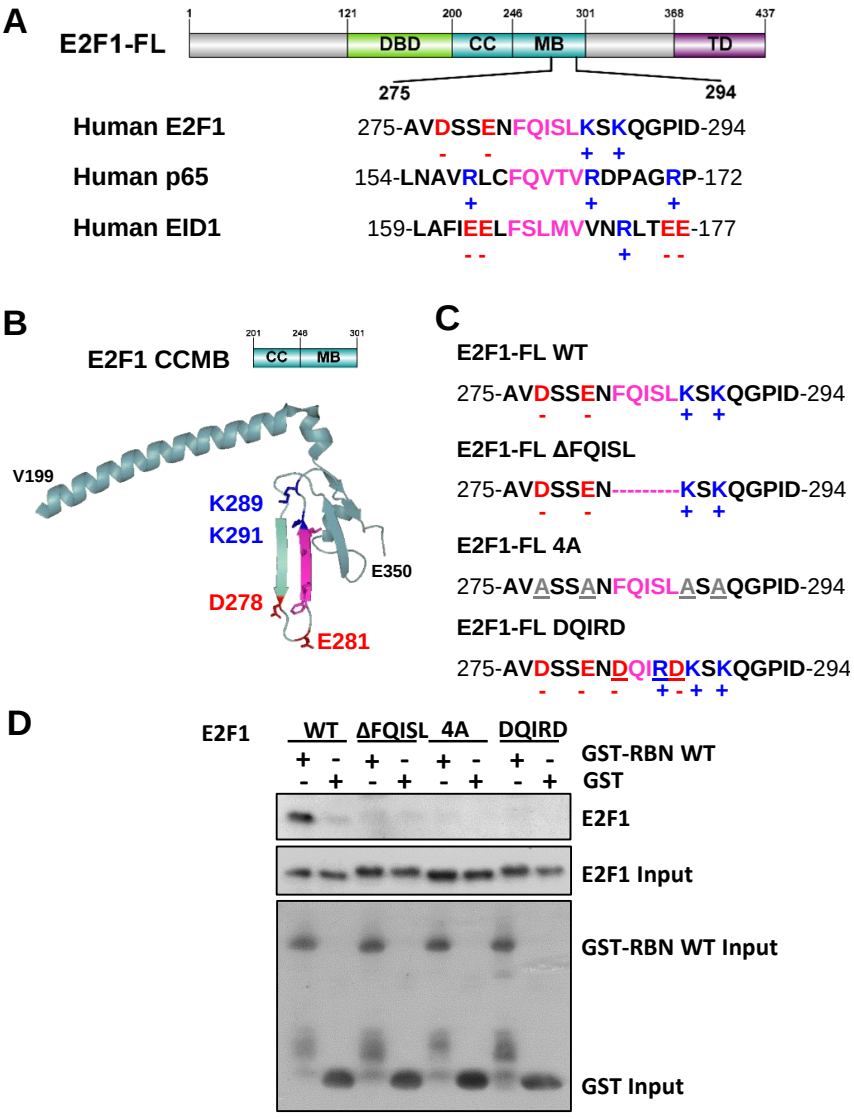

Figure 10. The ^{282}FQISL^{286} sequence of E2F1 and the charge of adjacent amino acids are key for RBN-E2F1 binding. A. Schematic diagram depicting the FxxxV/L motif of E2F1, p65 and EID1 and the charge of the adjacent amino acids. **B**. Crystal model of the CC-MB domain of E2F1. **C.** Schematic diagram showing the sequence of the different E2F1 mutants assayed. **D**. ^{282}ΔFQISL^{286} deletion, 4A and ^{282}DQIRD^{286} E2F1 mutants abolished the interaction with RBN. All proteins were purified from *E. Coli*. Empty GST was used as a negative control. GST and GST-RBN (1-379 aa) were pulled-down using Glutathione

Sepharose beads and incubated with the different His-E2F1 mutants. Co-precipitation of the E2F1 protein versions was analyzed by Western blotting.

The FxxxV/L motif of p65 is highly conserved and appears in other proteins that interact with the N-terminus of RB, such as EID1 (Hassler et al., 2007). We found that E2F1 also harbors a FxxxV/L (^{282}FQISL^{286}) motif located in its CC-MB domain (Figure 10A). To assess the importance of FxxxV/L motif of E2F, we performed pull-down experiments as described previously purifying a version of the E2F1 full-length deleting this motif (E2F1 ^{282}ΔFQISL^{286}). Like EID1 and p65, deletion of ^{282}ΔFQISL^{286} in E2F1 completely abolished RBN-E2F1 interaction (Figure 10D). Unlike p65, whose FxxxV/L sequence is surrounded by positively charged amino acids, the ^{282}FQISL^{286} sequence of E2F1 is surrounded by positively charged lysine residues and negatively charged amino acids (Figure 10A). To assess whether the differential charges in the amino acids surrounding the ^{282}FQISL^{286} motif affect the RBN-E2F1 interaction, we mutated the charged amino acids (D, E, K and K) to alanine (4A mutant) (Figure 10C, D). Furthermore, we substituted this E2F1 motif for ^{282}DQIRD^{286}, which is completely different in terms of sequence and charges (Figure 10C). Both mutants (4A and ^{282}DQIRD^{286}) eliminated the interaction between RBN-E2F1 similarly to the ^{282}ΔFQISL^{286} deletion mutant (Figure 10D), pointing out that both, the sequence of the ^{282}FQISL^{286} motif and the charges of the adjacent amino acids, were essential for binding between RBN and E2F1.

1.3 An RBN fragment of 146 amino acids is sufficient to interact with E2F1.

E2F1 ^{282}FQISL^{286} motif is sufficient for RB-E2F1 binding. To assess which is the minimal region of RBN that binds toE2F, we created a shorter RB N-terminal fragment of 146 amino acids (from amino acid 184 to 330) (Figure 11A) and performed binding assays as described previously. RBN (184-330 aa) fragment was still able of binding to E2F1 (Figure 11B).

RB S249 and T252 phosphorylation by p38 increased the affinity of RB for E2F (Gubern et al., 2016). Similarly, when the RBN (184-330 aa) protein version was phosphorylated *in vitro* at S249 and T252 by p38 or when using the RBN (184-330 aa) S249E/T252E phosphomimic mutant, binding to E2F1 increased. As expected, the non-phosphorylatable mutant of RB (S249A/T252) abolished the interaction with E2F1 (Figure 11B).

To further validate that the minimal interaction regions are the CC-MB domain of E2F and the 184-330 aa fragment of RBN, we performed a binding assay as described previously using these protein versions. E2F1 CC-MB domain and RBN (184-330 aa) protein version interacted *in vitro,* and this interaction is dependent on RB S249 and T252 phosphorylation (Figure 11C).

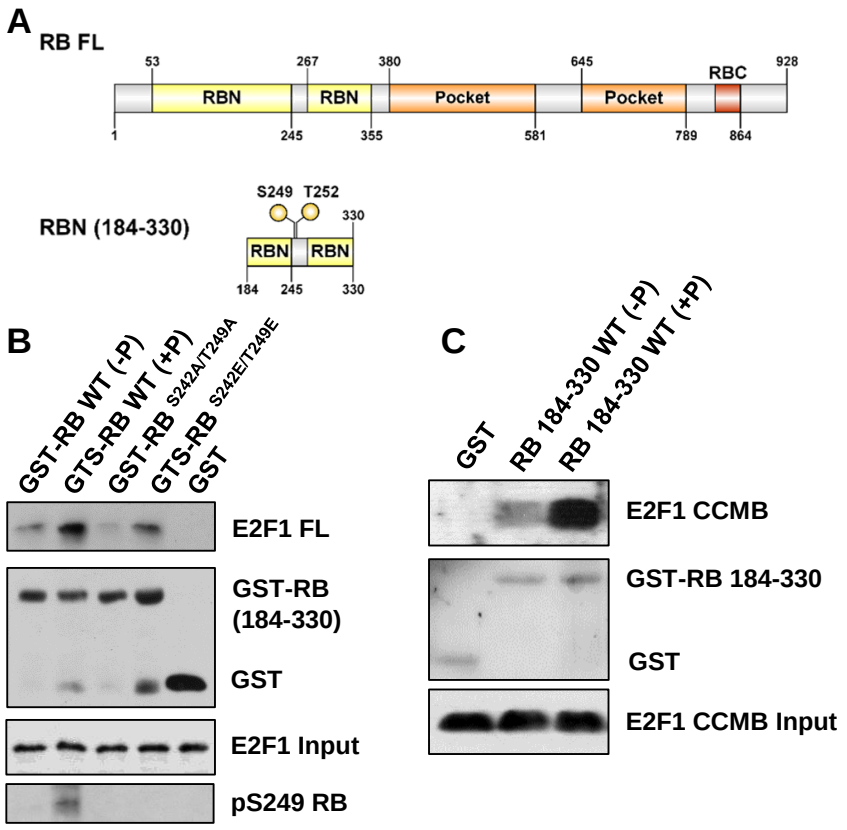

Figure 11. Binding of the RBN (184-330 aa) fragment and CCMB domain of E2F1. A. Schematic diagram depicting the RBN (184-330 aa) fragment. **B, C.** *In vitro* binding assay using purified E2F1 full-length (FL) and the indicated GST-RBN (184-330 aa) versions. RBN (184-330 aa) protein was incubated with His-E2F1 FL (B) or E2F1 CCMB domain (C). All proteins were purified from *E. Coli*. Empty GST was used as a negative control. GST and GST-RBN was pulled-down using Glutathione Sepharose beads and the co-precipitation of the E2F1 fragments was analyzed by western blotting. GST-RB (184-330 aa) was previously phosphorylated *in vitro* by p38, when is indicated (+P). **B-C**.

E2F1 CC-MB domain and RBN (184-330 aa) protein version constitute the minimal identified interaction regions between RB and E2F1. Both protein fragments are small enough to decipher the tertiary structure of the protein complex by NMR analysis. Once we

know the structure of the interaction surface, we will perform an *in-silico* compound screening that will increase the efficiency of the drug discovery process.

2. Setting up a cell-based assay to monitor RB activity amenable for HTS assays

As mentioned above, the RB phosphomimetic mutant not only reduces the expression of genes regulated by E2F and arrests the cell cycle but also reduces tumor proliferation. To address our main objective of identifying chemical compounds to restrict the proliferation of cancer cells considering RB as a therapeutic target, we developed different strategies. Apart from performing a screening of compounds *in silico* with the minimal region of RBN-E2F1 interaction described above (see section 1 of the results), we designed and developed a cell-based assay to monitor transcriptional RB activity amenable for conventional HTS assays.

The first step was designed an assay to monitor de RB activity, HEK293T cells were transfected with a plasmid containing a luciferase reporter E2F (pE2F-Luc) together with plasmids encoding HA-E2F1 and myc-RB (or GFP-RB). 48 hours after transfection, the cells were treated with different stresses (NaCl, H_2O_2, and Anisomycin) for 4 hours to activate p38 and a decrease in the transcription of the reporter upon stress was detected. We did not observe this reduction in E2F reporter transcription in cells that were transfected with the RB S249A/T252A mutant. However, the reporter signal decreased in cells transfected with the RB

S249E/T252E phosphomimetic mutant, independent of the stress treatment (Figure 12A and 12B).

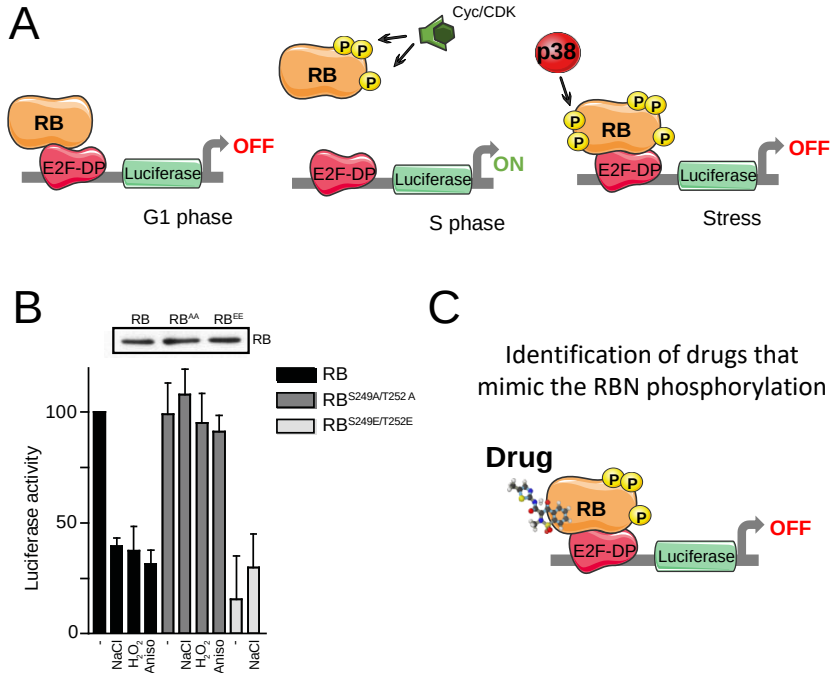

Figure 12. Cancer drug discovery assay. A. Schematic representation of the cell-based drug-screening tool to target retinoblastoma. HEK293T cell transfected with a luciferase E2F transcriptional reporter (pE2F-firefly-luciferase) together with plasmids encoding HA-E2F1 and GFP-RB. The transcription of E2F reporter is increased when Cyclin-CDK complex inhibits RB and is repressed upon stress when p38 phosphorylates RB at the S249/T252 sites. **B.** S249/T252 phosphorylation by p38 upon stress or a mutant phosphomimetic RB S249E/T252E repress E2F reporter transcription. RB S249A/T252A did not decrease reporter transcription independent of stress treatments. HEK293T cells were transfected with HA-E2F1 and pE2F-Luc together with wild-type myc-RB, RB S249A/T252A or RB S249E/T252E. Cells were treated with 100 mM NaCl, 400 mM H_2O_2, or 25 ng/mL Anisomycin (Aniso) for 4 hours. Adapted from Gubern *et al.,* 2016. **C.** Main objective of the drug discovery assay. Identification of drugs that mimic RBN phosphorylation.

The second step was to set up the large-scale assay to identify compounds capable of mimicking the phosphorylation at the S249/T252 sites of RB in order to increase its affinity for E2F, decrease the cell cycle regulatory genes expression, and arrest cell proliferation (Figure 12C). Since the candidates identified would have an effect on RB regulation and, therefore, an inhibitory effect on cell cycle progression, they could be good candidates to develop new antineoplastic therapies.

During the optimization process, the cell-based assay was developed and optimized in a 96, 384-well / plate format compatible with the use of HTS platforms and automated methodology. We performed a large number of assays to test different conditions (such as transfection condition, plate format, etc.) and the starting conditions selected for subsequent HTS assays are summarized in Table 3.

The cell line used was HEK293T cells because they are particularly easy to transfect and culture. Cells were seeded in a 384 well / plate format and cell were transfected with the three plasmids (pE2F-Luc, HA-E2F1 and myc-RB (or GFP-RB)) simultaneously (0.1 μg /total per well), using the reagent Fugene 6 transfection (from promega). The rate of transfection of each plasmid was an important test, because we observed that a high expression of RB reduced the luciferase signal too much, on the contrary, with a low expression of RB we would not detect those compounds that act on RB. The appropriate ratio of the plasmids was 1: 2: 8 for pE2F-Luc, HA-E2F1 and myc-RB plasmids, respectively. It should be noted that the expression of the plasmid myc-RB is lower than the

expression of GFP-RB, whose suitable ratio is 1: 1: 1/4 (pE2F-Luc, HA-E2F1 and GFP-RB plasmids, respectively). 48 hours after transfection, the cells were stressed. Anisomycin and H_2O_2 were used as positive control because they induced RB phosphorylation by p38 and reduces transcription of the reporter. Cells without treatment or treated with the dilution vehicle (dimethyl sulfoxide, DMSO) were used as negative control. After 4 hours of incubation at 37ºC the cells were lysed, we added Luciferase Assay Reagent (Promega) and the luminescence emitted in each well was measured in a Centro LB 960 microplate luminometer (Berthold technologies) (0.5 sec/read) (Table 3).

Table 3. Starting assay conditions selected for performing the HTS assays

	Starting conditions selected for HTS assays
Cell line	HEK29T cell Line
Assay Format	Optimized assay in a 96,384-well/plate format
Transfection conditions	Transfection Reagent: Fugene 6 Plasmids:E2F-luc, HA-E2F, Myc-RB or GFP-RB Plasmid ratio: 1:2:8 (E2F-luc, HA-E2F, Myc-RB) 1:1:1/4 (E2F-luc, HA-E2F, GFP-RB) DNA per well 384 plate format: 0.1 µg total DNA/well
Controls	Negative: DMSO Positive: Anisomycin or H_2O_2
Incubation conditions	37ºC 4 hours of incubation
Detection Reagent	Luciferase assay system (E1500 Promega)

To date, RB has been defined as a non-druggable protein, since no one has managed to design drugs that improve its tumor-suppressing activity. Our assay places RB as a possible therapeutic target and focuses on spotting optimal candidates for preclinical development.

3. Pilot HTS assays to identify compounds that regulates RB activity

The cell-based assay was then developed and optimized in a 96, 384-well/plates format compatible with the use of HTS platforms, and the methodology (see Experimental Procedures and section 1 of the results) was transferred to two drug discovery platforms for automation and large-scale screening development. A first pilot HTS was carried out at Innopharma (Santiago de Compostela University, Galicia) and a second pilot HTS, including certain methodological improvements was performed at the Centre for Drug Research and Development (CDRD) (Vancouver, Canada).

3.1 Screening platforms and chemical libraries

Innopharma and CDRD are pharmacological research platforms focused on filling the gap between basic research on new therapeutic mechanisms and their industrial application, carrying out projects that add value to scientific knowledge. Both entities provided the platforms to develop HTS assays. They provided expertise for miniaturization and development of HTS, equipment (automated dispensing systems, multifunctional plate readers) as well as compound libraries.

Innopharma screened a total of 4203 compounds from two different chemical libraries: DTP-NCI (2923 compounds) and Prestwick (1280 compounds). Additionally, the CDRD platform screened 5000 small molecules from two libraries, LOPAC and KD2. For confidentiality reasons, compounds will be named with the initial of the library (N for DTP-NCI, P for Prestwick and L/K

for LOPAC/KD2 library) followed by a number (N1: drug 1 from the DTP-NCI library, P1: drug 1 from the Prestwick library, L/K1: drug 1 from LOPAC/KD2 library).

3.1.1 DTP-NCI Chemical library

The Developmental Therapeutics Program (DTP) of the National Cancer Institute (NCI) facilitates the development of therapeutic agents for cancer. Its main aim is to turn "molecules into medicine for their use in public health". DTP maintains a repository of synthetic compounds and pure natural products, which are evaluated as possible anticancer drugs. The drug repository collection comes from a historical database of more than 600,000 compounds, which have been supplied to DTP from a diversity of sources worldwide. The DTP-NCI Chemical library available consists of 2,923 out of those 600,000 compounds from several subsets:

- **Diversity Set**: 1,596 compounds with high chemical diversity selected from 140,000 compounds library.
- **Mechanistic set**: Compounds that showed a broad range of growth inhibition patterns of 60 different cell lines in NCI screening assays. 813 out of 37,836 compounds have been selected.
- **Natural Product set**: 419 natural molecules that were selected from 140,000 compounds.
- **Approved Oncology Drugs set**: 95 drugs approved by the Food and Drug Administration (FDA).

3.1.2 PRESTWICK Chemical library

The Prestwick Chemical Library (PCL) is a collection of 1,280 small molecules with high chemical and pharmacological diversity. The drugs of this library are approved by the FDA, EMEA and other agencies. More than half of the drugs in the library are dedicated to the central nervous system, cardiovascular, metabolism and infectious diseases. The aim of using this library was to discover new uses for already approved drugs (drug repurposing). The main advantage of this strategy in drug development is that since these off-patent drugs have been fully evaluated, safety data are known and so the early cost and time needed to bring a drug to market could be spared. Indeed, the use of this library has demonstrated to be a high-quality tool for drug development, allowing the detection of new indications and mechanisms of action of several compounds.

3.1.3 LOPAC Library and extension KD2

The LOPAC and KD2 libraries are made up of 5,000 pharmacologically active compounds from known drugs from the SIGMA Aldrich Company. These molecules have shown high power and bioactive performance. This collection is composed of inhibitors, receptor ligands, pharma-developed tools, and approved drugs which impact most signaling pathways and covers all major drug target classes.

A clear advantage of using this library is that it is marketed, and the compounds are normalized and pre-solubilized in DMSO,

presenting a ready-to-use format that require less time-consuming sample preparation.

3.2 Optimization of cell-based HTS by Innopharma

As mentioned before, the protocol and materials of the cell-based assay that monitors RB activity were transferred to the Innopharma drug discovery platform for its automation.

The activity of the luciferase reporter was measured in HEK293T cells seeded in 384 well-plates and transfected in the 384 well-plate format with the plasmids E2F-luc, HA-E2F and myc-RB using Fugene 6 reagent. In parallel, GFP was included as a transfection efficiency control that was visualized 24 hours later in the Operetta High Content System (Perkin Elmer). 24 hours later, the transfected cells were treated with 0.5% DMSO as a negative control (vehicle in which the drugs are dissolved) and 50 μM Anisomycin as a positive control (Anisomycin induces RB phosphorylation by p38 and reduces transcription of the reporter; see Figure 5 and 12B). After 4 hours incubation at 37ºC the cells were lysed. 15 min later, the luciferase reagent was added for detection of the signal and luminescence was measured in a Tecan Infinite M1000Pro (0.5 sec/read). Concentrations of transfected plasmids, amounts of fetal bovine serum (FBS), types of culture media (DMEM / Opti-MEM) and other technical modifications were evaluated for the optimization and automation process (Figure 13).

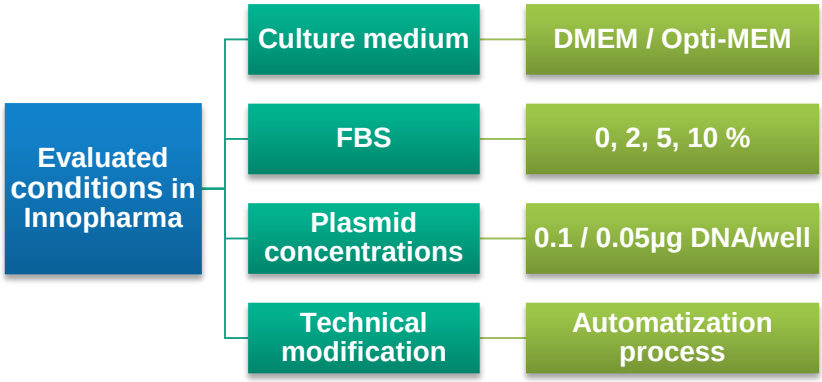

Figure 13. Schematic representation of the conditions evaluated for assay optimization. Innopharma assessed different conditions (type of culture medium, amount of FBS, concentrations of the transfected plasmids and other technical modifications) for the automatization of the process.

The optimum conditions for performing the HTS assay are shown in the Table 4. The results obtained with these conditions showed a correct signal/background ratio (or DMSO/Anisomycin) (S/B = 2), an adequate Z' for HTS (Z' = 0.46) and a variation adjusted to the quality criteria of below 10 % (CV = 5.7%) (Figure 14).

Table 4. Selected assay conditions for performing the HTS showing the best results in terms of quality standards.

Cell culture	Transfection per well	Treatments	Reagent
30,000 adherent cells DMEM 2%FBS	Fugene 6 transfection Reagent Plasmids: E2F-luc / HA-E2F / Myc-RB / GFP 0.1 µg total DNA/well	0.5% DMSO / 50µM Anisomycin 37ºC 4h incubation	Luciferase assay system (E1500 Promega)

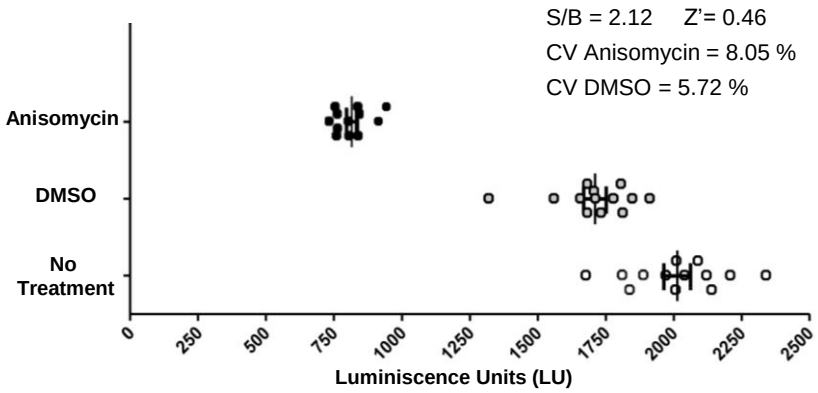

Figure 14. Automatization and optimization of the cell-based HTS assay by Innopharma. The assay was adjusted to quality standards. HEK293T cells were transfected with HA-E2F, E2F-luc, Myc-RB and GFP. 48 hours after, cells were treated with 0.5% DMSO as a negative control or 50 μM Anisomycin as a positive control for 4 hours at 37ºC. Luciferase activities are expressed using absolute luminescence units.

Taking into account that the aim of the screening assay was to identify new compounds for cancer therapy that mimic the effect of RB phosphorylation by p38, Innopharma first performed a small screening with 95 compounds from the Approved Oncology Drugs (AOD) set. The data obtained from this screening confirmed that the assay worked correctly after optimization and automatization processes, as Anisomycin caused a 2-fold reduction in luciferase activity compared with untreated cells or treated with DMSO. Positive compounds (hits) were defined using the approach [average – 2Standard deviation (SD)]. These assays were subject to a certain level of variability and a small assay window (2X). Therefore, it was decided to relax the quality criteria [average-2SD instead of average-3SD] to avoid losing interesting candidates,

although this implied increasing the validation effort to discard false positives.

From this small HST assay, we identified 9 hits at 1 and 10 µM that reduced luciferase activity with respect to the threshold level (better or similar effect as Anisomycin) (Figure 15A). Hits were then "cherry picked" and assayed again to confirm their activity. Drug N11, an antiangiogenic approved drug for the treatment of kidney cancer, was the only compound confirmed (Figure 15B).

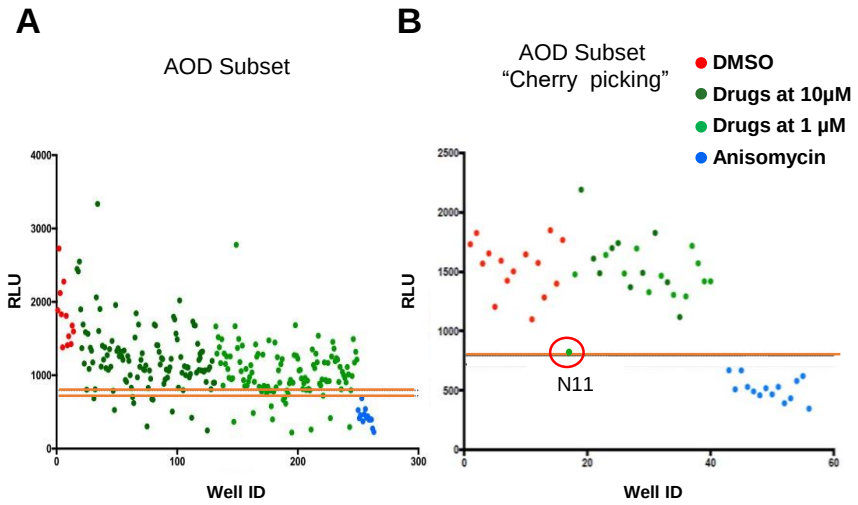

Figure 15. 1 hit from the AOD subset (DTP-NCI Chemical library) was identified and confirmed in the Innopharma pilot screening. A. 9 hits from the AOD subset were identified. HEK293T cells were transfected with HA-E2F, E2F-luc, Myc-RB and GFP. The cells were treated with the compounds at 10 and 1 µM, 0.5% DMSO as a negative control and 50 µM Anisomycin as a positive control for 4 hours at 37ºC. Hits were defined using the criteria [average - 2SD]. **B.** A single compound, N11 at 10 µM inhibited the luciferase reporter during the drug selection process or "cherry picking".

3.3 Identification of hits by cell-based pilot HTS assay using the DTP-NCI chemical library

The results of the small screening using the AOD subset demonstrated that the assay could be used in an automated HTS process. The primary pilot screening was then carried out with the complete DTP-NCI library (2,923 compounds) following the same protocol as the previous screening, but the compounds were only assayed at 1 µM. 46 hits were identified (hit rate = 1.5%) using the selection approach [average-2SD] (Figure 16A). Out of these 46 initially identified hits, 39 were confirmed during the "cherry picking" process (Final hit rate = 1.3%) (Figure 16B).

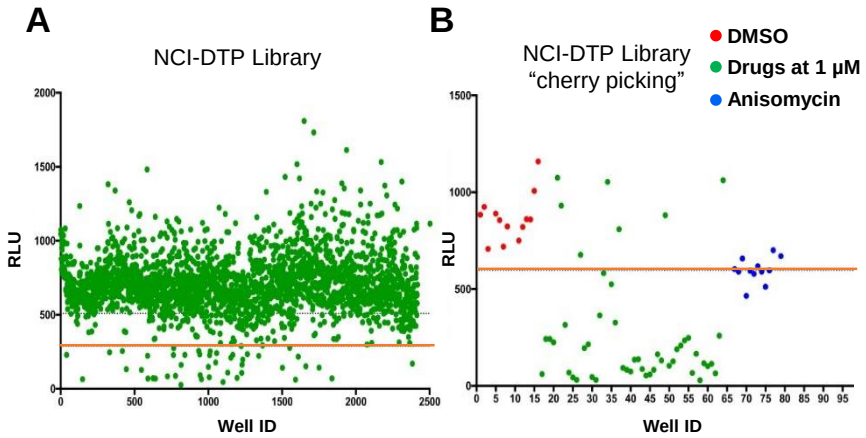

Figure 16. 39 hits from DTP-NCI Chemical library were identified and confirmed. A. 46 hits from whole DTP-NCI chemical library reduced the luciferase activity with respect to the threshold level (hit rate = 1.5%) **B.** 39 out of the 46 hits identified were confirmed during the drug selection process or "cherry picking". (hit rate = 1.3%). The luciferase activity was measured as relative luminescence units (RLU).

As in any HTS, false activities due to interferences with the technology (luciferase inhibitions, light quenching) or to a

compound's propensity to be active in a high number of screenings (frequent hitters) need to be removed. For this purpose, a bibliographic analysis was carried out. 14 out of the 39 confirmed hits were discarded for various reasons such as being luciferase inhibitors, unspecific translation inhibitors, duplicates, or frequent hitters (Table 6). The compounds' bioactivity in other screenings data were obtained from the PubChem web site. Thus, 25 compounds from the DTP-NCI Chemical library (from N1 to N25) were considered as drugs that specifically inhibited RB activity at 1 μM (Table 5).

Table 5. Hits that showed reduced RB activity and their bioactivity in other screening data from PubChem. Last column indicates the hits prioritized for further analysis.

Drug ID	Bioactivity in other screening assays	Read Out	Priority
N1	Small molecule inhibitors of shiga toxin asay	Luciferase	Prioritized hit
N2	Activators of apoptosis of cancer cells assay	Luciferase	Prioritized hit
N3	Yeast anticancer drug screen	Luciferase	Prioritized hit
N4	Small molecule inhibitors of shiga toxin assay	Luciferase	Prioritized hit
N5	Small molecule inhibitors of shiga toxin assay	Luciferase	Prioritized hit
N6	Activators of apoptosis of cancer cells assay	Luciferase	Prioritized hit
N7	Tyrosyl-DNA phosphodiesterase 1 inhibitors	Luciferase	Prioritized hit
N8	In vivo anticáncer drug HTS. Leukemia in mice	Tumor Size	Prioritized hit
N9	Human tumor cell line growth inhibition assay	Cell Growth	Prioritized hit
N10	Biochemical HTS to identify inhibitors of BCL2-related protein.	Fluorescence	Prioritized hit
N11	Inhibition of recombinant VEGFR2 (Axitinib)	Fluorescence	Prioritized hit
N12	HTS for inhibitors of the JAK2V617F mutant	Luciferase	Prioritized hit
N13	Modulators of MEK Kinase interactions assay	Fluorescence	Prioritized hit
N14	HTS to identify antagonists of GPR7 protein	Fluorescence	Prioritized hit
N15	Inhibition of JAK in BALB/c mouse B cells	Citometry	Prioritized hit
N16	Inhibitors of the HSP90 assay	Luciferase	Non-Prioritized hit
N17	Identification of inhibitors of shiga toxin	Luciferase	Non-Prioritized hit
N18	Tumor cell line growth inhibition HTS	Cell Growth	Non-Prioritized hit
N19	Leukemia cell line growth inhibition assay	Cell Growth	Non-Prioritized hit
N20	Inhibitors of the HSP90 assay	Luciferase	Non-Prioritized hit
N21	Inhibitors of the HSP90 assay	Luciferase	Non-Prioritized hit
N22	Apoptosis activators of cancer cells assay	Luciferase	Non-Prioritized hit
N23	Small molecule inhibitors of shiga toxin	Luciferase	Non-Prioritized hit
N24	RGS proteins interaction regulator assay	Fluorescence	Non-Prioritized hit
N25	Inhibitors of the ERK pathway assay	Luciferase	Non-Prioritized hit

Table 6. Discarded hits and bioactivity in other screenings data from PubChem**.**

Drug ID	Bioactivity in other screening assays	Read Out	DISCARD CAUSE
D N1	NCI tumor cell line growth inhibition assay	Cell Growth	False positive in other HTS
D N2	Anticancer drug HTS. Leukemia in mice	Tumor Size	False positive in other HTS
D N3	Anticancer drug HTS. Leukemia in mice	Tumor Size	False positive in other HTS
D N4	In vivo anticancer drug HTS	Tumor Size	False positive in other HTS
D N5	AIDS antiviral assay	Cell Growth	False positive in other HTS
D N6	Orphan nuclear receptor inhibitors assay	Luciferase	False positive in other HTS
D N7	SWI/SNF inhibitors assay	Luciferase	False positive in other HTS
D N8	Human tumor cell line growth inhibition HTS	Cell Growth	False positive in other HTS
D N9	HTS to identify inhibitors of luciferase	Lucifearse	Inhibitors of Luciferase
D N10	HTS to identify inhibitors of luciferase	Luciferase	Inhibitors of Luciferase
D N11	HTS to identify inhibitors of luciferase	Lucifearse	Inhibitors of Luciferase
D N12	Translation initiation inhibitors HTS	Fluorescence	Translation inhibitor
D N13	Inhibitors of the ERK pathway assay	Luciferase	Duplicate, Drug N25
D N14	Tumor cell line growth inhibition assay	Cell Growth	Druplicate, Drug N15

Next, the 25 positive hits were analyzed by a medical chemist. Structures of the hits were generated from the Pubchem ID and physical properties were calculated using Vortex (Dotmatics software). Compounds were analyzed by structural type and physical chemistry profile with particular emphasis on potential for cell penetration. According to these criteria, the hits can be further divided into 4 sub series, in which all the positive compounds are included, except for N15, which is a compound of natural origin and has a more complex structure. The four subseries are different at the structural level, all of them have a common aromatic group linked to different substituents characteristic of each chemical series. For confidentiality reasons, chemical structures will not be shown. The first series includes compounds N1, N3, N10, N12 and N14. The second series is made up of N2, N4, N6, N7, N8, and N11. Compound N5 are included in series 3. Finally, the fourth series is formed by compound N9 and N13.

According to the medical chemistry characterization, we prioritized 15 out of the 25 positive hits, which were commercially

available, for further studies. Overall, we ensured that non-prioritized compounds (N16-25) belonged to one of the four established chemical series. Thus, the 15 selected compounds (N1-15) guaranteed the representation of the chemical series and the optimization of resources.

Next, Innopharma determined the potency of the 15 prioritized hits by running a dose response assay (Figure 17) and estimating the IC50 (compound concentration necessary to inhibit the luciferase reporter gene by 50%) and the pIC50 (negative logarithm of the IC50 molar value) parameters for each compound (Table 7). The IC50 and pIC50 parameter allowed us to validate these selected hits and to rank them in terms of potency.

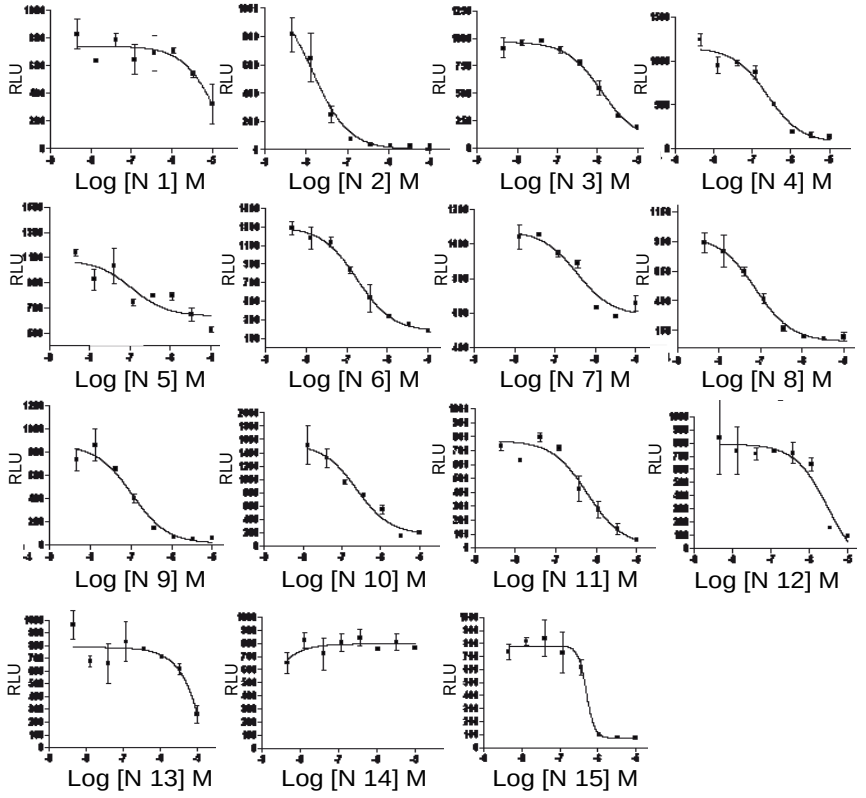

Figure 17. Dose response of 15 confirmed hits from the DTP-NCI library.

HEK293T cells were transfected with HA-E2F, E2F-luc, Myc-RB and GFP. The compounds concentrations assayed were 0.005, 0.01, 0.05, 0.1, 0.5, 1, 5, and 10 µM for 4h at 37ºC. The luciferase activity was measured as relative luminescence units (RLU).

Table 7. Classification of 15 prioritized hits from DTP-NCI, ranging from highest to lowest activity in the assay according to their IC50 and pIC50 values.

Drug ID	RB activity assay **IC_{50} (µM)**	RB activity assay **pIC_{50}**
N 2	0.01	7.84 ± 0.18
N 8	0.08	7.12 ± 0.11
N 9	0.10	6.98 ± 0.14
N 5	0.11	6.95 ± 0.37
N 6	0.18	6.74 ± 0.10
N 10	0.24	6.61 ± 0.19
N 4	0.25	6.60 ± 0.12
N 7	0.35	6.45 ± 0.21
N 15	0.50	6.30 ± 0.11
N 11	0.59	6.22 ± 0.15
N 3	1.27	5.89 ± 0.09
N 12	3.02	5.52 ± 0.36
N 1	15.20	4.81 ± 0.97
N 13	99.64	4
N 14	-	-

Although compound N14 was not active in this last dose-response assay, we did not discard it, due to its structural similarities with drug N12. We also did not rule out compound N13 which showed low activity because its structure was like N9 (Table 7).

Additionally, Innopharma performed a complementary assay to measure the cytotoxic capacity of the selected compounds using the cellTiter-Glo luminescent cell viability assay. This assay estimates the number of viable cells by quantifying the ATP present in the culture, as an indicator of metabolically active cells (Figure 18). The compounds' cytotoxicity capacity was measured by running dose response assays and quantifying IC50 and pIC50 (Table 8).

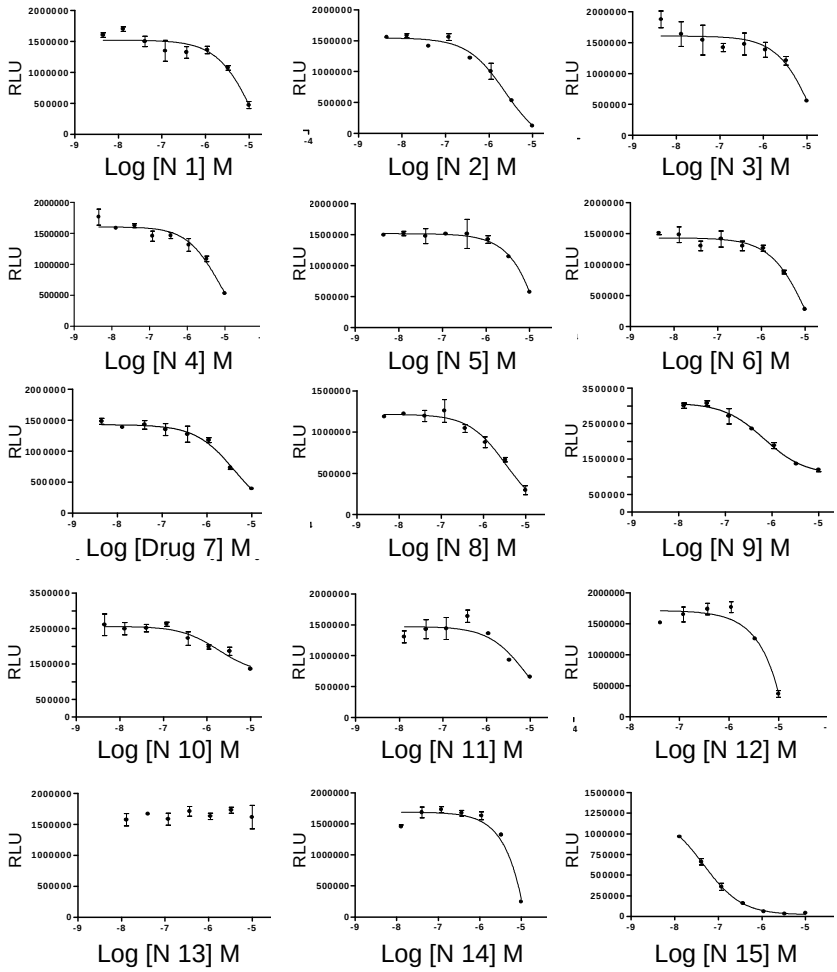

Figure 18. Dose-response of 15 selected hits from the DTP-NCI library to determine the cytotoxicity. Dose response of validated hits. The compound concentrations assayed were 0.005, 0.01, 0.05, 0.1, 0.5, 1, 5, and 10 μM for 4 hours at 37ºC. The luciferase activity was measured as relative luminescence units (RLU).

Table 8. Classification of 15 selected hits from DTP-NCI ranging from highest to lowest cytotoxic activity according to IC50 and pIC50 values.

Drug ID	Cytotoxic activity **IC_{50} (µM)**	Cytotoxic activity **pIC_{50}**
N 15	0.04	7.33 ± 0.05
N 9	0.68	6.17 ± 0.09
N 10	1.84	5.73 ± 0.26
N 2	2.34	5.63 ± 0.09
N 8	3.36	5.47 ± 0.16
N 7	4.10	5.38 ± 0.14
N 4	7.10	5.15 ± 0.23
N 11	8.46	5.07 ± 0.50
N 6	12.87	4.89 ± 0.28
N 1	14.63	4.83 ± 0.44
N 3	17.78	4.74 ± 0.73
N 5	55.07	4.25 ± 1.06
N 12	1680	2.77 ± 31.9
N 14	3409	2.46 ± 47.9
N 13	Non-cytotoxic at 10 µM	-

3.4 Identification of hits by cell-based pilot HTS using the Prestwick chemical library

The Prestwick library is a unique collection of 1,280 off-patent marketed compounds. The HST assay was performed as mentioned before, although assaying two concentrations (1 and 10 µM). 27 hits out of 1,280 were identified following the same selection criteria [average-2SD] as with the DTP-NCI library (Figure 19A). The "cherry picking" process was carried out according to the protocol used for the DTP-NCI library. 4 out of the 27 hits identified were confirmed (Figure 19B). Additionally, the potency of these 4 hits was characterized by using dose-response curves (Figure 19C) and the compounds were classified based on their potency (Table 9).

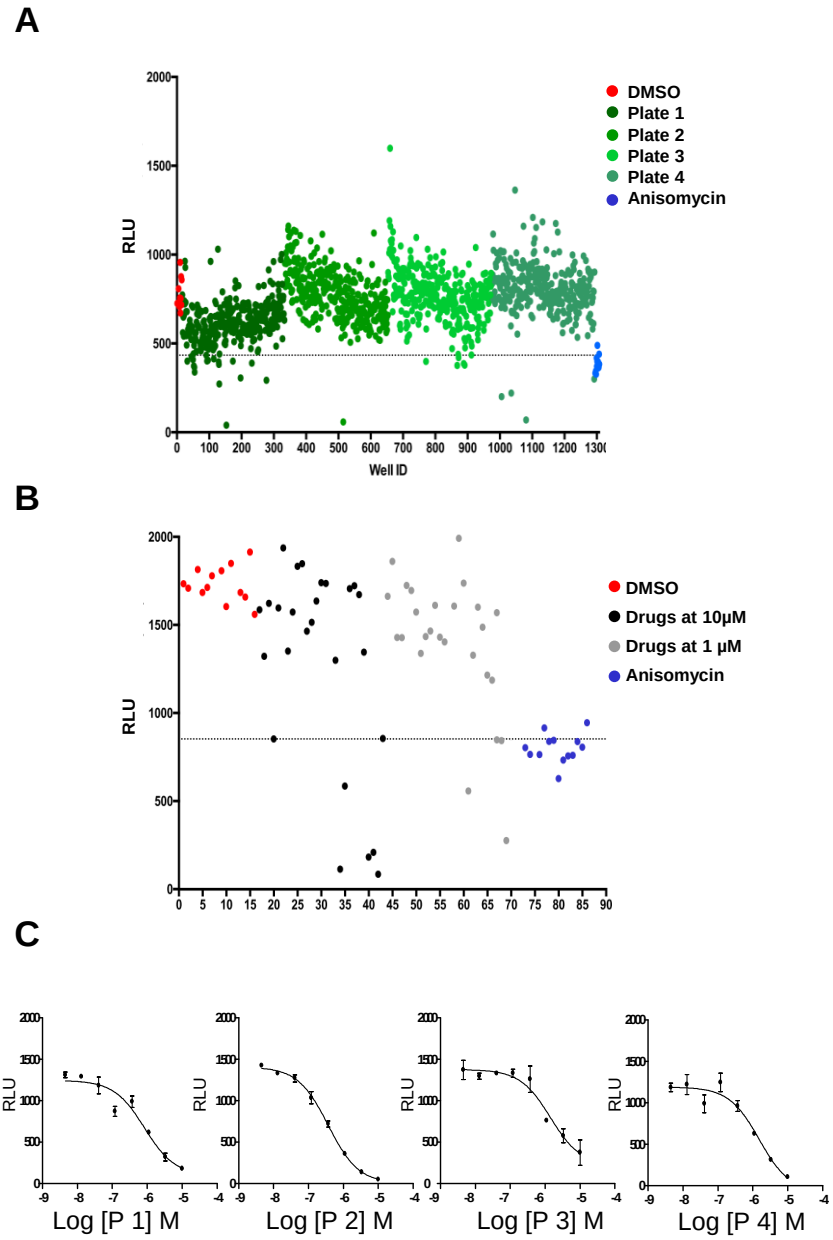

Figure 19. 4 hits from the Prestwick chemical library were identified and confirmed. A. 27 hits from the Prestwick chemical library were recognized. HEK293T cells were transfected with HA-E2F, E2F-luc, Myc-RB and GFP. The cells were treated with the compounds of the library at 1 or 10μM, 0.5% DMSO as a negative control or 50 μM Anisomycin as a positive control for 4 hours at

37ºC. Hits were defined using the criteria [average - 2SD]. **B.** 4 out of 27 initial identified hits inhibited the luciferase reporter at 1 µM during the drug selection process or "cherry picking". **C.** Dose response of validated hits. The compound concentrations assayed were 0.005, 0.01, 0.05, 0.1, 0.5, 1, 5, and 10 µM for 4 hours at 37ºC. The luciferase activity was measured as relative luminescence units (RLU).

Table 9. Classification of the 4 selected hits from highest to lowest activity according to its IC50 and pIC50 values and its medical indication.

Drug ID	**Indication**	RB activity assay **IC_{50} (µM)**	RB activity assay **pIC_{50}**
P 2	Antiparasirtic and antiviral	0.37	6.43 ± 0.04
P 1	Antiallergic	0.83	6.07 ± 0.15
P 3	Prevention of osteoporosis	1.41	5.85 ± 0.18
P 4	Antiallergic (asthma)	1.52	5.81 ± 0.16

The chemistry analysis based on the structure and physicochemical characteristics of these 4 compounds revealed that P1 and P2 were represented in series 2 and series 1, respectively, of the 4 chemical subseries classification defined for the NCI-DTP library hits. P3 and P4 increased the chemical diversity by not belonging to any of the previous classifications.

In addition, as with the DTP-NCI library, Innopharma performed a complementary assay to measure the cytotoxicity in a dose response of the selected compounds using the cellTiter-Glo luminescent cell viability assay. (Figure 20; Table 10).

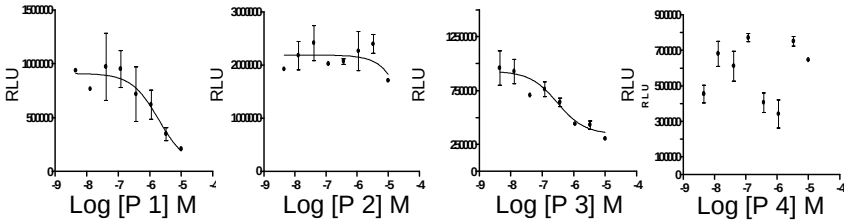

Figure 20. Dose-response of 4 selected hits from the Prestwick library to determine the compound cytotoxicity. Dose response of validated hits. The compounds concentrations assayed were 0.005, 0.01, 0.05, 0.1, 0.5, 1, 5, and 10 µM for 4 hours at 37ºC. The luciferase activity was measured as relative luminescence units (RLU).

Table 10. Classification of 4 selected hits from DTP-NCI ranging from highest to lowest activity in the cytotoxicity assay according to IC50 and pIC50 values.

Drug ID	Cytotoxic activity **IC_{50} (µM)**	Cytotoxic activity **pIC_{50}**
P 3	0.30	6.43 ± 0.04
P 1	1.93	6.07 ± 0.15
P 2	Non-cytotoxic at 10 µM	-
P 4	Non-cytotoxic at 10 µM	-

3.5 Optimization of the cell-based HTS by CDRD

It was not possible to perform a large-scale HTS assay at Innopharma due to platform funding issues and therefore we decided to look for an alternative.

We then established the cellular system and the optimization process of the assay to perform the HTS assay in the CDRD drug discovery platform (Vancouver, Canada). Specifically, and in comparison, with the procedure used for Innopharma, we improved the protocol to increase the assay window and decrease its variability.

HEK293T cells were only transfected with three plasmids E2F-luc, HA-E2F and GFP-RB, which increased the transfection efficiency. Moreover, we performed the cell transfection in bulk, instead of carrying out individual transfections per well to reduce assay variability. Also, the transfection reagent was changed to polyethylenimine (PEI) which is cheaper and easier to work with compared with Fugene 6. After 48 hours, transfected cells were harvested, washed, and resuspended in HBSS. Then, cells were seeded at 10,000 cells / 20 µl / well in plates preprinted with the compounds and incubated for 2 hours at 37ºC instead of Innopharma's conditions (30,000 adhered cells / well; 24 hours later, cells were treated with the drugs for 4 hours at 37ºC). Finally, to reduce the protocol steps, CDRD used the Bright-Glo detection reagent from Promega, which contains the detection reagent and lysis buffer in the same solution, instead of the conventional luciferase assay system with two different reagents. We added 20 µL Bright-Glo detection reagent / well, incubated at RT for 5 minutes and read on a Varioskan (0.5 sec/read) (Table 11).

Regarding quality criteria, the protocol used by CDRD showed robust results. CDRD achieved a suitable assay window using H_2O_2 at 1mM as a control. CDRD showed an assay window (S/B = 6.9) and Z' score (Z′ = 0.52) using 1 mM H_2O_2 as a control (Figure 21).

Table 11. Protocol modifications by CDRD regarding the assay conditions established by Innopharma.

	Innopharma protocol	Handicaps	Improvement in CDRD
CELL CULTURE	30.000 cell adhered/well; 4 hours at 37ºC	Time consuming protocol	10.000 cells in suspension/well 2 hours at 37ºC
PLASMIDS	E2F-luc, HA-E2F, Myc-RB, GFP	4 different plasmids	E2F-luc, HA-E2F, GFP-RB
TRANSFECTION	Transfection/well Fugene6 reagent	Hight variability More steps	One transfection in bulk PEI Reagent
CONTROLS	DMSO / 50µM Anisomycin	CDRD obtained a high assay window	Use as a control H2O2 at 1mM
DETECTION	Luciferase assay system	More steps (lysis reagent /mix /detection reagent)	Bright-Glo reagent (1 step)

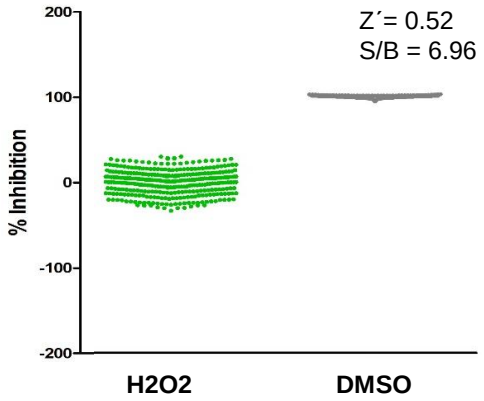

Figure 21. Development and optimization of the cell-based assay by CDRD. The assay was adjusted to the quality standards showing S/B=6.96 and Z´=0.52. HEK293T were transfected with HA-E2F, E2F-luc and GFP-RB. 48 hours after, the cells were harvested, seeded (10.000 cell/well) in 384 well/plate pretreated with 0.5% DMSO as a negative control or 1 mM H_2O_2 as a positive control and incubated for 2 hours at 37ºC. The percentage of inhibition of the luciferase activity is expressed relative to controls (DMSO and H_2O_2).

3.6 Identification of hits by a second cell-based pilot HTS assay using the LOPAC / KD2 chemical library

Next, the LOPAC/KD2 chemical library (5,000 pharmacologically active compounds distributed by SIGMA Aldrich) were assayed at 10 μM for 2 hours at 37ºC by the CDRD drug discovery platform. Out of the 5,000, 40 drugs reduced the expression of luciferase reporter with respect to the threshold level (hit rate = 0.8%). These hits were identified following the selection criteria [average - 3SD] (Figure 22).

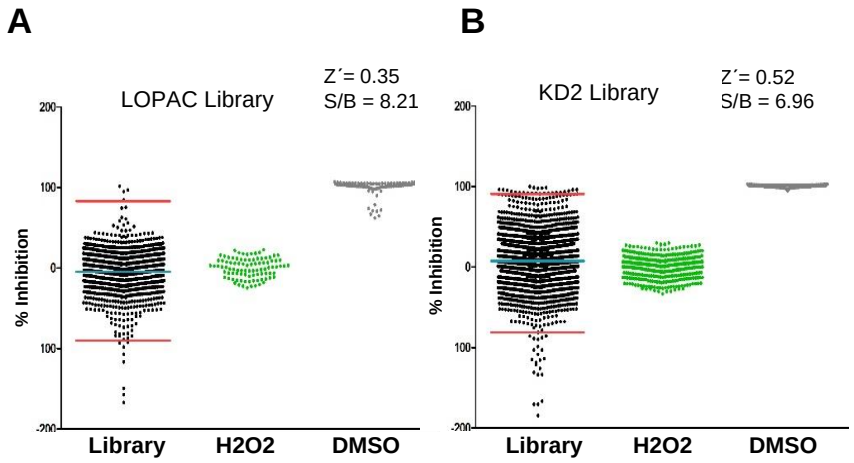

Figure 22. Pilot HTS assay with the LOPAC/KD2 chemical library identified 40 hits that affected RB activity. The assay was adjusted to the quality standards showing S / B = 8.21 – 6.96 and a Z´= 0.35 – 0.52. HEK293T cells were transfected with HA-E2F, E2F-luc and GFP-RB. 48 h after, the cells were harvest and 10,000 cells / well were seeded in 384 well-plates pretreated with the compounds at 10 μM, 0.5% DMSO as a negative control or 1 mM H_2O_2 as a positive control. Then, cells with the compounds were incubated for 2 hours at 37ºC. The percentage of inhibition of luciferase activity is expressed relative to controls (DMSO and H_2O_2).

The "Cherry picking" process was performed by diluting each compound 1:3 over 8 points starting at 30 μM to measure the potency of the compounds (Figure 23). Like Innopharma, CDRD also performed a complementary assay to measure the cytotoxic capacity of the selected compounds using the cellTiter-Glo luminescent cell viability assay. The ATP present in the culture as an indicator of metabolically active cells was measured by dose response assays, diluting each compound 1:3 over 8 points starting at 30 μM (Figure 23). Those compounds that showed greater inhibition of luciferase reporter expression than cytotoxicity, were selected. Thus, compounds whose % of inhibition of luciferase reporter expression (black dots Figure 23) that lay above the % of cell death (red dots Figure 23) and responded in a dose dependent concentration were considered as confirmed hits. The results revealed that 3 out of the 40 hits showed inhibition of luciferase reporter transcription with low toxicity. The medical chemical analysis did not include these three hits in the 4 series established for the Innopharma screening hits due to their complex structure as they are natural products.

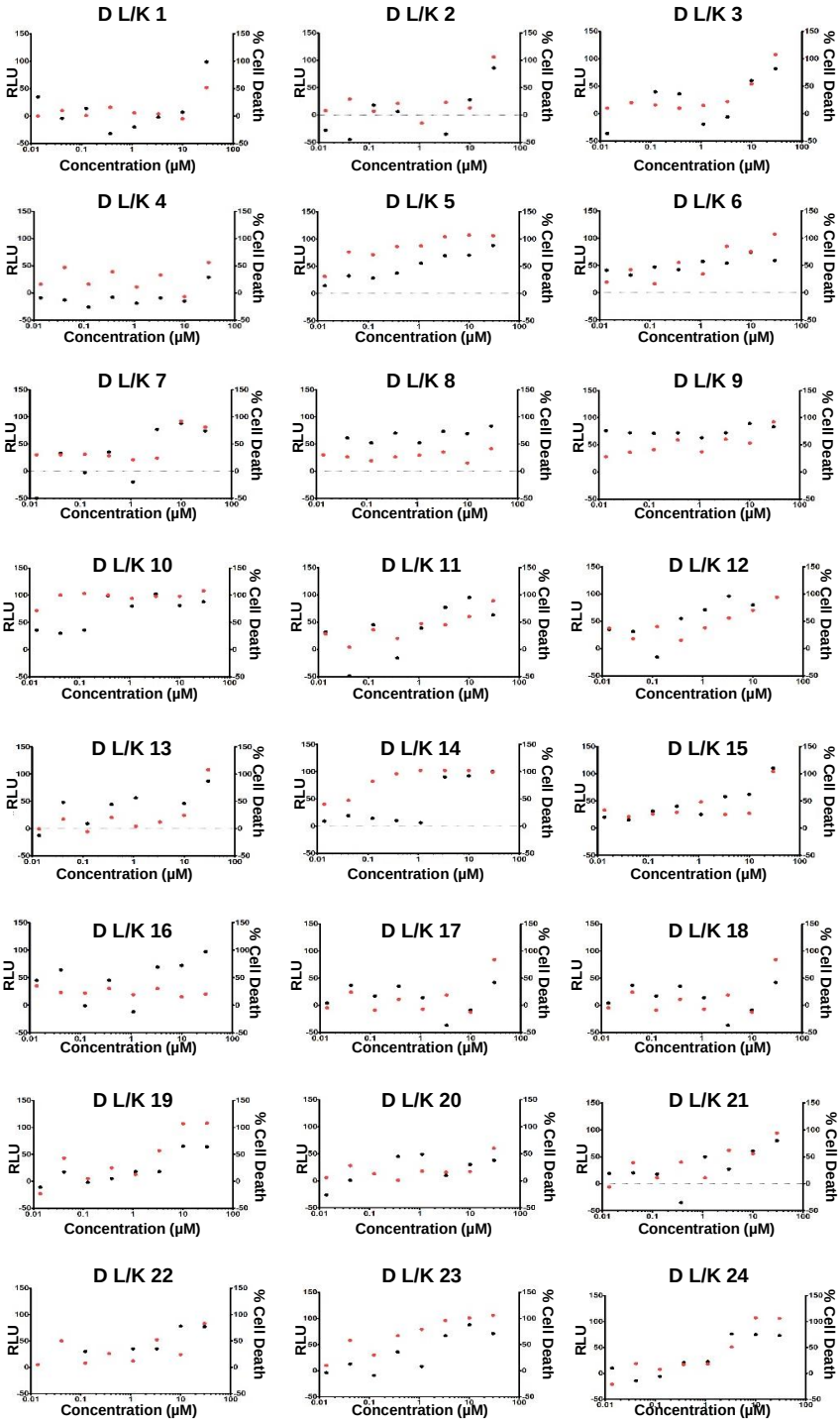
D L/K 1
D L/K 2
D L/K 3
D L/K 4
D L/K 5
D L/K 6
D L/K 7
D L/K 8
D L/K 9
D L/K 10
D L/K 11
D L/K 12
D L/K 13
D L/K 14
D L/K 15
D L/K 16
D L/K 17
D L/K 18
D L/K 19
D L/K 20
D L/K 21
D L/K 22
D L/K 23
D L/K 24
RLU
% Cell Death
Concentration (μM)

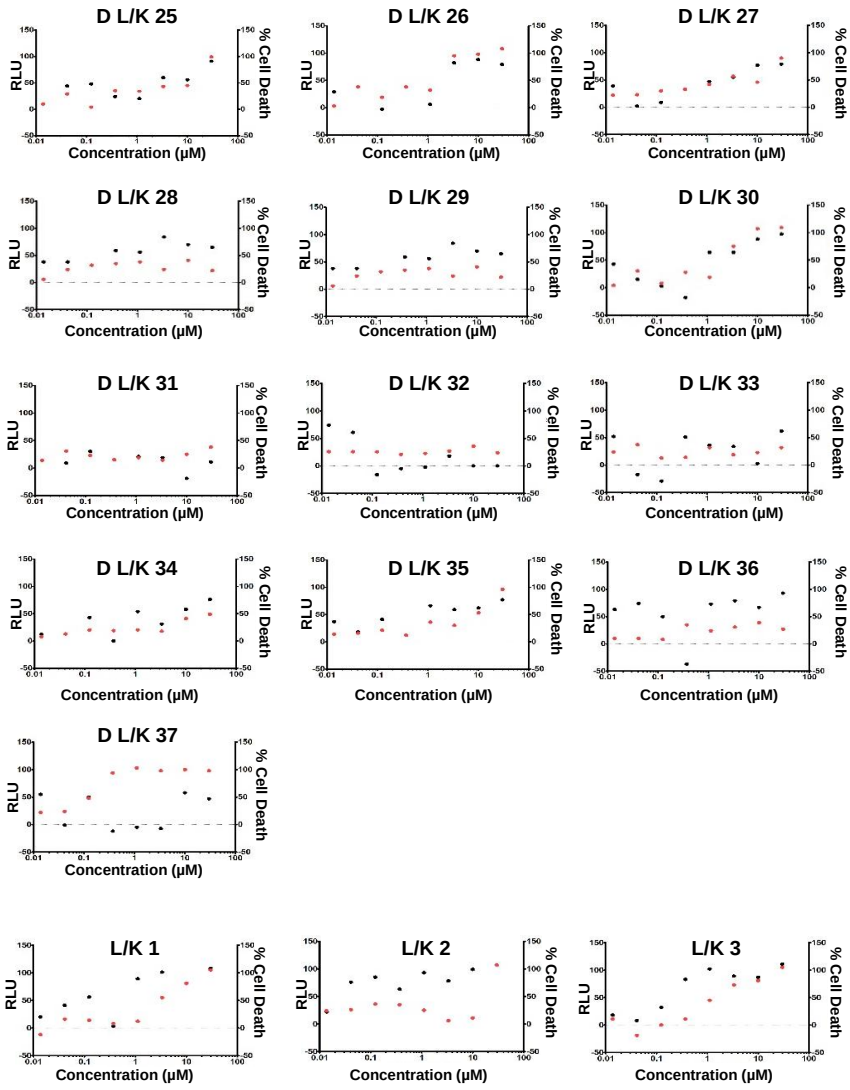

Figure 23. 3 of the 40 LOPAC/KD2 library hits showed inhibition of luciferase reporter expression and low toxicity. Dose response of validated hits in the RB activity assay (black dots) and in the cytotoxicity assay (red dots) is shown. The compound concentrations assayed were 0.01, 0.03, 0.1, 0.3, 1, 3, 10, and 30 μM for 2 hours at 37ºC. The percentage of inhibition of luciferase activities and cytotoxicity are expressed relative to controls (DMSO and H_2O_2).

4. Characterization of the 22 hits obtained by the Innopharma and CDRD HTS platforms

In summary, we selected 22 hits (15 from the DTP-NCI, 4 from Prestwick and 3 from LOPAC/KD2 chemical libraries), which reduced RB reporter activity. To identify leading drug candidates, we performed different secondary screenings to characterize their mechanism of action. The hit characterization assays can be divided into three groups according to their main purpose. The first group aimed to identify false positive compounds that nonspecifically inhibited the transcriptional machinery, interfered with luminescence, or quenched the light. The second group of assays was performed to identify candidates that prevented cell proliferation in cancer cell lines with high CDK activity. Then, we determined which compounds modulated cell cycle progression producing cell arrest in the G1 phase. Lastly, the fourth set of assays allowed us to select those candidates that promoted G1 phase arrest acting directly on RB and downregulating E2F-dependent genes, and to discard those compounds that are inhibitors of CDK or activators of p38. The different experimental readouts measured in the 4 assay groups are classified in the Figure 24.

Milestone 1: Discard false positive compounds that nonspecifically inhibit the transcriptional machinery or interfere with luminescence.

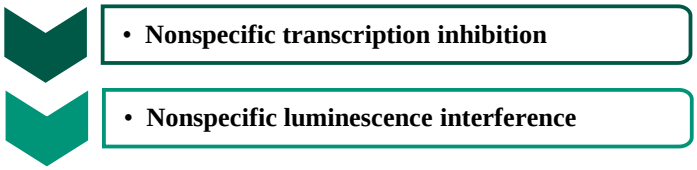

Milestone 2: Identify the candidates that prevent cell proliferation in cancer cell lines with high CDK activity.

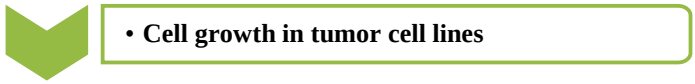

Milestone 3: Identify the candidates that modulate cell cycle progression arresting the cells in G1 phase

Milestone 4: Selection of candidates that promote a G1 arrest through the down-regulation of E2F-dependent genes, acting directly on RB and without behaving as inhibitors of CDK nor as activators of p38.

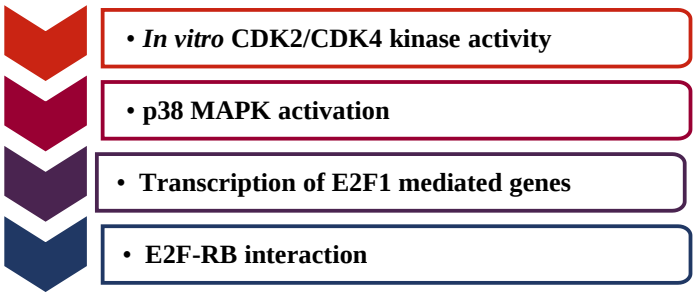

Figure 24. Schematic representation of main assays in the compound characterization process. Secondary characterization assays were divided into four groups (expressed in colors) in which different readouts were measured to discard false positive compounds and to identify the hits that directly stimulate RB activity mimicking phosphorylation by p38 MAPK.

4.1 Discard false positive compounds that non-specifically inhibited the transcriptional machinery or interfered with luminescence.

A key component of the success of a HTS strategy in drug discovery is the capacity to differentiate between promising drug leads and the false positives that can affect detection efforts. To discard those drugs whose effects were due to inhibition of the transcription machinery, HEK293T cells were transfected with a DOX-inducible GFP vector. After 24 hours at 37ºC, cells were treated with 10 μM drugs for 1 hour and GFP expression was induced with doxycycline overnight. Then, we measured GFP expression by flow cytometry. We discarded 3 (N2, N15 and L/K3) of the 22 candidate drugs due to their strong reduction of the GFP expression, suggesting that their effect in the HTS assays was due to their unspecific transcriptional inhibitory role (Figure 25A).

Additionally, to discard those drugs that inhibited luminescence in a non-specific way, HEK293T cells were transfected with a pGL3 plasmid constitutively expressing the firefly luciferase protein and were treated with the different compounds at 10 μM. The drugs N4 and N8 inhibited luciferase or quenched the light. Of note, we also detected the drugs N2, N15 and L/K3, but their effects may be due to inhibition of transcription (Figure 25B). According to these results, we discarded 5 false positive compounds (N2, N4, N8, N15, L/K3).

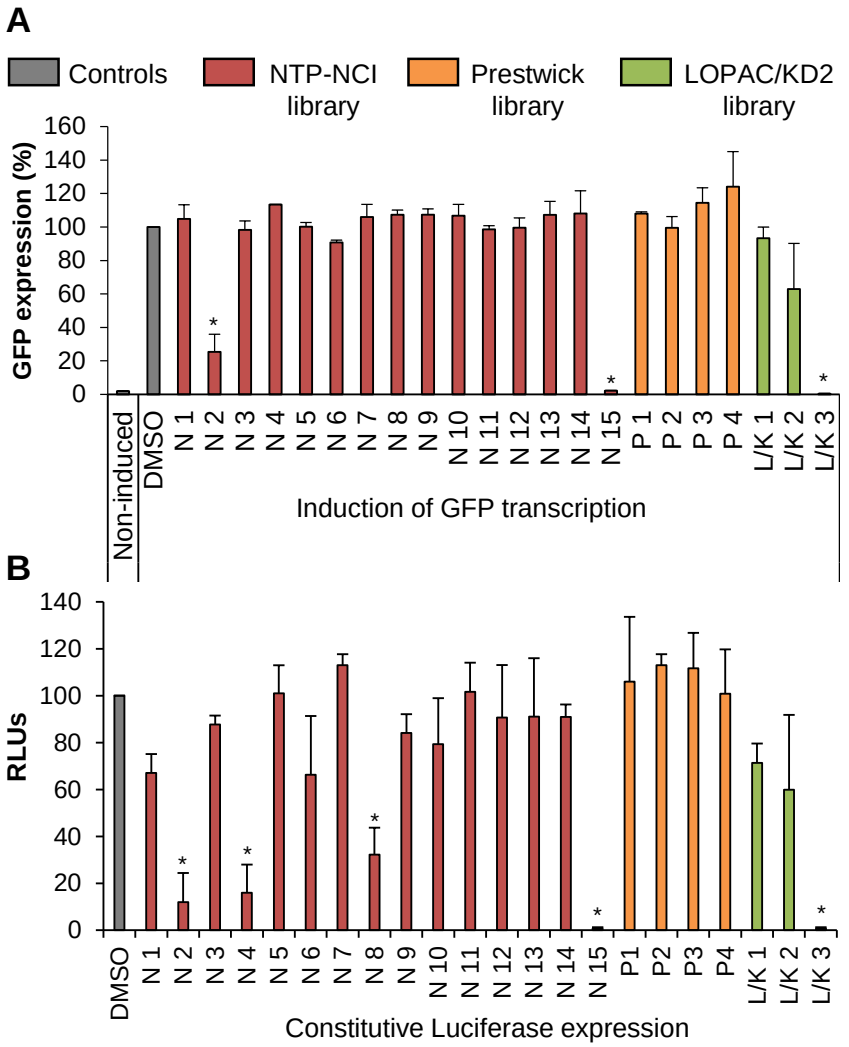

Figure 25. 5 of the 22 initially selected hits were discarded due to them inhibiting the transcriptional machinery, causing non-specific interferences in luminescence, or quenching the light. A. HEK293T cells were transfected with DOX-inducible GFP vector, after 24 hours at 37ºC cells were treated with 10 µM drugs and 1 hour later GFP expression was induced with doxycycline overnight. **B.** HEK293T cells were transfected with pGL3 vector constitutively expressed luciferase protein. After 24 hours at 37ºC cells were treated with 10 µM drugs. 4 hours later, cells were lysed with One-Glo reagent and Luciferase signal was measured**.** The luciferase activity was measured as relative

luminescence units (RLU). Data are shown as means ± SD of biological triplicates (* $p < 0.05$).

4.2 Identification of the HTS candidates that arrest cell growth in tumor cell lines

N-terminal RB phosphorylation restricted cell growth in three cancer cell lines with high CDK activity (Gubern et al., 2016). Thus, we analyzed the effect of the 17 hits in three tumor cell lines with high CDK activity MCF7 (breast), PK9 (pancreas) and 235J (bladder). Cells were plated at low density and treated with the different drugs in a dose response assay (performed by diluting each compound 1:2 over 5 points starting at 10 μM) for 4 days. Cell colonies were stained with crystal violet solution and quantified with ImageJ-plugin ColonyArea software (Guzmán et al., 2014) (Figure 26). 9 of the 17 hits reduced cell growth in the three tumor cell lines (MCF7, PK9 and 235J) at least at 10 μM (Table 12). In addition, drug N9 impaired cell growth only in the MCF7 cell line. The molecules of the N9 family were already described as growth inhibitors of breast cancer, thus we stopped prioritizing N9.

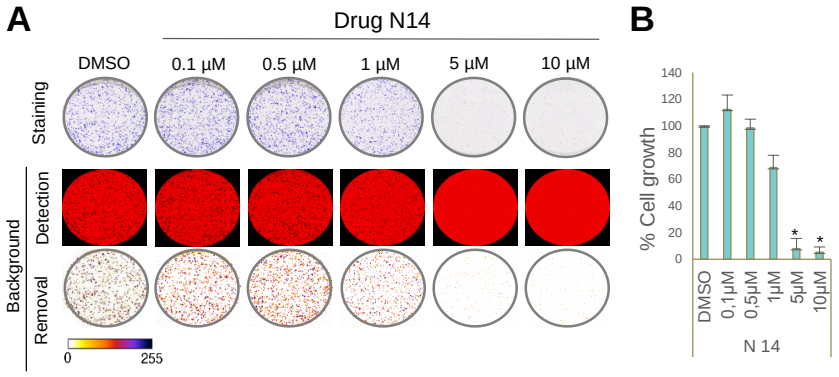

Figure 26. A representative colony assay of the 17 selected compounds in MCF7, PK9 and 235J cell tumor lines. A. Upper panel: Colony assay of MCF7

cells treated with the indicated concentrations of N14 and stained with crystal violet. Middle panel: Background detection with the ColonyArea plugin of ImageJ. Bottom panel: Image results after threshold and background removal by the "Colony_thresholder" macro. Colored bar represents the intensity scale shown in the threshold wells. Zero intensity (white) corresponds to areas where no cells were identified (background). **B**. Quantification of the growth area of colonies and intensity of staining using the Colony area plug-in of ImageJ. Data are shown as means ± SD of biological triplicates (* $p < 0.05$).

Table 12. Compounds that impaired tumor cell growth. Summary of the colony assay results in MCF7, PK9, and 235J cells treated with the17 hits in a dose response.

Library (Initial identified hits)	**Drug ID**	**Cell growth reduction**	**Effective concentration**
DTP-NCI (15 hits)	N1, N5, N6, N13	Non significant	-
	N3, N7	MCF7, 235J, PK9	10µM
	N10, N11, N12, N14	MCF7, 235J, PK9	5µM
	N9	MCF7	0,1 µM
Prestwick (4 hits)	P2	MCF7, 235J, PK9	10µM
	P3, P4, P1	Non significant	-
Lopac-KD2 (3 hits)	L/K 1	MCF7, 235J, PK9	5µM
	L/K 2	MCF7, 235J, PK9	1µM

4.3 Identification of the candidates that modulate cell cycle progression

The fact that 9 drugs impaired cell growth in tumor cell lines prompted us to test whether they would cause a cell cycle arrest in the G1 phase through the RB pathway. HEK293T cells were subjected to treatment with the drugs at 10 µM for 1 hour and then we added nocodazole (an inhibitor of microtubule formation to block cellular progression at G2/M). Exponentially growing cells

spend most of their time in G1, we used nocodazole after drug treatments to differentiate those drugs that arrested the cell in G1 from those that continue their cycle and are trapped in G2 / M by the nocodazole effect. After 16 hours, we followed the cell cycle with cytometry analyses. In the absence of drugs, control cells treated with nocodazole were arrested in G2/M (Figure 27, middle panel). In contrast, Anisomycin (used as a positive control) and 7 out of 9 drugs promoted a G1 arrest (Figure 27).

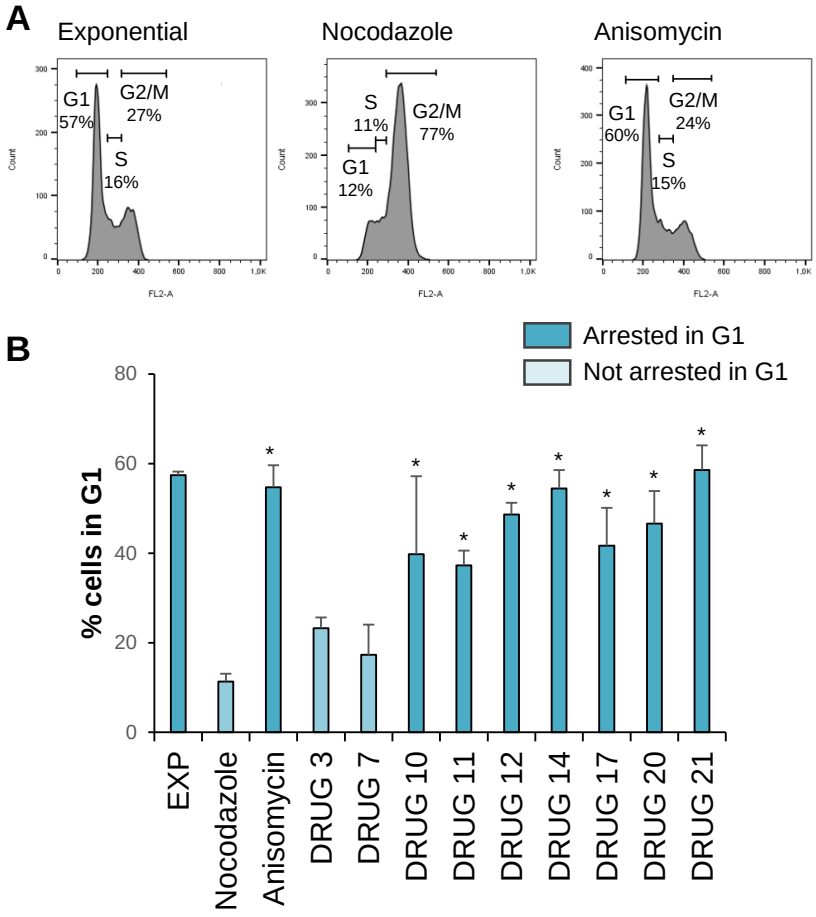

Figure 27. 7 of the 9 drugs that impaired tumor cell growth also caused cell cycle arrest in G1 phase. A. Representative cell cycle profiles from cytometry

assays. First panel: histogram of cells with exponential growth. Second histogram: cells treated with nocodazole Third histogram: cells treated with 150 μM Anisomycin 1 hour before being treated with nocodazole. **B**.7 compounds caused cell cycle arrested in G1 phase. Quantification of the percentage of cells in G1 after the drugs treatments and nocodazole addition. Data are shown as means ± SD of biological triplicates (* $p < 0.05$).

4.4 Identification of the candidates that act directly on RB activity increasing RB-E2F affinity

Tumor growth and cell cycle assays did not assess whether these 9 drugs acted directly on the RB pathway. For instance, if a drug activates the p38 signaling pathway or inhibits the action of CDKs, we could have obtained the same results in terms of cell cycle arrest and growth reduction in tumor cell lines. Thus, we assessed whether the candidate drugs were p38 activators or CDK inhibitors.

To assess the drugs' effect on CDK activity, we performed an *in vitro* kinase assay with purified proteins and radiolabeled-ATP. We used histone 1 (H1) as a non-specific substrate of CDK2 or CDK4 in the presence or not of drugs at 10 μM for 1 hour at 30ºC. We detected an inhibition of CDK4 with the drug L/K1 similar to the described inhibitor Palbociclib (Figure 28A). No drug inhibited CDK2 activity *in vitro* (Figure 28B).

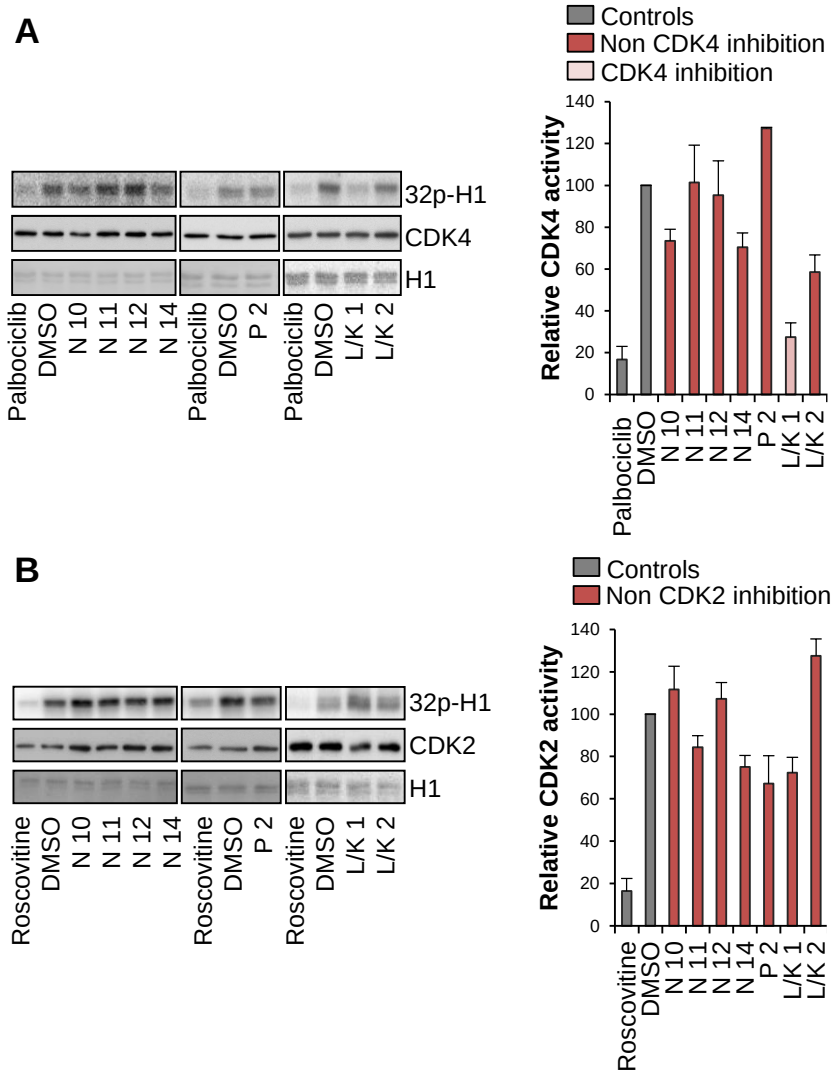

Figure 28. 1 out of the 7 drugs that arrested the cell cycle in G1, inhibited CDK4 activity *in vitro*. Representative Kinase assays with purified CDK4 **(A)** or CDK2 **(B)** proteins in the presence of drugs (10 μM) for 1 hour at 30ºC are shown. We measured the phosphorylation of H1 (a non-specific substrate of CDKs) using radiolabeled-ATP. Left panels show the quantification by ImageJ software of three independent kinase assays and data are shown as means ± SD.

To determine the drugs' effect on p38 activation, we treated HEK293T cells with the different 7 different drugs at 10 μM for 4 hours and analyzed phosphorylation of p38 by Western blot. The L/K2 drug increased the phosphorylation of p38, suggesting that this compound activates p38 (Figure 29).

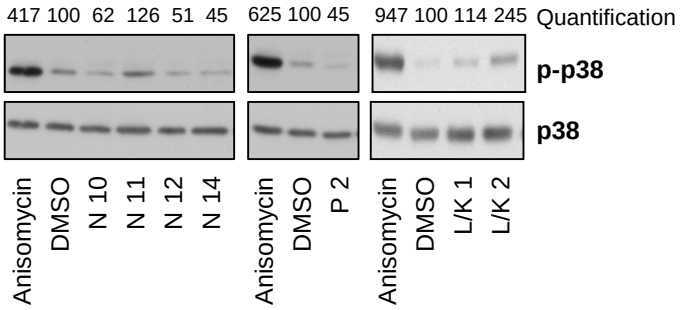

Figure 29. L/K2 drug activated p38. HEK293T cells were treated with the different drugs at 10 μM for 4 hours. The phosphorylation state of p38 was analyzed by Western blot and quantified by ImageJ software.

In summary, of the 7 drugs that arrested cells at G1 and showed reduced growth of cancer cell lines, 1 compound was able to activate p38 MAPK and another was a CDK4 inhibitor. Next, we assessed whether the 5 remaining drugs modulate cell cycle progression by increasing RB activity via downregulation of E2F-dependent genes. We analyzed the transcription of E2F-dependent genes in HEK293T cells subjected to treatments with the 5 drugs at 10 μM for 4 hours. The gene expression of E2F target genes (CycA2, CycE1, E2F1, BRCA1) was evaluated by qPCR. Drug treatments down-regulated the expression of E2F-dependent genes. p38 activators such as NaCl and Anisomycin were used as positive controls (Figure 30).

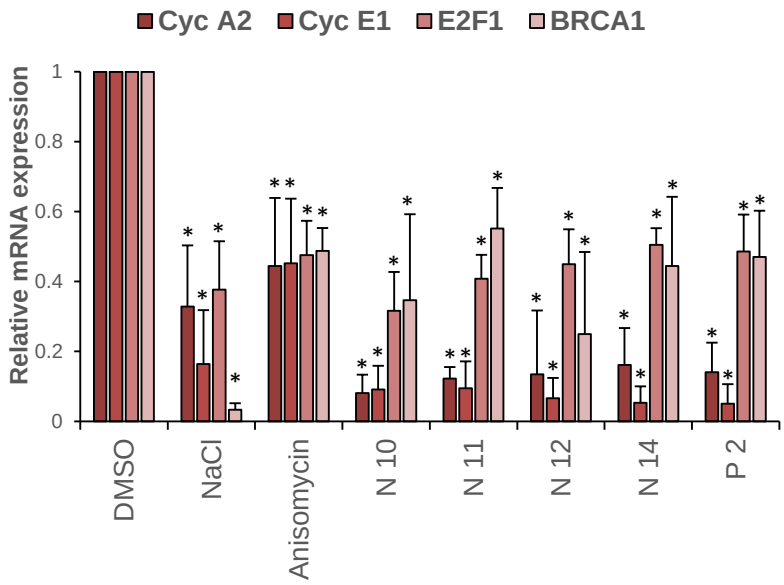

Figure 30. Drugs N10, N11, N12, N14 and P2 mediate E2F target gene repression. HEK293T cells were treated with the 5 different drugs at 10 μM for 4 hours. Anisomycin at 150 μM and NaCl at 100 mM were used as positive controls in the repression of E2F target genes. The mRNA levels of CycA2, CycE1, E2F1 and BRCA1 were assessed using real-time PCR. GAPDH mRNA was used for normalization. Data are shown as means ± SD of biological triplicates (* $p < 0,05$).

Phosphorylation of RB at S249 / T252 sites by p38 upon stress or the RB phosphomimetic mutant increased the interaction of RB-E2F (Gubern et al. 2018; see Introduction section). Thus, we assessed whether these drugs stimulate a conformational change in RB to promote an increase of E2F binding, mimicking the increased affinity between RBN S242E/T249E and E2F. To measure the binding RB-E2F affinity, we used Surface plasmon resonance (SPR) spectroscopy. SPR technology measures the binding affinities and kinetics of two interacting proteins in the absence or presence of small molecules. Recombinant His-tagged E2F was

randomly immobilized by amine coupling on a sensor chip, whilst in solution recombinant GST-tagged RBN and drugs flowed over the sensor surface. The optical method measured changes in refractive index at the sensor surface, detecting drug-induced changes in RB-E2F interaction. Dissociation equilibrium constants (KD) of RBN S242E/T249E and RBN S242A/T249A were used as controls of maximum and minimum affinity with E2F (a high-affinity interaction is characterized by a low KD). KD were calculated for each of the 5 selected drugs. Drugs N11, 12, 14 and P2 increased the affinity between RBN and E2F compared to the DMSO control, although the effect differed depending on the drug (Figure 31). While N12 and P2 drugs showed a KD (N12 KD =1.5 μM and P2 KD = 2.3 μM) similar to the phosphomimic mutant RBN S242E/T249E (KD = 1.1 μM), N11 showed a less pronounced effect and N14 had a slightly smaller KD than DMSO control (Figure 31B).

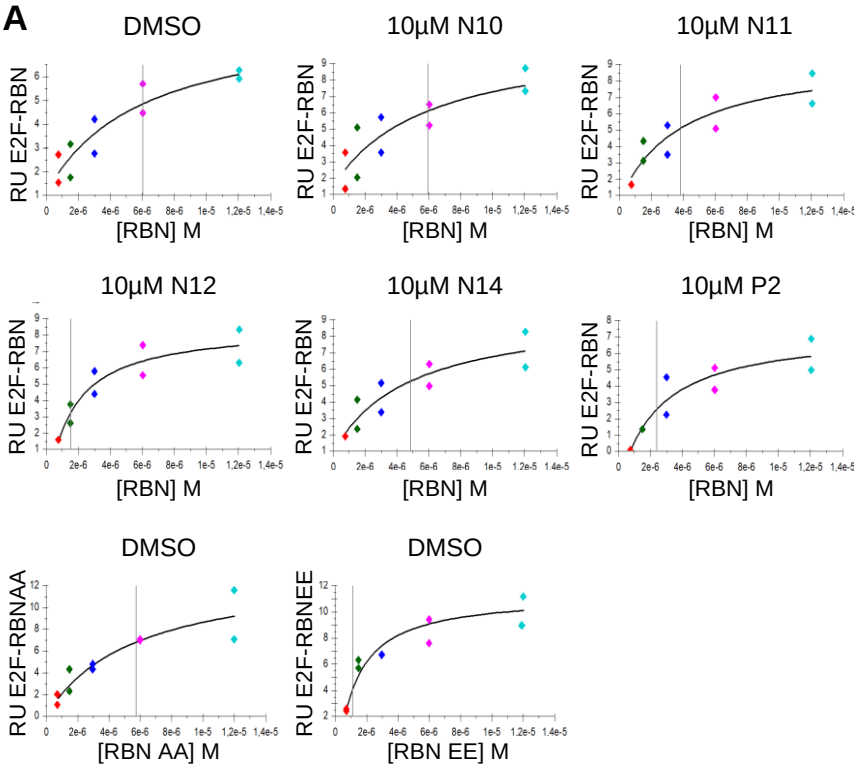

B

		KD (M)	Rmax(RU)	Chi²(RU²)
E2F-RBN	DMSO	5.99E-06	7.45	0.47
	N10	5.95E-06	9.20	1.51
	N11	3.82E-06	8.91	1.1.5
	N12	1.05E-06	10.59	0.89
	N14	4.83E-06	8,62	1,09
	P2	2.37E-06	9.77	1.16
E2F-RBNAA	DMSO	5.72E-06	13,40	1.65
E2F-RBNEE	DMSO	1.10-06	14.47	1.13

Figure 31. N12 and P2 drugs increased the affinity between RBN and E2F. **A.** SPR profiles were obtained using a Biacore T100. The alterations in the binding affinity of RBN-E2F by the 5 selected drugs were determined. E2F was randomly immobilized by amine coupling on a sensor chip (CM7) whilst the RBN, RBN S242E/T249E (RBNEE) or RBN S242A/T249A (RBNAA) flowed over the chip at a range of concentrations from 0.75 to 12 µM together with the drugs at 10 µM. DMSO remained constant at 0,1%. **B**. KD values were

determined by plotting concentration against response and fitting to a 1:1 binding model using Biacore Evaluation software. Rmax is the maximum analyte response. Chi^2 is a measure of the average deviation of the experimental data from the fitted curve.

To further validate these results, we performed an *in vitro* binding assay using His-E2F1 and GST-RBN and the N12 and P2 compounds. Purified GST-RBN protein not eluted from the glutathione beads was incubated overnight with eluted His-E2F1 protein and with the compounds N12 and P2 at 1 μM or DMSO (as negative control). GST-RBN protein bound to beads was pulled down by centrifugation and the co-precipitation with His-E2F1 proteins was analyzed by western blot. Both N12 and P2 increased E2F-RBN binding compared to DMSO control (Figure 32).

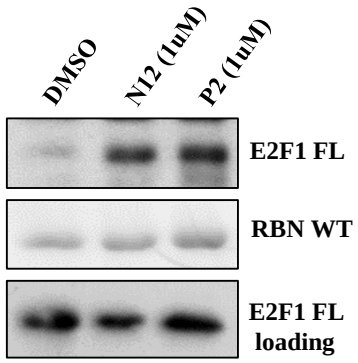

Figure 32. N12 and P2 **drugs increased the binding between RBN and E2F.** Recombinant GST-RBN (aa 1-379) was incubated with His-E2F1protein in presence of N12 and P2 at 1 μM overnight. All proteins were purified from *E. Coli*. GST-RBN was pulled-down using Glutathione Sepharose beads and the co-precipitation of E2F1 protein was analyzed by Western blotting.

We then analyzed the long-term effect of the drugs N12 and P2 (10 μM for 72 hours) on cell proliferation of wild type (WT) NIH-3T3 and RB knockout (KO) NIH-3T3 cells. The colony-forming

ability of NIH-3T3 was reduce by treatment for both drugs compared to DMSO-treated cells. In contrast, N12 and P2 had no effect on the colony-forming ability of RB KO cells, indicating that drugs P2 and N12 had an RB-dependent antiproliferative effect (Figure 33).

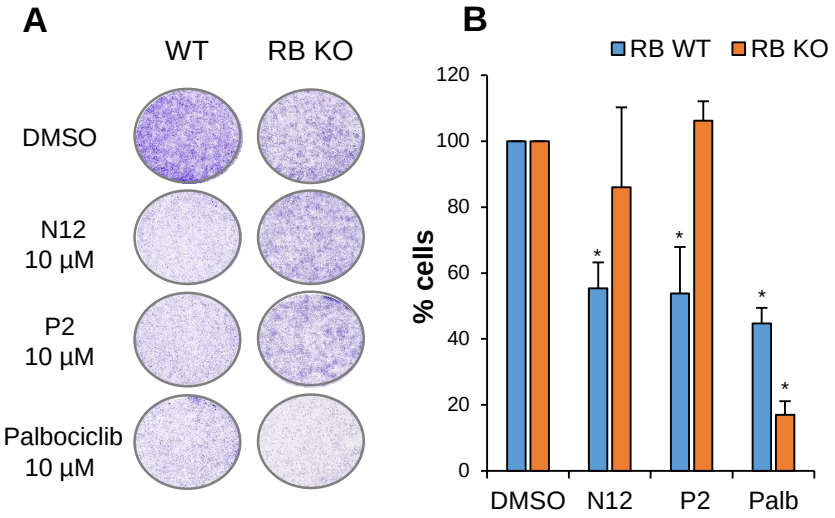

Figure 33. N12 and P2 drugs decreased NIH 3T3 cell proliferation in an RB-dependent manner. NIH-3T3 WT and NIH-3T3 RB KO cells were treated with N12 and P2 drugs at 10 µM for 72 hours and stained with crystal violet solution. Palbociclib at 10 µM was used as a control. **A.** Representative images of individual wells showing colony formation. **B**. Quantification of the growth area of colonies and intensity of the staining using the Colony area plug-in of ImageJ. Data are shown as means ± SD of biological triplicates (* $p < 0.05$).

To sum up, the initial 22 candidates were classified according to their mechanism of action on the RB signaling pathway by several secondary assays. Our data showed that 11 drugs inhibited tumor cell growth, 7 out of them arrested the cell cycle in G1 and 1 compound inhibited CDK activity, another compound activated p38 MAPK and 2 drugs increased the affinity of E2F1-RB. The two

compounds that directly increased the binding of E2F and RB (N12 and P2) also showed an RB-dependent antiproliferative effect, making them promising drugs for antitumor therapy.

5. Identification of compounds that regulate RB activity in a large-scale screening

Our previous screening assays asserted the success and feasibility of our novel RB targeting strategy. However, we did not have the opportunity to perform a large-scale HTS on the Innopharma and CDRD screening platforms. Innopharma did not have sufficient funding for the development of the project and the CDRD did not prioritize our proposal, so we looked for new alternatives. We now intend to continue our efforts to run a HTS with larger and newer chemical libraries to find new hits. In collaboration with the IRB drug discovery platform, we will run a HTS with 50,000 high quality and diverse library compounds. The representative collection of 50,000 molecules comes from the ChemDiv library of more than 1,500,000 compounds. Moreover, the library contains subsets focused on Protein-Protein-Interaction (PPI), central nervous system CNS, cancer, a diverse set, and a lead-like set, among others. Notably, 2,400 compounds belong to MCE (MedChemExpress) collection of FDA-approved drugs. This FDA-approved compounds have been completed extensive preclinical and clinical assays and have well-characterized bioactivities, safety, and bioavailability properties.

During the set-up for implementing the assay in the new automated platform, we defined and improved the protocols used in

Innopharma and CDRD. Table 13 shows the up-grades of the assay in terms of productivity, variability, and robustness.

Table 13. Protocol modifications and improvements by our laboratory in collaboration with the IRB drug discovery platform.

	IRB Protocol Changes	Improvements
CELL CULTURE MEDIUM	Replace DMEM with Opti-MEM	Two times higher signal detection
TRANSFECTION	One transfection in bulk with LTX PLUS Reagent	An increase in transfection efficiency
HEK293T CELLS	Seed 15,000-25,000 cells/well	Reduction of variability between wells
FROZEN CELLS	Cells frozen after transfection	A large batch of frozen cells, reduces variability between plates and assay days
AUTOMATION	Use of acoustic dispenser	Reduction of false positives and negatives, pipetting errors and compounds dead volume
CONTROLS	Use hits detected in previous screenings as positive controls	Increases the robustness of the test
DIFFERENT CONTROLS	Several hits with different action mechanisms used as controls	Better interpretation of the new results
DETECTION	Onle-Glo reagent (1 step)	One-Glo provides a more stable signal than Bright-Glo

These improvements in the protocol allowed us to increase the signal of the luciferase reporter gene, to increase the assay windows and to improve the automation and the productivity of the assay runs (Table 14). Of note, the use of several controls with known mechanisms of action (previous hits from Innopharma and CDRD HTSs) allowed us to have variable assay windows of S / B = 2-25,

which will help us to get a better interpretation of the new HTS results (e.g., hits obtained in the range of luminescence inhibitors).

Table 14. Improvement of the RB activity assay in terms of luciferase signal and S/B values comparing the IRB platform to Innopharma and CDRD platforms.

	Innopharma	**CDRD**	**IRB**
LUCIFERASE UNITS SIGNAL	500-2,000 RLUs DMSO conditions	3,000-5,000 RLUs DMSO conditions	20,000-80,000 RLUs DMSO conditions
S/B VALUE	S/B = 2-3 Anisomycin as a negative control	S/B = 6.7-8.21 H_2O_2 as a negative control	S/B = 2-25 Previous hits as a negative control

Currently, the RB activity assay is ready to start the HTS. IRB compound collection will be provided in three steps: pilot library (phase 1), library composed of 10,000 compounds (phase 2) and library composed of the remaining 40,000 compounds (phase 3). At the IRB platform the assay will be run in duplicate to increase reproducibility, reliability and robustness.

In addition, we have established a collaboration agreement with the European lead factory (ELF), which is a public-private partnership that aims to provide innovative drug discovery starting points. According to our experimental requirements, ELF assigned us the High-Throughput Biomedicine Unit at the Institute for Molecular Medicine Finland (FIMM) and gave us access to EU-OPENSCREEN 100,000 novel compounds. These 100,000 compounds belong to European Chemical Biology Library (ECBL), show unbiased chemical diversity and are unique having been designed by academic computational chemistry groups.

FIMM and our group have discussed the project and designed its screening workplan defining timelines, material transfer, supplies, and budget contributions from both sides. The EU-OPENSCREEN compound collection will be provided in three steps: pilot library of 5000 compounds (phase 1), library composed of 30,000 compounds (phase 2) and library composed of the remaining 70,000 compounds (phase 3). Currently, the assay, updated protocol, and materials have been transferred to the FIMM screening platform.

Results from first tests with 384 drugs, belonging to a set of drugs approved by the FDA for use in oncology, highlights the quality of the assay. Briefly, cells were transfected with E2F-luc, HA-E2F1, GFP-RB plasmids (1:1:1/4 plasmids proportion) in bulk using LTX plus reagent (15338100, Thermo Fisher). After 48h transfected cells were harvested, the cells were frozen in FBS 10% DMSO for later use. The cells for this assay were transfected at IRB and we shipped the transfected cells to FIMM for the test assays. At the FIMM platform, transfected cells were thawed, centrifuged at 1,000 rpm to remove the supernatant, and resuspended in DMEM with 2% FBS. Then cells were seeded at 12,500 cells/ 25 µl/well in plates pre-printed with the compounds in a dose response assay (performed by diluting each compound 1:10 over 5 points starting at 10 µM), Anisomycin at 150 µM, as a positive control, or DMSO (Vehicle) ,as a negative control, were incubated 4 hours at 37ºC. Finally, 25 µL of One-Glo detection reagent (E2610, Promega) per well were added after 30 min pre-equilibration at RT. After 5 minutes incubation, luminescence was read on EnVision plate reader from PerkinElmer (0.5 sec/read).

The assay was robust showing Z ' greater than 0.65 and CV less than 15%. We have already obtained two hits that have shown an IC50 around 1 μM. The promising results have demonstrated the success of the set-up and automation process to perform the next phases described before.

Access to the drug discovery state of the art facilities and their capabilities and experienced teams of both IRB Drug Screening Platform and EU-Openscreen-Drive facilities will provide us with the opportunity to advance the project from HTS to Hit to Lead. The two HTS platforms will be essential to run the screening campaigns with a large chemical library diversity and to discover novel chemical series. The hits will be validated by performing dose response curves to determine their IC50 and cytotoxicity, as done previously. Then, we will carry out secondary characterization assays, which we have already developed for the characterization of the hits obtained from the Innopharma and CDRD screening.

During the Hit refinement and Lead nomination process, the hits will be classified into chemical series and new compounds of the series will be synthesized. This phase will end with a group of compounds which has appropriate properties in terms of efficacy, safety and Drug Metabolism and Pharmacokinetics (DMPK) properties in both in vitro and in vivo assays. These properties will be further improved during the Lead Optimization process to finally nominate a Candidate ready to start the preclinical regulatory phase followed by human clinical trials.

STATEMENTS OF CONTRIBUTIONS

I have been involved in all the steps of this work

Dr. Radoslav Janostiak performed some binding assays (section 1).

The setting up of the large-scale screening (section 5) was performed in collaboration with Israel Ramos (Coordinator of IRB Barcelona Drug Screening platform).

DISCUSSION

According to the world health organization, cancer is one of the leading causes of death worldwide, causing around 10 million deaths in 2020 (https://gco.iarc.fr/today). Despite extraordinary advances in the treatment of many types of cancer in recent decades, effective treatments are still lacking for some forms of the disease. Advances in immunotherapy and targeted molecular therapies are transforming the treatment of cancer patients. But these new therapies only offer lasting clinical benefits to a few patients, for this reason new treatment approaches should be studied, or existing ones improved. Our current research allows the discovery of molecules targeting RB. To date, no drug targeting the RB protein has been identified. Due to its nature as a tumor suppressor it has been difficult to design compounds that increase its activity.

The phosphorylation of residues S249 / T252 at the RB N-terminus renders RB insensitive to CDK inactivation (Joaquin et al., 2017). The tumor antiproliferative capacity of a S249E / T252E phosphomimic mutant of RB (Gubern et al., 2016) and the evidence that RB-derived phosphomimetic peptide improve the therapeutic effectiveness of radiation *in vivo* (Jin et al., 2019) opens up new therapeutic opportunities. The main objective of this thesis was to identify and characterize molecules that emulate the phosphorylation effect of RB S249 / T252, making RB a super repressor insensitive to CDKs. These compounds could compromise the growth of tumors with high CDK activity or tumors with mutations that lead to RB inhibition.

The development of new drugs is costly and time-consuming, with estimates of over $US1 billion and 15 years for a product to reach the

market (Shechter et al., 2020). Several approaches have been used to increase the effectiveness in the search for drugs targeting RB pathway.

We proposed two approaches to identify molecules capable of mimicking the effect of RB N-terminal phosphorylation as a possible antineoplastic therapeutic strategy: 1. The computer-aided drugs design (CADD) to carry out an *in silico* screening predicting possible compounds that would increase the affinity between RB and E2F1. 2. The design and development of a cell-based assay to monitor RB activity suitable for conventional HTS technologies for developing new antitumor drugs.

1. Characterization of the RBN-E2F1 minimal interaction region

Our first approach to identify molecules that mimic the effect of RB N-terminal phosphorylation consisted in the use of CADD methods to carry out an in silico compound screening to predict possible compounds that would increase the affinity between RB and E2F1.

Although we knew that phosphorylation in the RB N-terminal domain at residues S249 / T252 stimulates a conformational change in RB that increases affinity towards E2F, this interaction surface still remains unknown (Gubern et al., 2016). The described crystal structure of RB does not include the RB region that contains these phosphorylated residues, due to the disordered nature of the region. The CADD analyzes and an in-silico drug screening require knowledge of the tertiary structure of the RBN-E2F1 interaction surface and due to the disordered nature of this N-terminal RB region,

we proposed to decipher the structure by NMR. To facilitate NMR analyzes we determined the minimal regions of E2F1 and RBN that are involved in the interaction by binding assays.

Recently, it has been shown that a 21 amino acid fragment of the RB N-terminal domain that contain residues S249 / T252 binds to p65 in a phosphorylation-dependent manner (Jin et al., 2018). The comparative study of the binding region described between RBN-p65 with the RBN-E2F shown that E2F has a similar sequence in its CC-MB domain. We identified that this E2F1 motif is sufficient for the E2F-RB binding. Moreover, we determined the region of the N-terminus RB (184-330 aa) that is required for interacting with E2F.

Both protein fragments (E2F1 CC-MB and RBN 194-330aa) are small enough to decipher the structure of interaction surfaces by NMR and investigate the effect of adding specific drugs. In addition to the possibility of performing an in-silico screening, the identification of the interaction regions will help us to more accurately characterize the impact of the identified hits on the affinity of both proteins.

2. Setting up a cell-based assay to monitor RB activity amenable for HTS assays

Our second approach to identify molecules that mimic the effect of RB N-terminal phosphorylation consisted in the design of an assay to monitor RB activity in cultured cells and its optimization for conventional HTS.

We have designed and developed a cell-based screening assay to follow the transcriptional activity of RB in cells using an E2F reporter system. The assay allowed us to study the effect of different stresses or molecules that affect this activity of RB. Upon different stresses (NaCl, H2O2, and Anisomycin) that activated p38, increased the RB activity resulting in a decrease in the transcription of the E2F1 reporter. Moreover, an RB S249E/T252E mutant that mimics the phosphorylation by p38 blocked gene expression even in the absence of stress stimuli (Gubern et al., 2016), a typical condition under which wild-type RB does not strongly repress transcription.

The capacity of the assay to detect the effect on RB activity after stress stimuli, suggested us a new use of the assay for the detection of drugs that enhance RB activity as possible antitumor therapy.

The purpose of the long optimization process was to adapt the assay to automated methods and HTS technology in drug discovery screening platforms. During the optimization stage different parameters were tested such as the plate format, the number of cells per well, transfection conditions and future controls, among others.

The assay was adjusted to quality standards (low variability and high signal with respect to background noise), ensuring the reproducibility of the biological characteristics.

Once the optimization process was finished, the starting conditions necessary to perform the HTS assays were established.

3. Pilot HTS assays to identify compounds that regulates RB activity

The efficient assay optimization established the starting conditions necessary for developing several compound screenings from different chemical libraries using the HTS methods.

Several pilot HTS assays allowed us to screen more than 9,000 molecules from three different libraries of great chemical diversity. This led to the detection and confirmation of 83 active compounds (hits) (39 drugs from the DTP-NCI, 4 drugs from Prestwick and 40 drugs from the LOPAC/KD2 libraries) with a similar or better effect on RB activity compared to cells induced by the p38 activator Anisomycin or H_2O_2 stress. 14 out of the 83 compounds were discarded because they were described as luciferase inhibitors, nonspecific translation inhibitors, duplicates, or false positives in other screening tests (frequent hitters). The IC50 and cell proliferation (cytotoxicity) of the remaining 69 hits were analyzed. Of these, 32 drugs were validated and 22 representative compounds from all the chemical series identified were selected for further analysis (15 from the DTP-NCI, 4 from the Prestwick and 3 from the LOPAC/KD2 libraries).

By chemistry analysis, we classified the 22 compounds into 4 main subseries based on their structure and physicochemical characteristics. 6 of the 22 hits identified had different chemical structures and were not included in this classification. All the hits profiled had proper values within the Lipinski guidelines and would be expected to be cell permeable. The Lipinski's guidelines define

molecular properties important for the pharmacokinetics of a drug in the human body, including its absorption, distribution, metabolism, and excretion ("ADME"). Moreover, the average molecular weight of the selected hits is low and the level of activity for such small molecules is encouraging. One possible issue is that the hits might be poorly soluble. In this case, small chemical modifications might solve this problem.

These results demonstrated the validity of our cell-based assay that monitors RB activity for identification of new compounds with high chemical diversity and future therapeutic interest.

4. Characterization of the 22 hits obtained by the Innopharma and CDRD HTS platforms

Phenotypic screening assays have led to the discovery of many of the current drugs. A phenotypic assay consists of testing a compound in cells, tissues, or animals to study whether it exerts the desired effects (Moffat et al., 2017). The identification of the therapeutic target and the molecular mechanism by which a drug exerts its function is often determined later and it is still a time-consuming and difficult process, making this the rate-limiting step in drug development (Jung and Kwon, 2015). Over the last quarter century, this lack of throughput has led to the use of a molecular approach that identifies drugs to treat unmet medical needs by targeting specific proteins, reducing molecular characterization efforts (Swinney, 2013). The relevance of our assay lies in the fact that it is an objective and unbiased-based assay to identify molecules that affect the RB signaling pathway in a cellular context.

Regardless of the assay design, subsequent complementary characterization assays are required to identify the direct target, function, or to ensure the elimination of false positives (Cho and Kwon, 2012). The RB activity HTS assay is based on a luciferase reporter and, thereby, it presents the risk of possible detection of false positives that interfere with the luciferase reporter gene or quench light. Indeed, from the 22 selected hits, we discarded 5 false-positive compounds that exhibited non-specific inhibition of the transcription machinery or interfered with luminescence. Notably, 3 out of the 5 discarded compounds belonged to chemical series number 2. The identification of a chemical series that includes several compounds that interfere with the assay is usefulness to detect possible false positives in future screenings. The other 2 discarded compounds were natural products. The natural molecules are not good starting points for future work as have poor physical chemistry and are very complex structures which would be very difficult to modify (Atanasov et al., 2021). The ratio of false positives was not excessively high (22.7%) indicating that there was a high probability that the remaining 17 candidates would present the desired effects.

Since our main aim was to discover effective compounds in cancer therapy, one of the key complementary assays consisted in evaluating the effect of the selected drugs on cell proliferation of tumor lines with high CDK activity. 9 compounds reduced the proliferation of the three tumor lines evaluated (MCF7, PK9 and 235J), suggesting a possible effectiveness in therapy. Moreover, drug N9 decreased cell proliferation of only the MFC7 breast cancer line. It should be noted that drug N9 belongs to the benzothiazole (Bz) family that has shown

effective antitumor activity in ER+ breast tumors (Callero and Loaiza-Pérez, 2011). Bz molecules trigger the aryl hydrocarbon receptor (AhR) receptor signaling pathway that leads to increased expression of CYP1A1 and CYP1B1 genes producing DNA damage and activating apoptosis mechanism in MCF7 cells (Callero and Loaiza-Pérez, 2011). Although N9 could modify the RB signaling pathway independent of the molecular mechanism described, we decided not to prioritize it, because its use in the treatment of breast cancer was already patented and undergoing clinical trials (Singh and Singh, 2014). The fact that these published results were related with our findings they served to validate our HTS approach.

We performed a second complementary assay, monitoring G1 cell cycle arrest. 7 out of the 9 antiproliferative drugs arrested the cell cycle in G1, indicating that they could target the RB pathway. However, the mechanism of action for arresting cells in G1 could lay at different levels of the RB signaling pathway; for instance, the drugs could trigger activation of p38 or inhibition of CDKs, as well increase the binding affinity of RB and E2F. Among the 7 candidate compounds that arrested the cycle in G1, 1 out of them inhibited CDK4 activity, another activated p38 and 2 of these compounds directly increased the RB-E2F1 binding. Furthermore, colony formation assays revealed a significant reduction of proliferation in NIH 3T3 cells treated with these 2 compounds compared in an RB-dependent manner.

Despite the numerous studies reporting an antitumor role of p38, many others showed that in more advanced stages of cancer this kinase promotes tumor development (Martínez-Limón et al., 2020).

Yet, evidence regarding antitumor efficacy by p38 inhibitors have made it the most studied therapeutic strategy (Canovas and Nebreda, 2021). However, p38 inhibitors have shown several side effects (Soni et al., 2019), probably due to the multifunctional nature of the kinase (Trempolec et al., 2013). Indeed, no p38 inhibitor drug has been currently approved for clinical use. Similarly, the study of p38 activators for antitumor therapy has not been assessed despite its function as a tumor suppressor (Choo et al., 2018; Hui et al., 2007). Thus, based on the previous data, *a priori*, the p38 activator compound identified in the HTS would not hold great expectations for its development as a clinical drug, but it could be useful in basic research.

In contrast, drug discovery of CDK inhibitors has progressed intensely over the last decade. Palbociclib, Abemaciclib, and Ribociclib are selective dual CDK4/6 inhibitors approved by the FDA for the treatment of hormone receptor positive metastatic breast cancer. These drugs have proven high clinical activity with controllable toxicity (Sánchez-Martínez et al., 2019). Nevertheless, *de novo* and acquired resistances are the main problems in the use of these inhibitors in the clinic (Portman et al., 2019). The use of new CDK inhibitors and the rational design of combination therapies could address the resistance and improve current therapies (Michaloglou et al., 2018; Rubio et al., 2019). Of note, our HTS assay showed to be a good approach for detecting new CDK inhibitors. Further characterization of the 2 CDK inhibitors identified should be addressed.

The two compounds that directly increased the binding of E2F and RB (N12 and P2) will offer a new and promising therapeutic strategy against cancer with clear advantages over the traditional approach (novel mechanism of action dominant over CDK activity) and applicable to most types of cancers (RB inactivation occurs in most of human cancers). Small molecule activators of RB will not only offer anti-proliferative therapy to cancer patients but also will boost immune response by decreasing PDL1 expression (Jin et al., 2018). Of note, drugs N12 and P2, in addition to belonging to the same chemical series, have a distinctive characteristic of one of the substituents within the same core. This distinguishing feature is not shared by other family members that have been discarded for various reasons, indicating a possible structure-activity relationship (SAR). Thus, next steps will be optimized these compounds, test similar ones of the same chemical series, and proceed to a hit-to-lead process.

5. Identification of compounds that regulate RB activity in a large-scale screening

The drug discovery process exhibits high rates of most drug failure. It is estimated that out of 10,000 molecules studied, only one will ever be approved by the FDA for clinical use (Harrer et al., 2019). Our previous screening assays asserted the success and feasibility of our novel RB targeting strategy. We now intend to continue our efforts to run a HTS with larger and newer chemical libraries to find new chemical starting points. The possibility of screening 150,000 molecules (50,000 molecules from the IRB drug platform and 100,000 from the UE. Open screen library) will increase

the chances of successful molecule development in the preclinical and clinical phase.

We expect promising results due to the success of the pilot screenings we have performed. Experience in the previous screenings on both drug discovery platforms and the setting up of the complementary assays for the characterization of the hits will improve productivity, organization, and development in the following larger scale screenings. By starting with a screening of 9,000 molecules, we obtained 2 potentially interesting molecules for antitumor therapy, which directly targeted RB. The use of larger libraries of up to 150,000 compounds will enormously increase the chances of detecting clinically relevant molecules. Many cancer patients could benefit from these compounds since more than 80% of tumors present mutations in the RB pathway and normally conserve a functional RB protein. This new mechanism of action places RB, which has been historically classified as a non-druggable protein, as a therapeutic target with great clinical potential.

CONCLUSIONS

The following conclusions can be reached from the results presented in this Ph.D. thesis:

- A novel mechanism of RB regulation by p38 MAPK, via phosphorylation at residues S249/T252 of RB, opens new venues for developing new drugs to treat cancer diseases.
- The optimization of a cell-based HTS assay that monitor RB activity has allowed screening more than 9,000 drugs from chemical libraries using HTS technologies to identify molecules that mimic the effect of RB S249/T252 phosphorylation.
- 22 identified compounds were selected for further analysis (15 from the DTP-NCI, 4 from Prestwick and 3 from the LOPAC/KD2 libraries).
- 5 false-positive compounds exhibited non-specific inhibition of the transcription machinery or interfered with luminescence.
- 9 compounds reduced the proliferation of the three tumor cell lines (MCF7, PK9, 235J) and 7 of them arrested the cell cycle in G1. Of these 7 compounds, 1 inhibited CDK4 activity and 1 activated p38.
- N12 and P2 compounds directly increased the affinity of RBN-E2F1 binding and showed activity in the RB signaling pathway in cell cultures.
- N12 and P2 belong to the same chemical series and have a distinctive characteristic of one of the substituents within the same core, indicating a possible structure-activity relationship.

- Both the previous screenings on drug discovery platforms and the set-up of all secondary tests for the hits characterization will increase productivity in the next larger scale screenings.
- Development of a larger screening of up to 150,000 compounds will enormously increase the chances of clinical success.
- Identifying RB-E2F1 minimal interaction regions will help us to define the structure of the new interaction surface and thus predict in silico potential molecules to act as therapeutic drugs.

SUPPLEMENTARY ARTICLE

Martínez-Limón, A., Joaquin, M., Caballero, M., Posas, F., and de Nadal, E. (2020). The p38 pathway: From biology to cancer therapy. Int. J. Mol. Sci. *21*. DOI: 10.3390/ijms21061913

REFERENCES

Adams, R.H., Porras, A., Alonso, G., Jones, M., Vintersten, K., Panelli, S., Valladares, A., Perez, L., Klein, R., and Nebreda, A.R. (2000). Essential role of p38α MAP kinase in placental but not embryonic cardiovascular development. Mol. Cell *6*, 109–116.

Ahlander, J., Chen, X.B., and Bosco, G. (2008). The N-terminal domain of the Drosophila retinoblastoma protein Rbf1 interacts with ORC and associates with chromatin in an E2F independent manner. PLoS One *3*, e2831.

Amat, R., Böttcher, R., Le Dily, F., Vidal, E., Quilez, J., Cuartero, Y., Beato, M., De Nadal, E., and Posas, F. (2019). Rapid reversible changes in compartments and local chromatin organization revealed by hyperosmotic shock. Genome Res. *29*, 18–28.

Arthur, J.S.C. (2008). MSK activation and physiological roles. Front. Biosci. *13*, 5866–5879.

Arthur, J.S.C., and Ley, S.C. (2013). Mitogen-activated protein kinases in innate immunity. Nat. Rev. Immunol. *13*, 679–692.

Atanasov, A.G., Zotchev, S.B., Dirsch, V.M., Orhan, I.E., Banach, M., Rollinger, J.M., Barreca, D., Weckwerth, W., Bauer, R., Bayer, E.A., et al. (2021). Natural products in drug discovery: advances and opportunities. Nat. Rev. Drug Discov. *20*, 200–216.

Attene-Ramos, M.S., Austin, C.P., and Xia, M. (2014). High Throughput Screening. In Encyclopedia of Toxicology: Third Edition, (Elsevier), pp. 916–917.

Attwooll, C., Denchi, E.L., and Helin, K. (2004). The E2F family: Specific functions and overlapping interests. EMBO J. *23*, 4709–4716.

Aulner, N., Danckaert, A., Ihm, J.E., Shum, D., and Shorte, S.L. (2019). Next-Generation Phenotypic Screening in Early Drug Discovery for Infectious Diseases. Trends Parasitol. *35*, 559–570.

Balog, E.R.M., Burke, J.R., Hura, G.L., and Rubin, S.M. (2011). Crystal structure of the unliganded retinoblastoma protein pocket domain. Proteins Struct. Funct. Bioinforma. *79*, 2010–2014.

Barnum, K.J., and O'Connell, M.J. (2014). Cell cycle regulation by checkpoints. Methods Mol. Biol. *1170*, 29–40.

Baudino, T. (2015). Targeted Cancer Therapy: The Next Generation of Cancer Treatment. Curr. Drug Discov. Technol. *12*, 3–20.

Ben-Levy, R., Hooper, S., Wilson, R., Paterson, H.F., and Marshall, C.J. (1998). Nuclear export of the stress-activated protein kinase p38 mediated by its substrate MAPKAP kinase-2. Curr. Biol. *8*, 1049–1057.

Beroukhim, R., Mermel, C.H., Porter, D., Wei, G., Raychaudhuri, S., Donovan, J., Barretina, J., Boehm, J.S., Dobson, J., Urashima, M., et al. (2010). The landscape of somatic copy-number alteration across human cancers. Nature *463*, 899–905.

Besson, A., Dowdy, S.F., and Roberts, J.M. (2008). CDK Inhibitors: Cell Cycle Regulators and Beyond. Dev. Cell *14*, 159–169.

Bhateja, P., Chiu, M., Wildey, G., Lipka, M.B., Fu, P., Yang, M.C.L., Ardeshir-Larijani, F., Sharma, N., and Dowlati, A. (2019). Retinoblastoma mutation predicts poor outcomes in advanced non small cell lung cancer. Cancer Med. *8*, 1459–1466.

Binné, U.K., Classon, M.K., Dick, F.A., Wei, W., Rape, M., Kaelin, W.G., Näär, A.M., and Dyson, N.J. (2007). Retinoblastoma protein and anaphase-promoting complex physically interact and functionally cooperate during cell-cycle exit. Nat. Cell Biol. *9*, 225–232.

Biondi, R.M., and Nebreda, A.R. (2003). Signalling specificity of Ser/Thr protein kinases through docking-site-mediated interactions. Biochem. J. *372*, 1–13.

Bollaert, E., de Rocca Serra, A., and Demoulin, J.B. (2019). The HMG box transcription factor HBP1: a cell cycle inhibitor at the crossroads of cancer signaling pathways. Cell. Mol. Life Sci. *76*, 1529–1539.

Brown, V.D., Phillips, R.A., and Gallie, B.L. (1999). Cumulative Effect of Phosphorylation of pRB on Regulation of E2F Activity. Mol. Cell. Biol. *19*, 3246–3256.

Bugai, A., Quaresma, A.J.C., Friedel, C.C., Lenasi, T., Düster, R., Sibley, C.R., Fujinaga, K., Kukanja, P., Hennig, T., Blasius, M., et al. (2019). P-TEFb Activation by RBM7 Shapes a Pro-survival Transcriptional Response to Genotoxic Stress. Mol. Cell *74*, 254-267.e10.

Burke, J.R., Deshong, A.J., Pelton, J.G., and Rubin, S.M. (2010). Phosphorylation-induced conformational changes in the retinoblastoma protein inhibit E2F transactivation domain binding. J. Biol. Chem. *285*, 16286–16293.

Burke, J.R., Hura, G.L., and Rubin, S.M. (2012). Structures of inactive retinoblastoma protein reveal multiple mechanisms for cell cycle control. Genes Dev. *26*, 1156–1166.

Cai, B., and Xia, Z. (2008). p38 MAP kinase mediates arsenite-induced apoptosis through FOXO3a activation and induction of Bim transcription. Apoptosis *13*, 803–810.

Cai, B., Chang, S.H., Becker, E.B.E., Bonni, A., and Xia, Z. (2006). p38 MAP kinase mediates apoptosis through phosphorylation of Bim EL at Ser-65. J. Biol. Chem. *281*, 25215–25222.

Callero, M.A., and Loaiza-Pérez, A.I. (2011). The Role of Aryl Hydrocarbon Receptor and Crosstalk with Estrogen Receptor in Response of Breast Cancer Cells to the Novel Antitumor Agents Benzothiazoles and Aminoflavone. Int. J. Breast Cancer *2011*, 1–9.

Cannell, I.G., Merrick, K.A., Morandell, S., Zhu, C.Q., Braun, C.J., Grant, R.A., Cameron, E.R., Tsao, M.S., Hemann, M.T., and Yaffe, M.B. (2015). A Pleiotropic RNA-Binding Protein Controls Distinct Cell Cycle Checkpoints to Drive Resistance of p53-Defective Tumors to Chemotherapy. Cancer Cell *28*, 623–637.

Canovas, B., and Nebreda, A.R. (2021). Diversity and versatility of p38 kinase signalling in health and disease. Nat. Rev. Mol. Cell Biol. 1–21.

Carbonell, C., Ulsamer, A., Vivori, C., Papasaikas, P., Böttcher, R., Joaquin, M., Miñana, B., Tejedor, J.R., de Nadal, E., Valcárcel, J., et al. (2019). Functional Network Analysis Reveals the Relevance of SKIIP in the Regulation of Alternative Splicing by p38 SAPK. Cell

Rep. *27*, 847-859.e6.

Cargnello, M., and Roux, P.P. (2011). Activation and Function of the MAPKs and Their Substrates, the MAPK-Activated Protein Kinases. Microbiol. Mol. Biol. Rev. *75*, 50–83.

Castaño, E., Kleyner, Y., and Dynlacht, B.D. (1998). Dual Cyclin-Binding Domains Are Required for p107 To Function as a Kinase Inhibitor. Mol. Cell. Biol. *18*, 5380–5391.

Cecchini, M.J., and Dick, F.A. (2011). The biochemical basis of CDK phosphorylation-independent regulation of E2F1 by the retinoblastoma protein. Biochem. J. *434*, 297–308.

Cheng, C.T., Kuo, C.Y., Ouyang, C., Li, C.F., Chung, Y., Chan, D.C., Kung, H.J., and Ann, D.K. (2016). Metabolic stress-induced phosphorylation of kap1 ser473 blocks mitochondrial fusion in breast cancer cells. Cancer Res. *76*, 5006–5018.

Chestukhin, A., Litovchick, L., Rudich, K., and DeCaprio, J.A. (2002). Nucleocytoplasmic Shuttling of p130/RBL2: Novel Regulatory Mechanism. Mol. Cell. Biol. *22*, 453–468.

Chicas, A., Wang, X., Zhang, C., McCurrach, M., Zhao, Z., Mert, O., Dickins, R.A., Narita, M., Zhang, M., and Lowe, S.W. (2010). Dissecting the Unique Role of the Retinoblastoma Tumor Suppressor during Cellular Senescence. Cancer Cell *17*, 376–387.

Chinnam, M., and Goodrich, D.W. (2011). RB1, Development, and Cancer (NIH Public Access).

Cho, Y.S., and Kwon, H.J. (2012). Identification and validation of bioactive small molecule target through phenotypic screening. Bioorganic Med. Chem. *20*, 1922–1928.

Choo, M.K., Kraft, S., Missero, C., and Park, J.M. (2018). The protein kinase p38α destabilizes p63 to limit epidermal stem cell frequency and tumorigenic potential. Sci. Signal. *11*.

Chow, C.W., and Davis, R.J. (2006). Proteins Kinases: Chromatin-Associated Enzymes? Cell *127*, 887–890.

Ciarmatori, S., Scott, P.H., Sutcliffe, J.E., McLees, A., Alzuherri, H.M., Dannenberg, J.-H., te Riele, H., Grummt, I., Voit, R., and White, R.J. (2001). Overlapping Functions of the pRb Family in the Regulation of rRNA Synthesis. Mol. Cell. Biol. *21*, 5806–5814.

Cisowski, J., and Bergo, M.O. (2017). What makes oncogenes mutually exclusive? Small GTPases *8*, 187–192.

Classon, M., and Harlow, E. (2002). The retinoblastoma tumour suppressor in development and cancer. Nat. Rev. Cancer *2*, 910–917.

Cobrinik, D. (2005). Pocket proteins and cell cycle control. Oncogene *24*, 2796–2809.

Coulthard, L.R., White, D.E., Jones, D.L., McDermott, M.F., and Burchill, S.A. (2009). p38MAPK: stress responses from molecular mechanisms to therapeutics. Trends Mol. Med. *15*, 369–379.

Croston, G.E. (2017). The utility of target-based discovery. Expert Opin. Drug Discov. *12*, 427–429.

Cuadrado, A., and Nebreda, A.R. (2010). Mechanisms and functions of p38 MAPK signalling. Biochem. J *429*, 403–417.

Cuenda, A., and Nebreda, A.R. (2009). p38δ and PKD1: Kinase Switches for Insulin Secretion. Cell *136*, 209–210.

Cuenda, A., and Rousseau, S. (2007). p38 MAP-Kinases pathway regulation, function and role in human diseases. Biochim. Biophys. Acta - Mol. Cell Res. *1773*, 1358–1375.

Cuenda, A., and Sanz-Ezquerro, J.J. (2017). p38γ and p38δ: From Spectators to Key Physiological Players. Trends Biochem. Sci. *42*, 431–442.

Cuevas, B.D., Abell, A.N., and Johnson, G.L. (2007). Role of mitogen-activated protein kinase kinase kinases in signal integration. Oncogene *26*, 3159–3171.

Dagnino, L., Zhu, L., Skorecki, K.L., and Moses, H.L. (1995). E2F-independent transcriptional repression by p107, a member of the retinoblastoma family of proteins. Cell Growth Differ. *6*, 191–198.

Dahiya, A., Wong, S., Gonzalo, S., Gavin, M., and Dean, D.C. (2001). Linking the Rb and polycomb pathways. Mol. Cell *8*, 557–569.

Dahlstrand, H.M., Lindquist, D., Björnestål, L., Ohlsson, A., Dalianis, T., Munck-Wikland, E., and Elmberger, G. (2005). P16INK4a correlates to human papillomavirus presence, response to radiotherapy and clinical outcome in tonsillar carcinoma. Anticancer Res. *25*, 4375–4383.

DeGregori, J., and Johnson, D. (2012). Distinct and Overlapping Roles for E2F Family Members in Transcription, Proliferation and Apoptosis. Curr. Mol. Med. *6*, 739–748.

Denechaud, P.D., Fajas, L., and Giralt, A. (2017). E2F1, a novel regulator of metabolism. Front. Endocrinol. (Lausanne). *8*, 311.

Dephoure, N., Zhou, C., Villén, J., Beausoleil, S.A., Bakalarski, C.E., Elledge, S.J., and Gygi, S.P. (2008). A quantitative atlas of mitotic phosphorylation. Proc. Natl. Acad. Sci. U. S. A. *105*, 10762–10767.

Dick, F.A. (2007). Structure-function analysis of the retinoblastoma tumor suppressor protein - Is the whole a sum of its parts? Cell Div. *2*, 26.

Dick, F.A., and Dyson, N. (2003). pRB contains an E2F1-specific binding domain that allows E2F1-induced apoptosis to be regulated separately from other E2F activities. Mol. Cell *12*, 639–649.

Dick, F.A., and Rubin, S.M. (2013a). Molecular mechanisms underlying RB protein function. Nat. Rev. Mol. Cell Biol. *14*, 297–306.

Dick, F.A., and Rubin, S.M. (2013b). Molecular mechanisms underlying RB protein function. Nat. Rev. | Mol. CELL Biol. *14*.

Dimri, G.P., Itahana, K., Acosta, M., and Campisi, J. (2000). Regulation of a Senescence Checkpoint Response by the E2F1 Transcription Factor and p14ARF Tumor Suppressor. Mol. Cell. Biol. *20*, 273–285.

Donzelli, M., and Draetta, G.F. (2003). Regulating mammalian

checkpoints through Cdc25 inactivation. EMBO Rep. *4*, 671–677.

Doza, Y.N., Cuenda, A., Thomas, G.M., Cohen, P., and Nebreda, A.R. (1995). Activation of the MAP kinase homologue RK requires the phosphorylation of Thr-180 and Tyr-182 and both residues are phosphorylated in chemically stressed KB cells. FEBS Lett. *364*, 223–228.

Duch, A., De Nadal, E., and Posas, F. (2012). The p38 and Hog1 SAPKs control cell cycle progression in response to environmental stresses. In FEBS Letters, (FEBS Lett), pp. 2925–2931.

Dümmler, A., Lawrence, A.M., and de Marco, A. (2005). Simplified screening for the detection of soluble fusion constructs expressed in E. coli using a modular set of vectors. Microb. Cell Fact. *4*.

Dyson, N., Howley, P., Munger, K., and Harlow, E. (1989). The human papilloma virus-16 E7 oncoprotein is able to bind to the retinoblastoma gene product. Science (80-.). *243*, 934–937.

Edmunds, J.W., and Mahadevan, L.C. (2004). MAP kinases as structural adaptors and enzymatic activators in transcription complexes. J. Cell Sci. *117*, 3715–3723.

Efimova, T., Broome, A.-M., and Eckert, R.L. (2004). Protein Kinase Cδ Regulates Keratinocyte Death and Survival by Regulating Activity and Subcellular Localization of a p38δ-Extracellular Signal-Regulated Kinase 1/2 Complex. Mol. Cell. Biol. *24*, 8167–8183.

Farooq, F., Balabanian, S., Liu, X., Holcik, M., and MacKenzie, A. (2009). p38 Mitogen-activated protein kinase stabilizes SMN mRNA through RNA binding protein HuR. Hum. Mol. Genet. *18*, 4035–4045.

Ferreiro, I., Joaquin, M., Islam, A., Gomez-Lopez, G., Barragan, M., Lombardía, L., Domínguez, O., Pisano, D.G., Lopez-Bigas, N., Nebreda, A.R., et al. (2010a). Whole genome analysis of p38 SAPK-mediated gene expression upon stress. BMC Genomics *11*, 144.

Ferreiro, I., Barragan, M., Gubern, A., Ballestar, E., Joaquin, M., and Posas, F. (2010b). The p38 SAPK is recruited to chromatin via its interaction with transcription factors. J. Biol. Chem. *285*, 31819–

31828.

Ferrigno, P., and Silver, P.A. (1999). Regulated nuclear localization of stress-responsive factors: How the nuclear trafficking of protein kinases and transcription factors contributes to cell survival. Oncogene *18*, 6129–6134.

Ferrigno, P., Posas, F., Koepp, D., Saito, H., and Silver, P.A. (1998). Regulated nucleo/cytoplasmic exchange of HOG1 MAPK requires the importin beta homologs NMD5 and XPO1. EMBO J. *17*, 5606–5614.

Fiorentino, F.P., Marchesi, I., and Giordano, A. (2013). On the role of retinoblastoma family proteins in the establishment and maintenance of the epigenetic landscape. J. Cell. Physiol. *228*, 276–284.

Fischer, M., and Müller, G.A. (2017). Cell cycle transcription control: DREAM/MuvB and RB-E2F complexes. Crit. Rev. Biochem. Mol. Biol. *52*, 638–662.

Flemington, E.K., Speck, S.H., and Kaelin, W.G. (1993). E2F-1-mediated transactivation is inhibited by complex formation with the retinoblastoma susceptibility gene product. Proc. Natl. Acad. Sci. U. S. A. *90*, 6914–6918.

Forcales, S. V., Albini, S., Giordani, L., Malecova, B., Cignolo, L., Chernov, A., Coutinho, P., Saccone, V., Consalvi, S., Williams, R., et al. (2012). Signal-dependent incorporation of MyoD-BAF60c into Brg1-based SWI/SNF chromatin-remodelling complex. EMBO J. *31*, 301–316.

Fouad, Y.A., and Aanei, C. (2017). Revisiting the hallmarks of cancer. Am. J. Cancer Res. *7*, 1016–1036.

Friend, S.H., Bernards, R., Rogelj, S., Weinberg, R.A., Rapaport, J.M., Albert, D.M., and Dryja, T.P. (1986). A human DNA segment with properties of the gene that predisposes to retinoblastoma and osteosarcoma. Nature *323*, 643–646.

Frolov, M. V., and Dyson, N.J. (2004). Molecular mechanisms of E2F-dependent activation and pRB-mediated repression. J. Cell Sci. *117*, 2173–2181.

Gabellini, C., Del Bufalo, D., and Zupi, G. (2006). Involvement of RB gene family in tumor angiogenesis. Oncogene *25*, 5326–5332.

Gaestel, M. (2016). MAPK-activated protein kinases (MKs): Novel insights and challenges. Front. Cell Dev. Biol. *3*.

Ganesh, K., and Massagué, J. (2021). Targeting metastatic cancer. Nat. Med. *27*, 34–44.

Giacinti, C., and Giordano, A. (2006). RB and cell cycle progression. Oncogene *25*, 5220–5227.

Gladden, A.B., and Diehl, J.A. (2005). Location, location, location: The role of cyclin D1 nuclear localization in cancer. J. Cell. Biochem. *96*, 906–913.

Gong, X., Ming, X., Deng, P., and Jiang, Y. (2010). Mechanisms regulating the nuclear translocation of p38 MAP kinase. J. Cell. Biochem. *110*, 1420–1429.

Gordon, E., Ravicz, J., Liu, S., Chawla, S., and Hall, F. (2018). Cell cycle checkpoint control: The cyclin G1/Mdm2/p53 axis emerges as a strategic target for broad-spectrum cancer gene therapy - A review of molecular mechanisms for oncologists. Mol. Clin. Oncol. *9*, 115–134.

Gräb, J., and Rybniker, J. (2019). The Expanding Role of p38 Mitogen-Activated Protein Kinase in Programmed Host Cell Death. Microbiol. Insights *12*, 117863611986459.

Gubern, A., Joaquin, M., Marquès, M., Maseres, P., Garcia-Garcia, J., Amat, R., González-Nuñez, D., Oliva, B., Real, F.X., de Nadal, E., et al. (2016). The N-Terminal Phosphorylation of RB by p38 Bypasses Its Inactivation by CDKs and Prevents Proliferation in Cancer Cells. Mol. Cell *64*, 25–36.

Guil, S., Long, J.C., and Cáceres, J.F. (2006). hnRNP A1 Relocalization to the Stress Granules Reflects a Role in the Stress Response. Mol. Cell. Biol. *26*, 5744–5758.

Guiley, K.Z., Liban, T.J., Felthousen, J.G., Ramanan, P., Litovchick, L., and Rubin, S.M. (2015). Structural mechanisms of DREAM

complex assembly and regulation. Genes Dev. *29*, 961–974.

Guo, X., Ngo, B., Modrek, A., and Lee, W.-H. (2014). Targeting Tumor Suppressor Networks for Cancer Therapeutics. Curr. Drug Targets *15*, 2–16.

Gupta, J., and Nebreda, A.R. (2015). Roles of p38α mitogen-activated protein kinase in mouse models of inflammatory diseases and cancer. FEBS J. *282*, 1841–1857.

Guzmán, C., Bagga, M., Kaur, A., Westermarck, J., and Abankwa, D. (2014). ColonyArea: An ImageJ Plugin to Automatically Quantify Colony Formation in Clonogenic Assays. PLoS One *9*, e92444.

Han, J., Wu, J., and Silke, J. (2020). An overview of mammalian p38 mitogen-activated protein kinases, central regulators of cell stress and receptor signaling. F1000Research *9*.

Hanahan, D., and Weinberg, R.A. (2011). Hallmarks of cancer: The next generation. Cell *144*, 646–674.

Harbour, J.W., Luo, R.X., Dei Santi, A., Postigo, A.A., and Dean, D.C. (1999). Cdk phosphorylation triggers sequential intramolecular interactions that progressively block Rb functions as cells move through G1. Cell *98*, 859–869.

Harrer, S., Shah, P., Antony, B., and Hu, J. (2019). Artificial Intelligence for Clinical Trial Design. Trends Pharmacol. Sci. *40*, 577–591.

Hassler, M., Singh, S., Yue, W.W., Luczynski, M., Lakbir, R., Sanchez-Sanchez, F., Bader, T., Pearl, L.H., and Mittnacht, S. (2007). Crystal Structure of the Retinoblastoma Protein N Domain Provides Insight into Tumor Suppression, Ligand Interaction, and Holoprotein Architecture. Mol. Cell *28*, 371–385.

Helin, K., Wu, C.L., Fattaey, A.R., Lees, J.A., Dynlacht, B.D., Ngwu, C., and Harlow, E. (1993). Heterodimerization of the transcription factors E2F-1 and DP-1 leads to cooperative trans-activation. Genes Dev. *7*, 1850–1861.

Hemmilä, I.A., and Hurskainen, P. (2002). Novel detection strategies

for drug discovery. Drug Discov. Today *7*.

Henley, S.A., and Dick, F.A. (2012). The retinoblastoma family of proteins and their regulatory functions in the mammalian cell division cycle. Cell Div. *7*, 10.

Van Den Heuvel, S., and Dyson, N.J. (2008). Conserved functions of the pRB and E2F families. Nat. Rev. Mol. Cell Biol.

Hiebert, S.W., Chellappan, S.P., Horowitz, J.M., and Nevins, J.R. (1992a). The interaction of pRb with E2F inhibits the transcriptional activity of E2F. Genes Dev *6*, 177–185.

Hiebert, S.W., Chellappan, S.P., Horowitz, J.M., and Nevins, J.R. (1992b). The interaction of RB with E2F coincides with an inhibition of the transcriptional activity of E2F. Genes Dev. *6*, 177–185.

Hilgendorf, K.I., Leshchiner, E.S., Nedelcu, S., Maynard, M.A., Calo, E., Ianari, A., Walensky, L.D., and Lees, J.A. (2013). The retinoblastoma protein induces apoptosis directly at the mitochondria. Genes Dev. *27*, 1003–1015.

Ho, J., and Benchimol, S. (2003). Transcriptional repression mediated by the p53 tumour suppressor. Cell Death Differ. *10*, 404–408.

Hollern, D.P., Swiatnicki, M.R., Rennhack, J.P., Misek, S.A., Matson, B.C., McAuliff, A., Gallo, K.A., Caron, K.M., and Andrechek, E.R. (2019). E2F1 Drives Breast Cancer Metastasis by Regulating the Target Gene FGF13 and Altering Cell Migration. Sci. Rep. *9*, 1–13.

Hotamisligil, G.S., and Davis, R.J. (2016). Cell signaling and stress responses. Cold Spring Harb. Perspect. Biol. *8*.

Hu, Q.J., Dyson, N., and Harlow, E. (1990). The regions of the retinoblastoma protein needed for binding to adenovirus E1A or SV40 large T antigen are common sites for mutations. EMBO J. *9*, 1147–1155.

Hui, L., Bakiri, L., Mairhorfer, A., Schweifer, N., Haslinger, C., Kenner, L., Komnenovic, V., Scheuch, H., Beug, H., and Wagner, E.F.

(2007). p38α suppresses normal and cancer cell proliferation by antagonizing the JNK-c-Jun pathway. Nat. Genet. *39*, 741–749.

Ianari, A., Natale, T., Calo, E., Ferretti, E., Alesse, E., Screpanti, I., Haigis, K., Gulino, A., and Lees, J.A. (2009). Proapoptotic Function of the Retinoblastoma Tumor Suppressor Protein. Cancer Cell *15*, 184–194.

Indovina, P., Marcelli, E., Casini, N., Rizzo, V., and Giordano, A. (2013). Emerging Roles of RB Family: New Defense Mechanisms Against Tumor Progression. J. Cell. Physiol *228*, 525–535.

Islam, M.A., Xu, Y., Tao, W., Ubellacker, J.M., Lim, M., Aum, D., Lee, G.Y., Zhou, K., Zope, H., Yu, M., et al. (2018). Restoration of tumour-growth suppression in vivo via systemic nanoparticle-mediated delivery of PTEN mRNA. Nat. Biomed. Eng. *2*, 850–864.

Iversen, P.W., Eastwood, B.J., Sittampalam, G.S., and Cox, K.L. (2006). A comparison of assay performance measures in screening assays: Signal window, Z′ factor, and assay variability ratio. J. Biomol. Screen. *11*, 247–252.

Ji, P., Jiang, H., Rekhtman, K., Bloom, J., Ichetovkin, M., Pagano, M., and Zhu, L. (2004). An Rb-Skp2-p27 pathway mediates acute cell cycle inhibition by Rb and is retained in a partial-penetrance Rb mutant. Mol. Cell *16*, 47–58.

Jin, S., Tong, T., Fan, W., Fan, F., Antinore, M.J., Zhu, X., Mazzacurati, L., Li, X., Petrik, K.L., Rajasekaran, B., et al. (2002). GADD45-induced cell cycle G2-M arrest associates with altered subcellular distribution of cyclin B1 and is independent of p38 kinase activity. Oncogene *21*, 8696–8704.

Jin, X., Ding, D., Yan, Y., Li, H., Wang, B., Ma, L., Ye, Z., Ma, T., Wu, Q., Rodrigues, D.N., et al. (2019). Phosphorylated RB Promotes Cancer Immunity by Inhibiting NF-κB Activation and PD-L1 Expression. Mol. Cell *73*, 22-35.e6.

Joaquin, M., Gubern, A., González-Nuñez, D., Josué Ruiz, E., Ferreiro, I., De Nadal, E., Nebreda, A.R., and Posas, F. (2012). The p57 CDKi integrates stress signals into cell-cycle progression to promote cell survival upon stress. EMBO J. *31*, 2952–2964.

Joaquin, M., de Nadal, E., and Posas, F. (2017). An RB insensitive to CDK regulation. Mol. Cell. Oncol. *4*.

Jung, H.J., and Kwon, H.J. (2015). Target deconvolution of bioactive small molecules: The heart of chemical biology and drug discovery. Arch. Pharm. Res. *38*, 1627–1641.

Kent, L.N., and Leone, G. (2019). The broken cycle: E2F dysfunction in cancer. Nat. Rev. Cancer *19*, 326–338.

Keseru, G.M., and Makara, G.M. (2006). Hit discovery and hit-to-lead approaches. Drug Discov. Today *11*, 741–748.

Khidr, L., and Chen, P.L. (2006). RB, the conductor that orchestrates life, death and differentiation. Oncogene *25*, 5210–5219.

Kishi, H., Nakagawa, K., Matsumoto, M., Suga, M., Ando, M., Taya, Y., and Yamaizumi, M. (2001). Osmotic Shock Induces G1 Arrest through p53 Phosphorylation at Ser33 by Activated p38MAPK without Phosphorylation at Ser15 and Ser20. J. Biol. Chem. *276*, 39115–39122.

Knudsen, E.S., and Wang, J.Y. (1996). Differential regulation of retinoblastoma protein function by specific Cdk phosphorylation sites. J. Biol. Chem. *271*, 8313–8320.

Knudsen, E.S., and Wang, J.Y. (1997). Dual mechanisms for the inhibition of E2F binding to RB by cyclin-dependent kinase-mediated RB phosphorylation. Mol. Cell. Biol. *17*, 5771–5783.

Knudsen, E.S., and Wang, J.Y.J. (2010). Targeting the RB-pathway in cancer therapy. Clin. Cancer Res. *16*, 1094–1099.

Knudsen, E.S., Nambiar, R., Rosario, S.R., Smiraglia, D.J., Goodrich, D.W., and Witkiewicz, A.K. (2020). Pan-cancer molecular analysis of the RB tumor suppressor pathway. Commun. Biol. *3*, 1–12.

Knudson, A.G. (1971). Mutation and cancer: statistical study of retinoblastoma. Proc. Natl. Acad. Sci. U. S. A. *68*, 820–823.

Kogan, S., and Carpizo, D. (2016). Pharmacological targeting of

mutant p53. Transl. Cancer Res. *5*, 698–706.

Kontomanolis, E.N., Koutras, A., Syllaios, A., Schizas, D., Mastoraki, A., Garmpis, N., Diakosavvas, M., Angelou, K., Tsatsaris, G., Pagkalos, A., et al. (2020). Role of oncogenes and tumor-suppressor genes in carcinogenesis: A review. Anticancer Res. *40*, 6009–6015.

Kyriakis, J.M., and Avruch, J. (2012). Mammalian MAPK signal transduction pathways activated by stress and inflammation: A 10-year update. Physiol. Rev. *92*, 689–737.

Lacy, S., and Whyte, P. (1997). Identification of a p130 domain mediating interactions with cyclin A/cdk 2 and cyclin E/cdk 2 complexes. Oncogene *14*, 2395–2406.

Lafarga, V., Cuadrado, A., Lopez de Silanes, I., Bengoechea, R., Fernandez-Capetillo, O., and Nebreda, A.R. (2009). p38 Mitogen-activated protein kinase- and HuR-dependent stabilization of p21(Cip1) mRNA mediates the G(1)/S checkpoint. Mol. Cell. Biol. *29*, 4341–4351.

Lavia, P., and Jansen-Dürr, P. (1999). E2F target genes and cell-cycle checkpoint control. Bioessays *21*, 221–230.

Lawson, S.K., Dobrikova, E.Y., Shveygert, M., and Gromeier, M. (2013). p38 Mitogen-Activated Protein Kinase Depletion and Repression of Signal Transduction to Translation Machinery by miR-124 and -128 in Neurons. Mol. Cell. Biol. *33*, 127–135.

Lee, C., Chang, J.H., Lee, H.S., and Cho, Y. (2002). Structural basis for the recognition of the E2F transactivation domain by the retinoblastoma tumor suppressor. Genes Dev. *16*, 3199–3212.

Lee, W., Bookstein, R., Hong, F., Young, L., Shew, J., and Lee, E. (1987). Human retinoblastoma susceptibility gene: cloning, identification, and sequence. Science (80-.). *235*, 1394–1399.

Lee, Y.-R., Chen, M., and Paolo Pandolfi, P. (2018). The functions and regulation of the PTEN tumour suppressor: new modes and prospects. Nat. Rev. Mol. Cell Biol.

Li, W., Zhu, J., Dou, J., She, H., Tao, K., Xu, H., Yang, Q., and Mao, Z. (2017). Phosphorylation of LAMP2A by p38 MAPK couples ER stress to chaperone-mediated autophagy. Nat. Commun. *8*.

Litovchick, L., Chestukhin, A., and DeCaprio, J.A. (2004). Glycogen synthase kinase 3 phosphorylates RBL2/p130 during quiescence. Mol. Cell. Biol. *24*, 8970–8980.

Liu, X., and Hu, C. (2020). Novel Potential Therapeutic Target for E2F1 and Prognostic Factors of E2F1/2/3/5/7/8 in Human Gastric Cancer. Mol. Ther. - Methods Clin. Dev. *18*, 824–838.

Ludlow, J.W., Glendening, C.L., Livingston, D.M., and DeCarprio, J.A. (1993). Specific enzymatic dephosphorylation of the retinoblastoma protein. Mol. Cell. Biol. *13*, 367–372.

MacDonald, J.I., and Dick, F.A. (2012). Posttranslational modifications of the retinoblastoma tumor suppressor protein as determinants of function. Genes and Cancer *3*, 619–633.

Malumbres, M., and Barbacid, M. (2001). To cycle or not to cycle: A critical decision in cancer. Nat. Rev. Cancer *1*, 222–231.

Manning, A.L., Longworth, M.S., and Dyson, N.J. (2010). Loss of pRB causes centromere dysfunction and chromosomal instability. Genes Dev. *24*, 1364–1376.

Markham, D., Munro, S., Soloway, J., O'Connor, D.P., and La Thangue, N.B. (2006). DNA-damage-responsive acetylation of pRb regulates binding to E2F-1. EMBO Rep. *7*, 192–198.

Martínez-Limón, A., Joaquin, M., Caballero, M., Posas, F., and de Nadal, E. (2020). The p38 pathway: From biology to cancer therapy. Int. J. Mol. Sci. *21*.

Massagué, J. (2004). G1 cell-cycle control and cancer. Nature *432*, 298–306.

McBrayer, S.K., Olenchock, B.A., DiNatale, G.J., Shi, D.D., Khanal, J., Jennings, R.B., Novak, J.S., Oser, M.G., Robbins, A.K., Modiste, R., et al. (2018). Autochthonous tumors driven by Rb1 loss have an ongoing requirement for the RBP2 histone demethylase. Proc. Natl.

Acad. Sci. U. S. A. *115*, E3741–E3748.

McLendon, R., Friedman, A., Bigner, D., Van Meir, E.G., Brat, D.J., Mastrogianakis, G.M., Olson, J.J., Mikkelsen, T., Lehman, N., Aldape, K., et al. (2008). Comprehensive genomic characterization defines human glioblastoma genes and core pathways. Nature *455*, 1061–1068.

McNair, C., Xu, K., Mandigo, A.C., Benelli, M., Leiby, B., Rodrigues, D., Lindberg, J., Gronberg, H., Crespo, M., De Laere, B., et al. (2018). Differential impact of RB status on E2F1 reprogramming in human cancer. J. Clin. Invest. *128*, 341–358.

Michaloglou, C., Crafter, C., Siersbaek, R., Delpuech, O., Curwen, J.O., Carnevalli, L.S., Staniszewska, A.D., Polanska, U.M., Cheraghchi-Bashi, A., Lawson, M., et al. (2018). Combined inhibition of mtor and cdk4/6 is required for optimal blockade of e2f function and long-term growth inhibition in estrogen receptor–positive breast cancer. Mol. Cancer Ther. *17*, 908–920.

Mittnacht, S. (1998a). Control of pRB phosphorylation. Curr. Opin. Genet. Dev. *8*, 21–27.

Mittnacht, S. (1998b). Control of pRB phosphorylation. Curr. Opin. Genet. Dev. *8*, 21–27.

Miura, H., Kondo, Y., Matsuda, M., and Aoki, K. (2018). Cell-to-Cell Heterogeneity in p38-Mediated Cross-Inhibition of JNK Causes Stochastic Cell Death. Cell Rep. *24*, 2658–2668.

Moffat, J.G., Vincent, F., Lee, J.A., Eder, J., and Prunotto, M. (2017). Opportunities and challenges in phenotypic drug discovery: An industry perspective. Nat. Rev. Drug Discov. *16*, 531–543.

Morris, L.G.T., and Chan, T.A. (2015). Therapeutic targeting of tumor suppressor genes. Cancer *121*, 1357–1368.

Mudgett, J.S., Ding, J., Guh-Siesel, L., Chartrain, N.A., Yang, L., Gopal, S., and Shen, M.M. (2000). Essential role for p38α mitogen-activated protein kinase in placental angiogenesis. Proc. Natl. Acad. Sci. U. S. A. *97*, 10454–10459.

Mulligan, G.J., Wong, J., and Jacks, T. (1998). p130 Is Dispensable in Peripheral T Lymphocytes: Evidence for Functional Compensation by p107 and pRB. Mol. Cell. Biol. *18*, 206–220.

Münger, K., Werness, B.A., Dyson, N., Phelps, W.C., Harlow, E., and Howley, P.M. (1989). Complex formation of human papillomavirus E7 proteins with the retinoblastoma tumor suppressor gene product. EMBO J. *8*, 4099–4105.

Narasimha, A.M., Kaulich, M., Shapiro, G.S., Choi, Y.J., Sicinski, P., and Dowdy, S.F. (2014). Cyclin D activates the Rb tumor suppressor by mono-phosphorylation. Elife *2014*.

Ogawa, H., Ishiguro, K.I., Gaubatz, S., Livingston, D.M., and Nakatani, Y. (2002). A complex with chromatin modifiers that occupies E2f- and Myc-responsive genes in G0 cells. Science (80-.). *296*, 1132–1136.

Olsen, J. V., Vermeulen, M., Santamaria, A., Kumar, C., Miller, M.L., Jensen, L.J., Gnad, F., Cox, J., Jensen, T.S., Nigg, E.A., et al. (2010). Quantitative phosphoproteomics revealswidespread full phosphorylation site occupancy during mitosis. Sci. Signal. *3*.

Otto, T., and Sicinski, P. (2017). Cell cycle proteins as promising targets in cancer therapy. Nat. Rev. Cancer *17*, 93–115.

Ovejero, S., Bueno, A., and Sacristán, M.P. (2020). Working on genomic stability: From the S-phase to mitosis. Genes (Basel). *11*.

Owens, D.M., and Keyse, S.M. (2007). Differential regulation of MAP kinase signalling by dual-specificity protein phosphatases. Oncogene *26*, 3203–3213.

Paul, D. (2020). The systemic hallmarks of cancer. J. Cancer Metastasis Treat. *2020*.

Peuget, S., Zhu, J., Sanz, G., Singh, M., Gaetani, M., Chen, X., Shi, Y., Saei, A.A., Visnes, T., Lindstrom, M.S., et al. (2020). Thermal proteome profiling identifies oxidative-dependent inhibition of the transcription of major oncogenes as a new therapeutic mechanism for select anticancer compounds. Cancer Res. *80*, 1538–1550.

Peyressatre, M., Prével, C., Pellerano, M., and Morris, M.C. (2015). Targeting cyclin-dependent kinases in human cancers: From small molecules to peptide inhibitors. Cancers (Basel). *7*, 179–237.

Phong, M.S., Van Horn, R.D., Li, S., Tucker-Kellogg, G., Surana, U., and Ye, X.S. (2010). p38 Mitogen-Activated Protein Kinase Promotes Cell Survival in Response to DNA Damage but Is Not Required for the G2 DNA Damage Checkpoint in Human Cancer Cells. Mol. Cell. Biol. *30*, 3816–3826.

Polager, S., and Ginsberg, D. (2008). E2F - at the crossroads of life and death. Trends Cell Biol. *18*, 528–535.

Portman, N., Alexandrou, S., Carson, E., Wang, S., Lim, E., and Caldon, C.E. (2019). Overcoming CDK4/6 inhibitor resistance in ER-positive breast cancer. Endocr. Relat. Cancer *26*, R15–R30.

Puri, P.L., Wu, Z., Zhang, P., Wood, L.D., Bhakta, K.S., Han, J., Feramisco, J.R., Karin, M., and Wang, J.Y.J. (2000). Induction of terminal differentiation by constitutive activation of p38 MAP kinase in human rhabdomyosarcoma cells. Genes Dev. *14*, 574–584.

Purvis, J.E., and Lahav, G. (2013). Encoding and decoding cellular information through signaling dynamics. Cell *152*, 945–956.

Qin, X.Q., Chittenden, T., Livingston, D.M., and Kaelin, W.G. (1992). Identification of a growth suppression domain within the retinoblastoma gene product. Genes Dev. *6*, 953–964.

Raman, M., Earnest, S., Zhang, K., Zhao, Y., and Cobb, M.H. (2007). TAO kinases mediate activation of p38 in response to DNA damage. EMBO J. *26*, 2005–2014.

Real, S., Meo-Evoli, N., Espada, L., and Tauler, A. (2011). E2F1 regulates cellular growth by mTORC1 signaling. PLoS One *6*.

Regot, S., Hughey, J.J., Bajar, B.T., Carrasco, S., and Covert, M.W. (2014). High-sensitivity measurements of multiple kinase activities in live single cells. Cell *157*, 1724–1734.

Reinhardt, H.C., Aslanian, A.S., Lees, J.A., and Yaffe, M.B. (2007). p53-Deficient Cells Rely on ATM- and ATR-Mediated Checkpoint

Signaling through the p38MAPK/MK2 Pathway for Survival after DNA Damage. Cancer Cell *11*, 175–189.

Remy, G., Risco, A.M., Iñesta-Vaquera, F.A., González-Terán, B., Sabio, G., Davis, R.J., and Cuenda, A. (2010). Differential activation of p38MAPK isoforms by MKK6 and MKK3. Cell. Signal. *22*, 660–667.

Ren, S., and Rollins, B.J. (2004). Cyclin C/cdk3 promotes Rb-dRen, Shengjun, and Barrett J. Rollins. 2004. "Cyclin C/Cdk3 Promotes Rb-Dependent G0 Exit." Cell 117(2):239–51.ependent G0 exit. Cell *117*, 239–251.

Reynolds, C.H., Betts, J.C., Blackstock, W.P., Nebreda, A.R., and Anderton, B.H. (2000). Phosphorylation sites on tau identified by nanoelectrospray mass spectrometry: Differences in vitro between the mitogen-activated protein kinases ERK2, c-Jun N-terminal kinase and P38, and glycogen synthase kinase- 3β. J. Neurochem. *74*, 1587–1595.

Reyskens, K.M.S.E., and Arthur, J.S.C. (2016). Emerging roles of the mitogen and stress activated kinases MSK1 and MSK2. Front. Cell Dev. Biol. *4*.

Rodier, G., Makris, C., Coulombe, P., Scime, A., Nakayama, K., Nakayama, K.I., and Meloche, S. (2005). p107 inhibits G1 to S phase progression by down-regulating expression of the F-box protein Skp2. J. Cell Biol. *168*, 55–66.

Roelofs, P.A., Goh, C.Y., Chua, B.H., Jarvis, M.C., Stewart, T.A., McCann, J.L., McDougle, R.M., Carpenter, M.A., Martens, J.W.M., Span, P.N., et al. (2020). Characterization of the mechanism by which the rb/e2f pathway controls expression of the cancer genomic dna deaminase apobec3b. Elife *9*, 1–64.

Rubin, S.M., Gall, A.L., Zheng, N., and Pavletich, N.P. (2005). Structure of the Rb C-terminal domain bound to E2F1-DP1: A mechanism for phosphorylation-induced E2F release. Cell *123*, 1093–1106.

Rubio, C., Martínez-Fernandez, M., Segovia, C., Lodewijk, I., Suarez-Cabrera, C., Segrelles, C., Lopez-Calder, F., Munera-

Maravilla, E., Santos, M., Bernardini, A., et al. (2019). CDK4/6 inhibitor as a novel therapeutic approach for advanced bladder cancer independently of RB1 status. Clin. Cancer Res. *25*, 390–402.

Sabio, G., Arthur, J.S.C., Kuma, Y., Peggie, M., Carr, J., Murray-Tait, V., Centeno, F., Goedert, M., Morrice, N.A., and Cuenda, A. (2005). p38γ regulates the localisation of SAP97 in the cytoskeleton by modulating its interaction with GKAP. EMBO J. *24*, 1134–1145.

Sánchez-Martínez, C., Lallena, M.J., Sanfeliciano, S.G., and de Dios, A. (2019). Cyclin dependent kinase (CDK) inhibitors as anticancer drugs: Recent advances (2015–2019). Bioorganic Med. Chem. Lett. *29*, 126637.

Sandler, H., and Stoecklin, G. (2008). Control of mRNA decay by phosphorylation of tristetraprolin. In Biochemical Society Transactions, (Biochem Soc Trans), pp. 491–496.

Sangwan, M., McCurdy, S.R., Livne-Bar, I., Ahmad, M., Wrana, J.L., Chen, D., and Bremner, R. (2012). Established and new mouse models reveal E2f1 and Cdk2 dependency of retinoblastoma, and expose effective strategies to block tumor initiation. Oncogene *31*, 5019–5028.

Schaal, C., Pillai, S., and Chellappan, S.P. (2014). The Rb-E2F transcriptional regulatory pathway in tumor angiogenesis and metastasis. In Advances in Cancer Research, (Academic Press Inc.), pp. 147–182.

Schindler, E.M., Hindes, A., Gribben, E.L., Burns, C.J., Yin, Y., Lin, M.H., Owen, R.J., Longmore, G.D., Kissling, G.E., Arthur, J.S.C., et al. (2009). p38δ mitogen-activated protein kinase is essential for skin tumor development in mice. Cancer Res. *69*, 4648–4655.

Schneider, G. (2018). Automating drug discovery. Nat. Rev. Drug Discov. *17*, 97–113.

Scott, P.H., Cairns, C.A., Sutcliffe, J.E., Alzuherri, H.M., McLees, A., Winter, A.G., and White, R.J. (2001). Regulation of RNA polymerase III transcription during cell cycle entry. J. Biol. Chem. *276*, 1005–1014.

Shechter, S., Thomas, D.R., and Jans, D.A. (2020). Application of In Silico and HTS Approaches to Identify Nuclear Import Inhibitors for Venezuelan Equine Encephalitis Virus Capsid Protein: A Case Study. Front. Chem. *8*, 573121.

Sherr, C.J., and Roberts, J.M. (1999). CDK inhibitors: Positive and negative regulators of G1-phase progression. Genes Dev. *13*, 1501–1512.

Singh, M., and Singh, S. (2014). Benzothiazoles: How Relevant in Cancer Drug Design Strategy? Anticancer. Agents Med. Chem. *14*, 127–146.

Sinha, S., and Vohora, D. (2017). Drug Discovery and Development: An Overview. In Pharmaceutical Medicine and Translational Clinical Research, (Elsevier Inc.), pp. 19–32.

Slobodnyuk, K., Radic, N., Ivanova, S., Llado, A., Trempolec, N., Zorzano, A., and Nebreda, A.R. (2019). Autophagy-induced senescence is regulated by p38α signaling. Cell Death Dis. *10*.

Smith, M.T., Guyton, K.Z., Kleinstreuer, N., Borrel, A., Cardenas, A., Chiu, W.A., Felsher, D.W., Gibbons, C.F., Goodson, W.H., Houck, K.A., et al. (2020). The key characteristics of carcinogens: Relationship to the hallmarks of cancer, relevant biomarkers, and assays to measure them. Cancer Epidemiol. Biomarkers Prev. *29*, 1887–1903.

Soni, S., Anand, P., and Padwad, Y.S. (2019). MAPKAPK2: The master regulator of RNA-binding proteins modulates transcript stability and tumor progression. J. Exp. Clin. Cancer Res. *38*.

Soustek, M.S., Balsa, E., Barrow, J.J., Jedrychowski, M., Vogel, R., Smeitink, J., Gygi, S.P., and Puigserver, P. (2018). Inhibition of the ER stress IRE1α inflammatory pathway protects against cell death in mitochondrial complex I mutant cells. Cell Death Dis. *9*.

Stevaux, O., and Dyson, N.J. (2002). A revised picture of the E2F transcriptional network and RB function. Curr. Opin. Cell Biol. *14*, 684–691.

Stramucci, L., Pranteda, A., and Bossi, G. (2018). Insights of

Crosstalk between p53 Protein and the MKK3/MKK6/p38 MAPK Signaling Pathway in Cancer. Cancers (Basel). *10*, 131.

Sumara, G., Formentini, I., Collins, S., Sumara, I., Windak, R., Bodenmiller, B., Ramracheya, R., Caille, D., Jiang, H., Platt, K.A., et al. (2009). Regulation of PKD by the MAPK p38δ in Insulin Secretion and Glucose Homeostasis. Cell *136*, 235–248.

Sun, A., Bagella, L., Tutton, S., Romano, G., and Giordano, A. (2007). From G0 to S phase: A view of the roles played by the retinoblastoma (Rb) family members in the Rb-E2F pathway. J. Cell. Biochem. *102*, 1400–1404.

Surget, S., Descamps, G., Brosseau, C., Normant, V., Maïga, S., Gomez-Bougie, P., Gouy-Colin, N., Godon, C., Béné, M.C., Moreau, P., et al. (2014). RITA (Reactivating p53 and Inducing Tumor Apoptosis) is efficient against TP53abnormal myeloma cells independently of the p53 pathway. BMC Cancer *14*, 437.

Swinney, D.C. (2013). Phenotypic vs. Target-based drug discovery for first-in-class medicines. Clin. Pharmacol. Ther. *93*, 299–301.

Takahashi, Y., Rayman, J.B., and Dynlacht, B.D. (2000). Analysis of promoter binding by the E2F and pRB families in vivo: Distinct E2F proteins mediate activation and repression. Genes Dev. *14*, 804–816.

Talluri, S., and Dick, F.A. (2012). Regulation of transcription and chromatin structure by pRB: Here, there and everywhere. Cell Cycle *11*, 3189–3198.

Tanoue, T., Adachi, M., Moriguchi, T., and Nishida, E. (2000). A conserved docking motif in MAP kinases common to substrates, activators and regulators. Nat. Cell Biol. *2*, 110–116.

Tanoue, T., Maeda, R., Adachi, M., and Nishida, E. (2001). Identification of a docking groove on ERK and p38 MAP kinases that regulates the specificity of docking interactions. EMBO J. *20*, 466–479.

Thomas, D.M., Carty, S.A., Piscopo, D.M., Lee, J.S., Wang, W.F., Forrester, W.C., and Hinds, P.W. (2001). The retinoblastoma protein acts as a transcriptional coactivator required for osteogenic

differentiation. Mol. Cell *8*, 303–316.

Thomas, D.M., Yang, H.S., Alexander, K., and Hinds, P.W. (2003). Role of the retinoblastoma protein in differentiation and senescence. Cancer Biol. Ther. *2*, 124–130.

Thoms, H.C., Dunlop, M.G., and Stark, L.A. (2007). p38-mediated inactivation of cyclin D1/cyclin-dependent kinase 4 stimulates nucleolar translocation of RelA and apoptosis in colorectal cancer cells. Cancer Res. *67*, 1660–1669.

Thornton, T.M., and Rincon, M. (2009). Non-classical p38 map kinase functions: Cell cycle checkpoints and survival. Int. J. Biol. Sci. *5*, 44–52.

Tiedje, C., Holtmann, H., and Gaestel, M. (2014). The role of mammalian MAPK signaling in regulation of cytokine mRNA stability and translation. J. Interf. Cytokine Res. *34*, 220–232.

Tognetti, S., Jiménez, J., Viganò, M., Duch, A., Queralt, E., de Nadal, E., and Posas, F. (2020). Hog1 activation delays mitotic exit via phosphorylation of Net1. Proc. Natl. Acad. Sci. U. S. A. *117*, 8924–8933.

Tomida, T., Takekawa, M., and Saito, H. (2015). Oscillation of p38 activity controls efficient pro-inflammatory gene expression. Nat. Commun. *6*.

Trempolec, N., Dave-Coll, N., and Nebreda, A.R. (2013). SnapShot: P38 MAPK substrates. Cell *152*, 924-924.e1.

Trimarchi, J.M., and Lees, J.A. (2002). Sibling rivalry in the E2F family. Nat. Rev. Mol. Cell Biol. *3*, 11–20.

Vandel, L., Nicolas, E., Vaute, O., Ferreira, R., Ait-Si-Ali, S., and Trouche, D. (2001). Transcriptional Repression by the Retinoblastoma Protein through the Recruitment of a Histone Methyltransferase. Mol. Cell. Biol. *21*, 6484–6494.

Vélez-Cruz, R., and Johnson, D.G. (2017). The retinoblastoma (RB) tumor suppressor: Pushing back against genome instability on multiple fronts. Int. J. Mol. Sci. *18*.

Verona, R., Moberg, K., Estes, S., Starz, M., Vernon, J.P., and Lees, J.A. (1997). E2F activity is regulated by cell cycle-dependent changes in subcellular localization. Mol. Cell. Biol. *17*, 7268–7282.

Vijayaraghavan, S., Moulder, S., Keyomarsi, K., and Layman, R.M. (2018). Inhibiting CDK in Cancer Therapy: Current Evidence and Future Directions. Target. Oncol. *13*, 21–38.

Wagner, E.F., and Nebreda, Á.R. (2009). Signal integration by JNK and p38 MAPK pathways in cancer development. Nat. Rev. Cancer *9*, 537–549.

Wang, H., Bauzon, F., Ji, P., Xu, X., Sun, D., Locker, J., Sellers, R.S., Nakayama, K., Nakayama, K.I., Cobrinik, D., et al. (2010). Skp2 is required for survival of aberrantly proliferating Rb1-deficient cells and for tumorigenesis in Rb1+/ mice. Nat. Genet. *42*, 83–88.

Wei, Y., An, Z., Zou, Z., Sumpter, R., Su, M., Zang, X., Sinha, S., Gaestel, M., and Levine, B. (2015). The stress-responsive kinases MAPKAPK2/MAPKAPK3 activate starvation-induced autophagy through Beclin 1 phosphorylation. Elife *2015*.

Wells, J., Boyd, K.E., Fry, C.J., Bartley, S.M., and Farnham, P.J. (2000). Target Gene Specificity of E2F and Pocket Protein Family Members in Living Cells. Mol. Cell. Biol. *20*, 5797–5807.

Whyte, P., Williamson, N.M., and Harlow, E. (1989). Cellular targets for transformation by the adenovirus E1A proteins. Cell *56*, 67–75.

Wiggin, G.R., Soloaga, A., Foster, J.M., Murray-Tait, V., Cohen, P., and Arthur, J.S.C. (2002). MSK1 and MSK2 Are Required for the Mitogen- and Stress-Induced Phosphorylation of CREB and ATF1 in Fibroblasts. Mol. Cell. Biol. *22*, 2871–2881.

Wirt, S.E., and Sage, J. (2010). P107 in the public eye: An Rb understudy and more. Cell Div. *5*, 1–13.

Woo, M.S., Sánchez, I., and Dynlacht, B.D. (1997). p130 and p107 use a conserved domain to inhibit cellular cyclin-dependent kinase activity. Mol. Cell. Biol. *17*, 3566–3579.

Wu, S., Lopez, J., Salcido, K., Zocchi, L., Wu, J., and Benavente, C.

(2020). UHRF1 drives the poor prognosis associated with RB loss in osteosarcoma. BioRxiv 2020.05.24.113647.

Xiao, B., Spencer, J., Clements, A., Ali-Khan, N., Mittnacht, S., Broceno, C., Burghammer, M., Perrakis, A., Marmorstein, R., and Gamblin, S.J. (2003). Crystal structure of the retinoblastoma tumor suppressor protein bound to E2F and the molecular basis of its regulation. Proc. Natl. Acad. Sci. *100*, 2363–2368.

Yao, G., Lee, T.J., Mori, S., Nevins, J.R., and You, L. (2008). A bistable Rb-E2F switch underlies the restriction point. Nat. Cell Biol. *10*, 476–482.

Zarkowska, T., and Mittnacht, S. (1997). Differential phosphorylation of the retinoblastoma protein by G1/S cyclin-dependent kinases. J. Biol. Chem. *272*, 12738–12746.

Zhang, J., and Bowden, G.T. (2012). Activation of p38 MAP kinase and JNK pathways by UVA irradiation. Photochem. Photobiol. Sci. *11*, 54–61.

Zhang, J.H., Chung, T.D.Y., and Oldenburg, K.R. (1999). A simple statistical parameter for use in evaluation and validation of high throughput screening assays. J. Biomol. Screen. *4*, 67–73.

Zhang, Y., Liu, G., and Dong, Z. (2001). MSK1 and JNKs Mediate Phosphorylation of STAT3 in UVA-irradiated Mouse Epidermal JB6 Cells. J. Biol. Chem. *276*, 42534–42542.

Zhang, Y., Cho, Y.Y., Petersen, B.L., Zhu, F., and Dong, Z. (2004). Evidence of STAT1 phosphorylation modulated by MAPKs, MEK1 and MSK1. Carcinogenesis *25*, 1165–1175.

Zhang, Y.Y., Mei, Z.Q., Wu, J.W., and Wang, Z.X. (2008). Enzymatic activity and substrate specificity of mitogen-activated protein kinase p38α in different phosphorylation states. J. Biol. Chem. *283*, 26591–26601.